EXPERIMENTS WITH A "PLANE MIRROR" ELECTRON ENERGY ANALYSER

Thesis

Submitted by

JAMES GIBSON

for the degree of

Master of Philosophy

University of Edinburgh

October, 1976.

DECLARATION

I declare that:-

(a) This thesis has been composed by me.

(b) The work is entirely my own except where specifically indicated.

(Signed)

J. GIBSON.

ACKNOWLEDGEMENTS.

I wish to thank Professor W.S. Cochrane and Professor N.E. Feather for giving me the opportunity to carry out this research. I am indebted to Professor P.S. Farago for the idea of the project and his invaluable assistance throughout the course of the experiment. I wish also to thank Dr. R.C. Dougal who compiled the computer program which enabled me to evaluate my results, Dr. D.M. Campbell, Dr. A.G.A. Rae and Dr. I.C. Malcolm for advice at various stages of the experiment and the technical staff of the Physics department for assistance rendered. Finally I would like to thank Mrs. N. Burgoyne for her excellent work in the typing of this thesis.

ABSTRACT OF THESIS

The properties of a plane mirror electrostatic energy analyser are discussed when using a low energy electron beam with an angle of incidence of 30 degrees to the front plate of the analyser. Factors affecting the energy resolution of the analyser under second order focusing conditions are discussed and an analyser constructed so that its various characteristics can be tested under practical conditions. Using a thermionic electron source the electron ballistics of the analyser are checked and calculations made from the measurements to determine the energy resolution of the analyser. Values of percentage resolution of the analyser of around one per cent are obtained and the thermal spread of the electron source is also evaluated.

The use of such an analyser as an instrument to detect back-scattering of electrons from a gaseous source is discussed and a short description is given of an experiment using the analyser to observe the inelastically scattered electrons produced at an angle of 180 degrees when the 6^1P_1, 6^3P_0 and 6^3P_1 states of the mercury atom are excited by an electron beam which is energy selected by the same analyser.

C O N T E N T S

		Page
CHAPTER 1	INTRODUCTION	1
CHAPTER 2	THEORY OF THE EXPERIMENT	5
2.1	The Plane Mirror Electrostatic Energy Analyser - Ballistics.	5
2.2	The Plane Mirror Electrostatic Energy Analyser - Energy Resolution.	8
2.3	Analyser as an Instrument to Detect Backscattering.	11
CHAPTER 3	THE APPARATUS	12
3.1	Plane Mirror Electrostatic Energy Analyser	12
3.2	Electron Gun	16
3.3	Electron Detector	17
3.4	Ancillary Apparatus	18
CHAPTER 4	EXPERIMENTAL METHOD	22
4.1	Setting up of Basic Experimental Parameters	22
4.2	Data Measurement and Recording	23
CHAPTER 5	EVALUATION OF RESULTS	27
5.1	Electron Ballistics	27
5.2	Interpretation of Shapes of Measured Spectra	29
5.3	Calculation of Resolution	34
CONCLUSION		38
APPENDICES		
I	Measurements of Inelastic Scattering from the Mercury Atom	39
II	Electronic circuits	45
III	Procedure for Activating Cathode	52
IV	Mathematical Steps for the Interpretation of Shapes of Measured Spectra	53
REFERENCES		

CHAPTER 1

INTRODUCTION

One of the most basic problems in electron ballistics is the motion of electrons of a known initial energy in a uniform electric field. An electron emitted at an arbitrary angle into a uniform electric retarding field will follow a parabolic trajectory in that field. Given that two electrons are emitted by a point source with the same initial kinetic energy, but with different angles, then their trajectories will, in general, cross each other. A well known example (Pierce:1949) is that electrons of the same initial kinetic energy, emitted within a small angular range about an angle of 45° from a point source located on the more positive plate of a plane parallel condenser, will be focused on this plane provided that the initial velocities of the electrons lie in a plane parallel to the electric field.

This is the basis of the electron energy analyser developed by Yarnold and Bolton (1949) and studied in some detail by Harrower (1955) in the energy range 100 to 900 eV. In these cases, since there is no force acting in the direction perpendicular to the electric field, focusing takes place in one direction only.

Two directional focusing can be achieved by using the type of field developed between two co-axial cylinders. Electrons, with the same initial energy, emitted within a small range of solid angle by a point source situated on the symmetry axis, can be brought to a focus on this axis (Blauth:1957) (Sar-el:1967). As well as its two directional focusing property, such a cylindrical mirror satisfies the requirements of second order focusing for a specific combination of experimental parameters (Zashkvara:1966). The

performance/

performance of such a cylindrical mirror as an energy analyser can be shown to surpass that of a hemispherical analyser (Hafner:1968).

Green and Proca (1970) showed that if the source slit and collector slit of a plane mirror energy analyser are located in a field free region, then electrons of the same initial kinetic energy, emitted within a small angular range about an angle of 30° from a point source, will come to a focus under second order focusing conditions. The minimum image size of such an analyser was also studied.

The use of various types of energy analysers in the study of electron-atom interactions means that the resultant scattered electrons can be analysed very accurately and their energy distributions found. Schulz (1962) devised a method of studying the vibrational excitation of nitrogen molecules by electrons in the energy range 1.5 to 4eV using two identical 127 - degree electrostatic analysers, the first to produce essentially monoenergetic electrons and the second tuned to an energy loss process. The plane mirror energy analyser has been used in experiments to study the angular distribution of electrons scattered with well defined energy (Lassettre: 1964) and as a part of a simple photoelectron spectrometer (Eland: 1968). These analysers are of the type which accept electrons emitted at an angle of 45 degrees as is the one used by Malcolm (1976) in his apparatus to study angular momentum dependent collision processes in sodium.

All these types of apparatus mentioned latterly cannot be used to observe scattering out to angles of 180 degrees because of the interference of the source. The apparatus that does enable observations/

observations to be made at these angles was developed by Gagge (1933) who employed a uniform magnetic field to deflect the electrons in a circular path. A plane mirror electrostatic analyser with a 30 degree entrance angle can be used as an instrument for the measurement and study of 180 degree inelastically scattered electrons from a gaseous source. The beam of scattered electrons will follow a different path from the source beam and this particular experiment will be discussed more fully in the appendix.

Although a study into the angular resolution of the plane mirror electrostatic analyser with a 30 degree entrance angle (120 degree analyser) has been made by Green and Proca, as previously mentioned, a project to study the energy resolution of such an analyser under second order focusing conditions was carried through.

The theoretical background of the electrostatic analyser is discussed in chapter two, and in conjunction with the relationships formulated an analyser was constructed and operated with a simple thermionic source, the description of both of which are dealt with in chapter three. When operating the analyser, two methods of data collection were used both of which have distinct advantages and these are discussed in chapter four along with other factors important to the working of the analyser. The general performance and charac-:teristics of the analyser using low energy electrons were checked and measurements to determine the energy resolution were made. These calculations and results were based on certain assumed characteristics of the thermionic electron source used and upon the analyser having a Gaussian instrument function, all of which are discussed in chapter five. As well as obtaining values of resolution of less than one

percent/

percent certain characteristics of the thermionic source were obtained.

An experiment to detect inelastically scattered electrons from mercury at an angle of 180 degrees to the incident beam direction was carried out. Some results were obtained and although the success was very limited due to parameters changing during the long counting times involved, the analyser as an instrument for the observation of back-scattering is feasible. This experiment was done in a qualitative rather than quantitative manner and is discussed in the appendix.

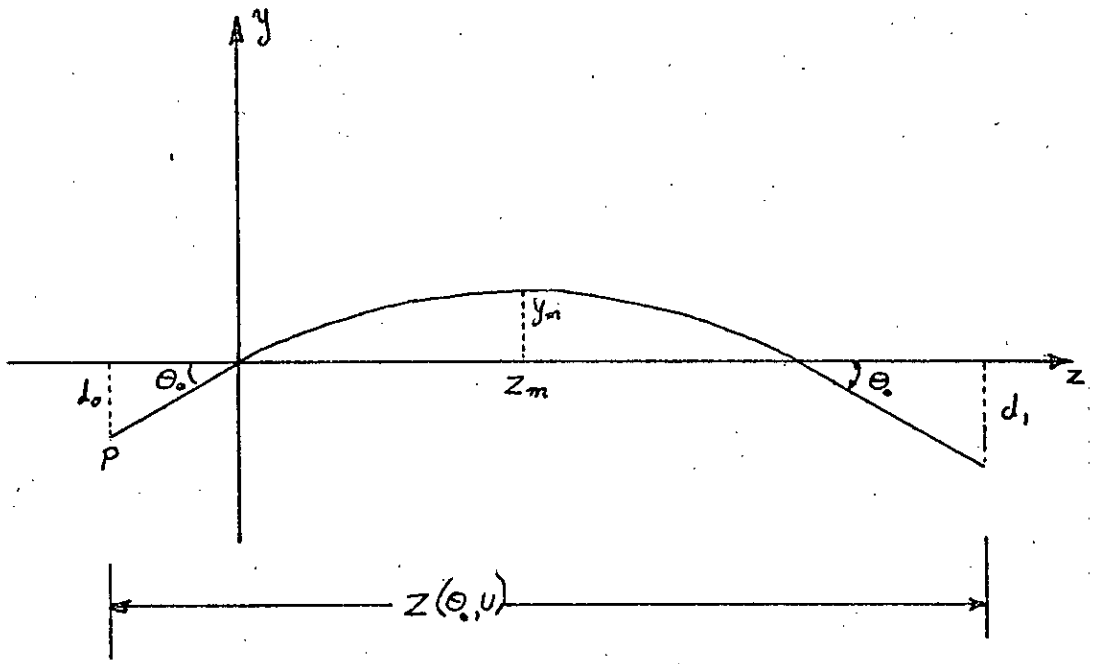

Figure 2.1

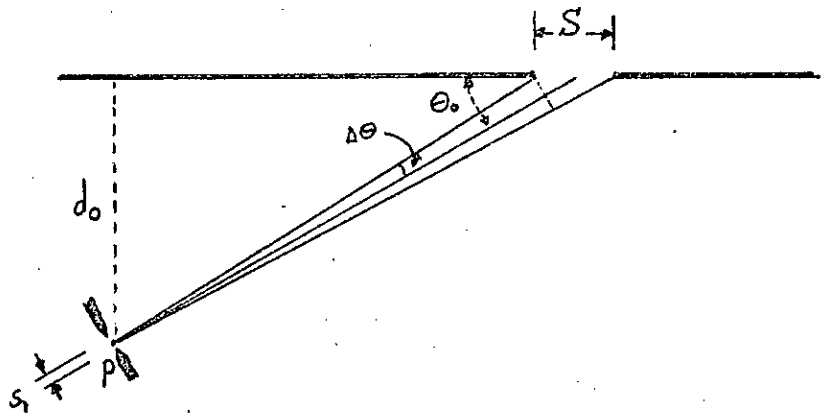

Figure 2.2

CHAPTER 2

THEORY OF THE EXPERIMENT

2.1 The Plane Mirror Electrostatic Energy Analyser - Ballistics

If an electron is emitted from a point source P, which is situated in a field free region, as it enters the half plane $y \geq 0$ in which there is a uniform electric field Ey parallel to the y axis, then the electron is subject to a constant acceleration a (see fig. 2.1)

where $a = -\frac{e\,Ey}{m}$

e being the electron charge and m the electron mass.

If time t = o at (zy) = (o,o) then the usual equations of trajectory can be written.

$$y = v_{oy}\,t - \frac{e\,Ey\,t^2}{2m}$$

$$z = v_{oz}\,t - \frac{e\,Ez\,t^2}{2m}$$

and as Ez = 0

$$z = v_{oz}\,t = v_o \cos\theta_o\,t$$

If the initial kinetic energy of the electron is eU

$$v_o^2 = \frac{2\,eU}{m}$$

To find the maximum penetration of the electron in the electric field

$$\frac{dy}{dt} = v_{oy} - \frac{eEy}{m}\,t$$

which gives a value of t_{max} and therefore a value of y_{max}

$$y_{max} = \frac{U}{Ey}\sin^2\theta_o$$

Similarly/

Similarly the other co-ordinate of this maximum position can be found

$$Z_{max} = \frac{U}{Ey} \sin 2\theta_o$$

The total distance from source to focus can be found

$$Z = Z_o + Z_i + 2Z_{max}$$

$$Z(\theta, U) = (d_o + d_1)\cot\theta_o + \frac{2U}{Ey} \sin 2\theta_o$$

If another electron of the same initial energy U leaves the source at a slightly different angle $\theta_o + \Delta\theta$ it will reach $y = d_1$ at a distance $Z(\theta_o + \Delta\theta, U)$

Using a Taylor expansion $Z(\theta_o+\Delta\theta,U)=Z(\theta_o,U)+\left(\frac{dZ}{d\theta}\right)_{\theta_o}\Delta\theta+\frac{1}{2}\left(\frac{d^2Z}{d\theta^2}\right)_{\theta_o}(\Delta\theta)^2 + \cdots$

First order focusing occurs if, in the first order approximation, $Z(\theta_o + \Delta\theta, U)$ is independent of $\Delta\theta$

i.e. $\left(\frac{dZ}{d\theta}\right)_{\theta_o} = 0$

By differentiation this condition becomes

$$\frac{Ey(d_o+d_1)}{4U} = \sin^2\theta_o \cos 2\theta_o$$

Thus for a given initial energy eU, there is a range of angles θ_o for which first order focusing occurs. Second order focusing will occur if, in addition, the condition

$\left(\frac{d^2Z}{d\theta^2}\right)_{\theta_o} = 0$ is satisfied.

That is if $\frac{Ey\,(d_o + d_1)}{4U} = 2\sin^4\theta_o$

First order and second order focusing conditions are simultaneously satisfied only if $\theta_o = 30^o$

From this the following useful relationships are obtained

$$\frac{U}{Ey} = 2(d_o + d_1)$$

$$y_{max} = \tfrac{1}{2}(d_o + d_1)$$

$$Z_{max} = \sqrt{3}\,(d_o + d_1)$$

$$Z(30^o, U) = 3\sqrt{3}\,(d_o + d_1)$$

The error due to the third order focusing effect is given by the fourth term of the Taylor expansion

$$\Delta Z_3 = \frac{1}{6}\left(\frac{d^3 Z}{d\theta^3}\right)_{\theta_o} (\Delta\theta)^3$$

If it is assumed that the higher order effects are very much smaller for small values of $\Delta\theta$, then effectively all electrons emitted from the point source P within the cone $\theta_o - \Delta\theta$ to $\theta_o + \Delta\theta$ will cross the plane $y = d_1$ at points $Z - \Delta Z_3$ to $Z + \Delta Z_3$. Thus, choosing a collector slit of width $2\,|\Delta Z_3|$ will allow the collection of most electrons emitted within the range $\theta_o \pm \Delta\theta$ assuming that all the electrons have the same energy. The required width of the collector slit for this condition turns out to be

$$2\,|\Delta Z_3| = 32(d_o + d_1)(\Delta\theta)^3$$

This implies that monoenergetic electrons emitted in the cone $\theta_o \pm \Delta\theta$ go to $Z \pm \frac{32}{2}(d_o + d_1)(\Delta\theta)^3$

2.2 The Plane Mirror Electrostatic Energy Analyser - Energy Resolution.

The following reasoning is similar to that used by Aksela et al (1970) in his study of an electron spectograph with coaxial cylindrical electrodes.

Consider the shift of the image of a point source formed at a fixed angle of incidence $\theta_o = 30^o$ if the energy of the incident electrons changes from U to $U \pm \Delta U$

$$\Delta Z(\theta_o, U \pm \Delta U) = \pm \frac{dZ}{dU} \Delta U = \pm D \frac{\Delta U}{U}$$

where the quantity $D = \frac{dZ}{dU} \cdot U$

This quantity is called the 'energy dispersion coefficient' of the analyser at the nominal energy U

If a slit of width s is considered to be in the image plane then the fractional energy spread in the transmitted beam is

$$R_{(s)} = \frac{\Delta U}{U} = \frac{1}{2} \frac{s}{D}$$

If it is considered once again that there is an angular spread $\pm \Delta\theta$ about the nominal angle of incidence θ_o but $\Delta U = 0$ then under second order focusing conditions, where $\theta_o = 30^o$, if a slit of width $2 \left| \Delta Z(\pm \Delta\theta, U) \right|$ is placed in the image plane, the initially divergent beam will be fully transmitted but the slit will allow a fractional energy spread

$$R_{(\Delta\theta)} = \frac{\Delta U}{U} = \frac{2 \left| \Delta Z(\pm \Delta\theta, U) \right|}{2 \quad D}$$

$$= \frac{1}{2 \times 3 D} \left| \frac{d^3 Z}{d\theta^3} \quad (\Delta\theta)^3 \right|$$

In general, if a point source emits an electron beam of angular spread $\pm \Delta\theta$ about the nominal angle $\theta_o = 30^o$ and there is/

is a slit of width s in the image plane, the resulting energy resolution is

$$\frac{\Delta U}{U} = R = R_{(\Delta\theta)} + R_{(s)}$$

$$R = \frac{1}{D}\left\{\frac{1}{2}s + \frac{1}{6}\left|\frac{d^3Z}{d\theta^3}(\Delta\theta)^3\right|\right\}$$

This result can be readily extended to the case of a source of finite width. If the source has a slit of width s_1 and a slit in the image plane has width s_2 then the previous considerations are valid to a point within the source slit and therefore the latter relationship will hold to the case of a finite source as well, provided s is replaced by $s_1 + s_2$

$$D = \left(\frac{dZ}{dU}\right).U = \frac{2U}{Ey}\sin 2\theta_o$$

$$= 2\sqrt{3}\,(d_o + d_1)$$

The aperture angle of the incident beam is defined by the geometry shown in fig. 2.2.

$$\Delta\theta = \frac{\frac{1}{2}S\sin\theta_o}{d_o/\sin\theta_o} = \frac{S}{8d_o}$$

From previous equations $\frac{1}{3}\frac{d^3Z}{d\theta^3} = 32(d_o + d_1)$

Substituting this and the relationships for D and $\Delta\theta$ in the equation for R gives

$$R = \frac{1}{4\sqrt{3}}\left\{\frac{s}{d_o+d_1} + \frac{1}{16}\left(\frac{S}{d_o}\right)^3\right\}$$

From this it is apparent that in the case of a small aperture S the third order focusing term makes very little contribution to the energy spread of the transmitted beam. The main obstacle to high resolution is/

is the finite size of the source and image slit rather than the spherical aberration. In fact, unless the contribution to R due to the finite slit widths is reduced considerably, the second order focusing contribution to the energy resolution of the analyser is unimportant. In practice, however, it is customary to make the two contributions comparable so that

$$\frac{S}{d_o + d_1} = \frac{1}{16}\left(\frac{S}{d_o}\right)^3$$

which would yield

$$R = \frac{1}{\sqrt{3}}\,\frac{s_1 + s_2}{2(d_o + d_1)}$$

This gives a theoretical value to the energy resolution of a plane mirror electrostatic energy analyser which has an entrance angle of 30 degrees.

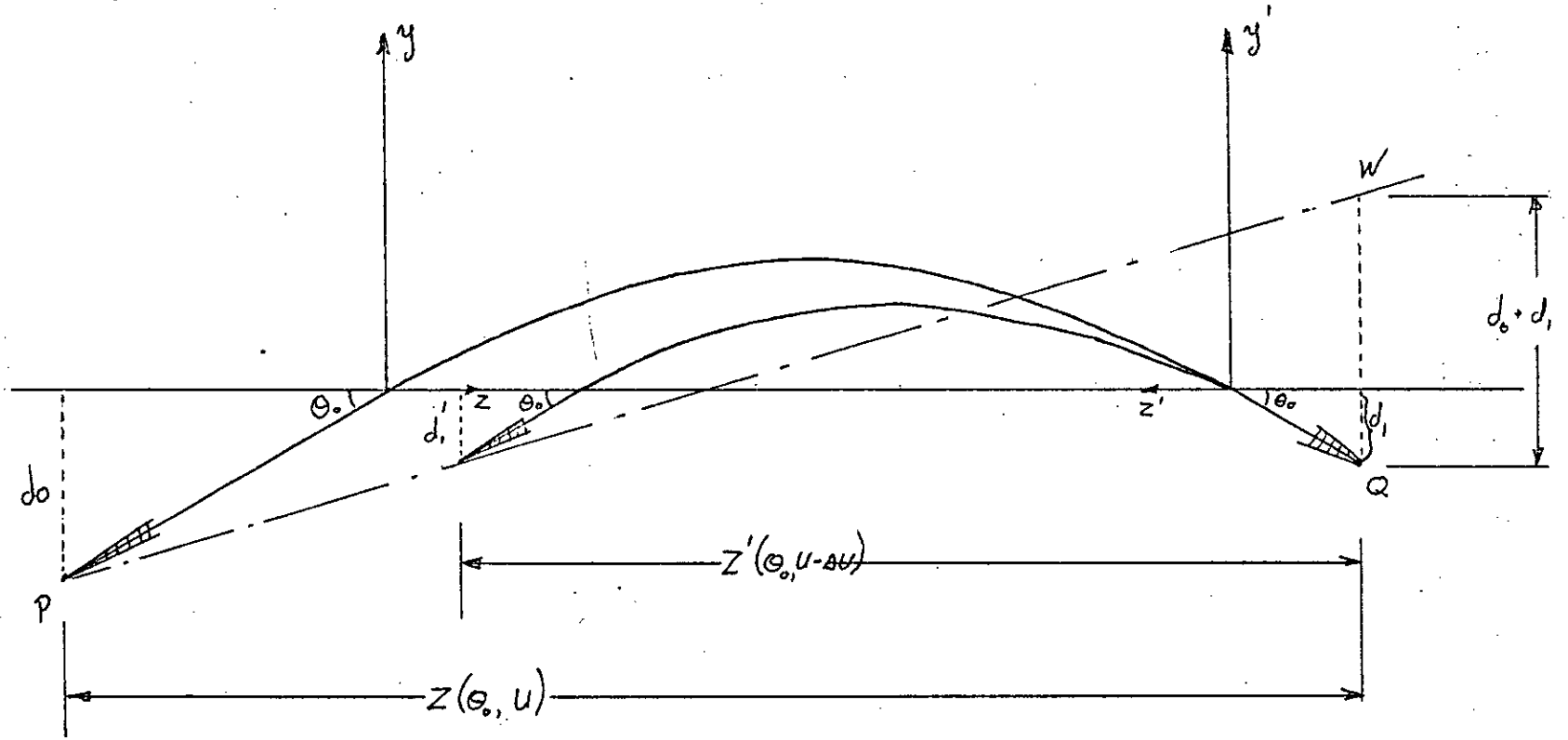
y
y'
W
$d_0 + d_1$
θ_0
z
θ_0
d_1
z'
θ_0
d_1
d_0
Q
P
$Z'(\theta_0, u-\Delta u)$
$Z(\theta_0, u)$

Figure 2.3

2.3 Analyser as an Instrument to Detect Backscattering

Suppose electrons leaving point source P and focusing on Q (Fig. 2.3) are inelastically scattered at 180 degrees to the incident direction then the motion of these scattered electrons is governed by all the previous considerations except that the source position is $y = d_1$. There is a different initial energy of these electrons of $U' = U - \Delta U$ where ΔU is the energy loss of the electrons due to the inelastic scattering, and the direction of the Z axis is reversed. For the backscattered beam the position of the focus at $y = d_1'$ can be found by the relationship

$$\frac{Ey\,(d_1 + d_1')}{U - \Delta U} = \frac{1}{2}$$

The value of Ey must be the same as that for the incident beam as the same analyser is used for both incident and backscattered beams.

$$Z'(\theta_o, U-\Delta U) = (d_o + d_1)\cot\theta_o + \frac{2(U - \Delta U)}{Ey} \sin 2\theta_o$$

which gives the other relationships

$$\frac{d_1 + d_1'}{d_o + d_1} = \frac{\Delta U}{U}$$

$$\frac{Z'(\theta_o, U - \Delta U)}{Z(\theta_o, U)} = 1 - \frac{\Delta U}{U}$$

$$\frac{d_1 + d_1'}{Z(\theta_o, U - \Delta U)} = \frac{d_o + d_1}{Z(\theta_o, U)}$$

On this basis, the position of the focus of backscattered electrons can readily be obtained for any energy loss $\frac{\Delta U}{U}$

For various energy losses the corresponding foci are located on a straight line as illustrated in figure 2.3.

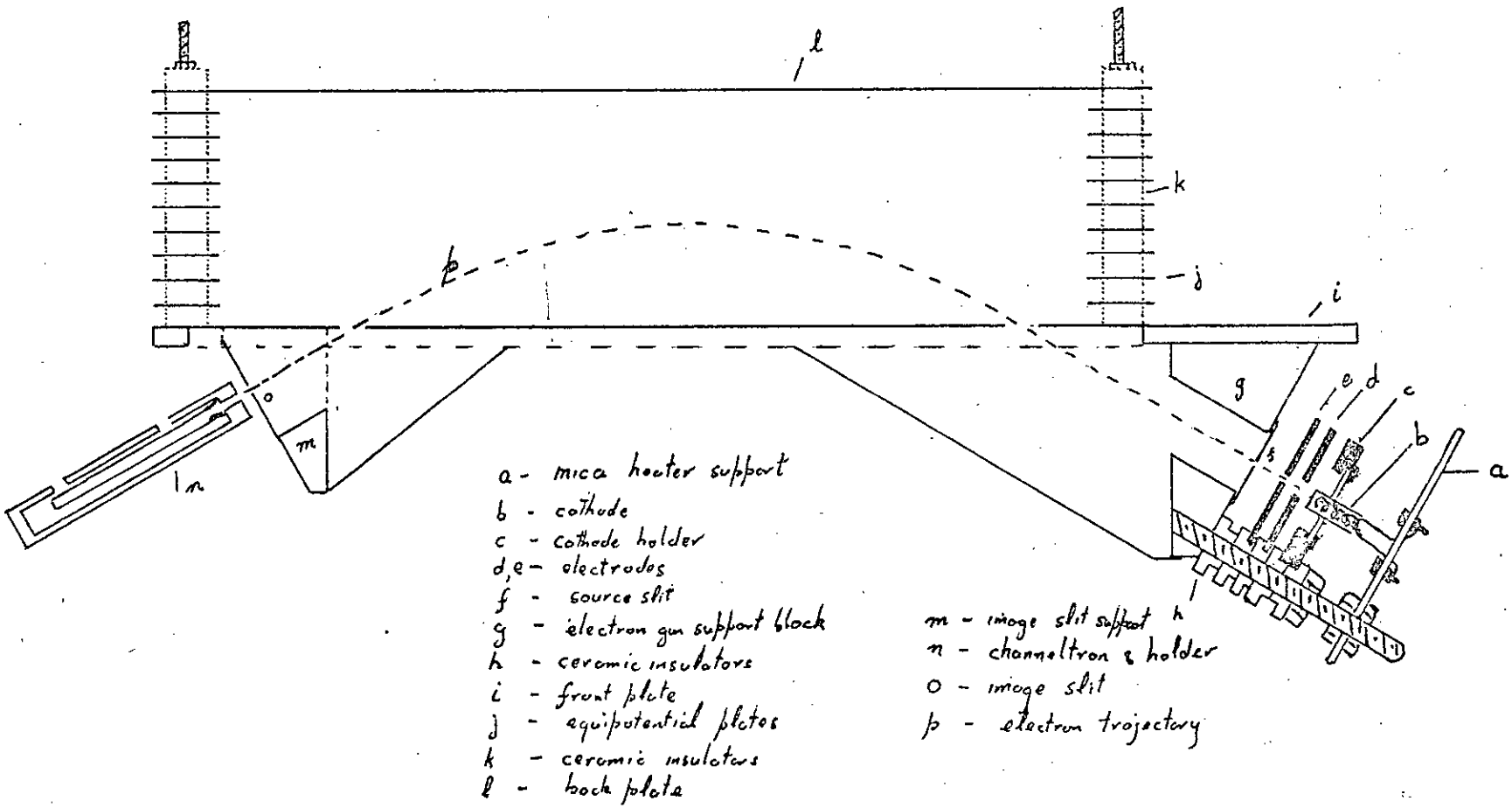
l
k
j
i
p
g
e
d
c
b
a
o
m
n
h
a - mica heater support
b - cathode
c - cathode holder
d,e - electrodes
f - source slit
g - electron gun support block
h - ceramic insulators
i - front plate
j - equipotential plates
k - ceramic insulators
l - back plate
m - image slit support
n - channeltron & holder
o - image slit
p - electron trajectory

Figure 3.1

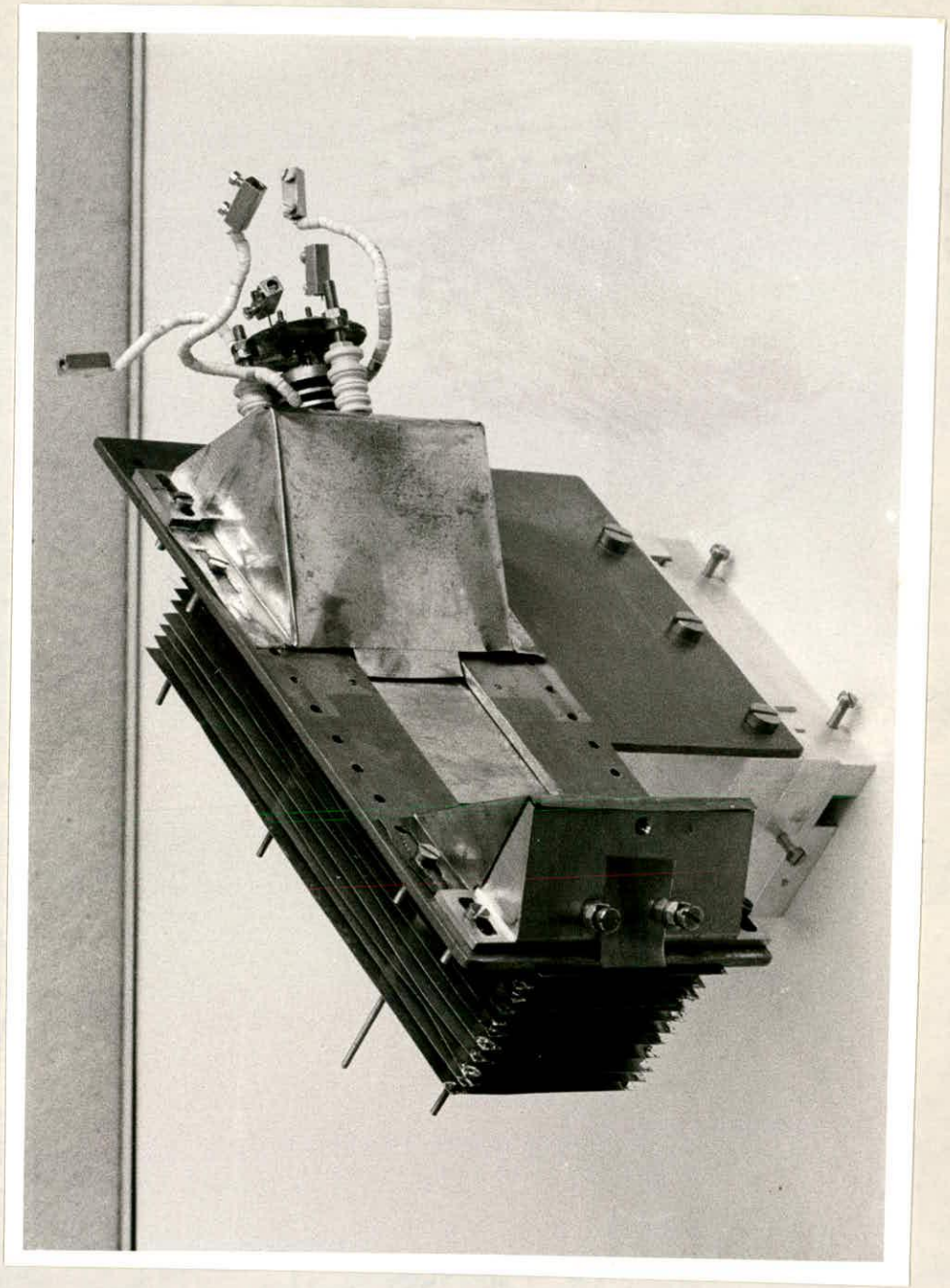

Figure 3.1a Analyser Assembly.

CHAPTER 3
THE APPARATUS

3.1 Plane Mirror Electrostatic Energy Analyser

The analyser shown in figure (3.1) consisted of a front plate, back plate and nine guard plates separated by stepped ceramic insulators and held together by eight 10 B.A. brass threaded rods inserted through the centre of the insulators at eight positions along the plates. These threaded rods were screwed to a 2.5 mm thick copper sheet which was in direct contact with the front plate. This sheet acted as a support for the electron gun and collector slit as well as being bolted to a system of slides, made from dural, which enabled the whole analyser assembly to be moved on the baseplate.

The front, back and guard plates were cut from 0.15 mm copper sheet to be 150 x 50 mm in size. Each plate had eight 4 mm diameter holes which fitted the steps in the ceramic insulators. The entrance and exit apertures in the front plate, as well as the large rectangular 130 x 30 mm holes in the guard plates were all made by spark machining. The back plate of course had only the holes for the ceramic insulators. The guard plates were equally spaced using the ceramic insulators and joined electrically by resistors in such a way that a voltage of ten percent of the total voltage between front and back plates was dropped between adjacent guard plates. In this way a uniform electric field was set up inside the analyser with no danger of external fields penetrating from the sides.

For reasons of space the value of Z max was taken to be 50 mm.

$$\therefore \quad d_o + d_1 = \frac{Z \text{ max}}{\sqrt{3}} = 28.9 \text{ mm}$$

d_o was chosen to be 20 mm and therefore d_1 was 8.9 mm.

The/

The maximum depth of penetration of the electron beam in the analyser could then be found

$$y_{max} = \tfrac{1}{2}(d_o + d_1) = 14.45 \text{ mm}$$

This meant that the back plate of the analyser had to be at least this distance from the front plate and so a distance of about twice this value was taken to ensure that there could be no appreciable electron scattering from the back plate. The distance between front and back plates was b taken to be 34.5 mm and then the voltage on the back plate Eb as a function of Ey was

$$Eb = 0.0345\ Ey$$

Given this voltage Eb then a beam of electrons passing through the analyser would have an energy of

$$U = \frac{Z_{max}\ Eb}{\sin 2\theta_o \times 0.0345} = 1.6735\ Eb$$

The source slit was made 0.26 x 1.0 mm and the image slit 0.2 x 1.85 mm giving a value of s_1 of 0.26 mm and s_2 0.2 mm.

Ignoring the apertures in the front plate, a value of energy resolution was

$$R = \frac{1}{\sqrt{3}} \frac{s_1 + s_2}{2(d_o + d_1)} = 0.00459 = 0.459\%$$

Therefore a theoretical size of entrance aperture S could be calculated, assuming the second order focus term to be of the same value as the source-image slit term.

$$S = d_o \left[16(s_1 + s_2)/(d_o + d_1)\right]^{\frac{1}{3}} = 12.68 \text{ mm}$$

A reduction of S would have little advantage yet a value of 6 mm was chosen as this was a convenient size when machining took place. The main result might be a reduction in transmitted intensity which is proportional to S for a possibly moderate gain in resolving power/

power.

Since focusing effects take place for trajectories which lie in a plane parallel to the electric field (the focusing plane), it is obvious that no similar effect will take place in the direction orthogonal to this plane. Velocity components of the electrons orthogonal to the focusing plane are not affected. Slit dimensions s_1, s_2 and S are therefore measured in the focusing plane and dimensions in the direction orthogonal to the focusing plane are arbitrary for measurements of energy resolution although consideration of fringing field effects is necessary.

The region in which the uniform field of the analyser will be disturbed is confined to the neighbourhood of the entrance and exit apertures. In the case of a narrow slit, this field extends along, and is symmetrical with respect to, the mid-plane along the slit as well as being normal to the plane of the slit. The depth of the disturbed region measured along the normal to the slit is of the same order as the width of the slit. Thus a long narrow slit acts as a cylindrical lens which has an effect on the electron velocity component perpendicular to the slit but has little effect on the electron velocity component parallel to the slit. The exceptions to this case are electrons which pass in the immediate vicinity of the slit ends.

From this it follows that the slits in the front plate of the analyser should be relatively long in the focusing plane and narrow in the direction at right angles to the focusing plane. This is important for the source side slit because the incoming electron beam is decelerated and the fringing field acts as a defocusing lens. To allow for any divergence of the beam at right angles to the focusing field/

field the output slit on the front plate of the analyser should be made slightly wider than the source side slit. In the region of this slit the field is slightly focusing and the overall effect of the two slits in the direction orthogonal to the focusing plane of the analyser should be slightly focusing. This situation is analogous to the symmetrical three aperture lens where the outer electrodes have the same potential and the central electrode is negative with respect to the outer electrodes. The front plate of the analyser is at earth potential and the back plate at some negative potential.

The source and image slits are in field free regions and therefore their dimensions in the direction orthogonal to the focusing plane of the analyser play no part in the performance of the system. In practice, however, it was thought not advisable to make these larger than the corresponding dimensions of the slits in the analyser front plate. These front plate dimensions are

source side aperture	6 x 1 mm
image side aperture	6 x 2.2 mm

The source and image slits were spark machined on 0.15 mm copper sheet and they were mounted on brass blocks which were machined such that the electron beam at an angle of 30 degrees would focus in the appropriate dimensions of the slits.

These blocks were mounted on the front support plate and copper sheets were manufactured to enclose the blocks and the front plate of the analyser so that a field free region was set up.

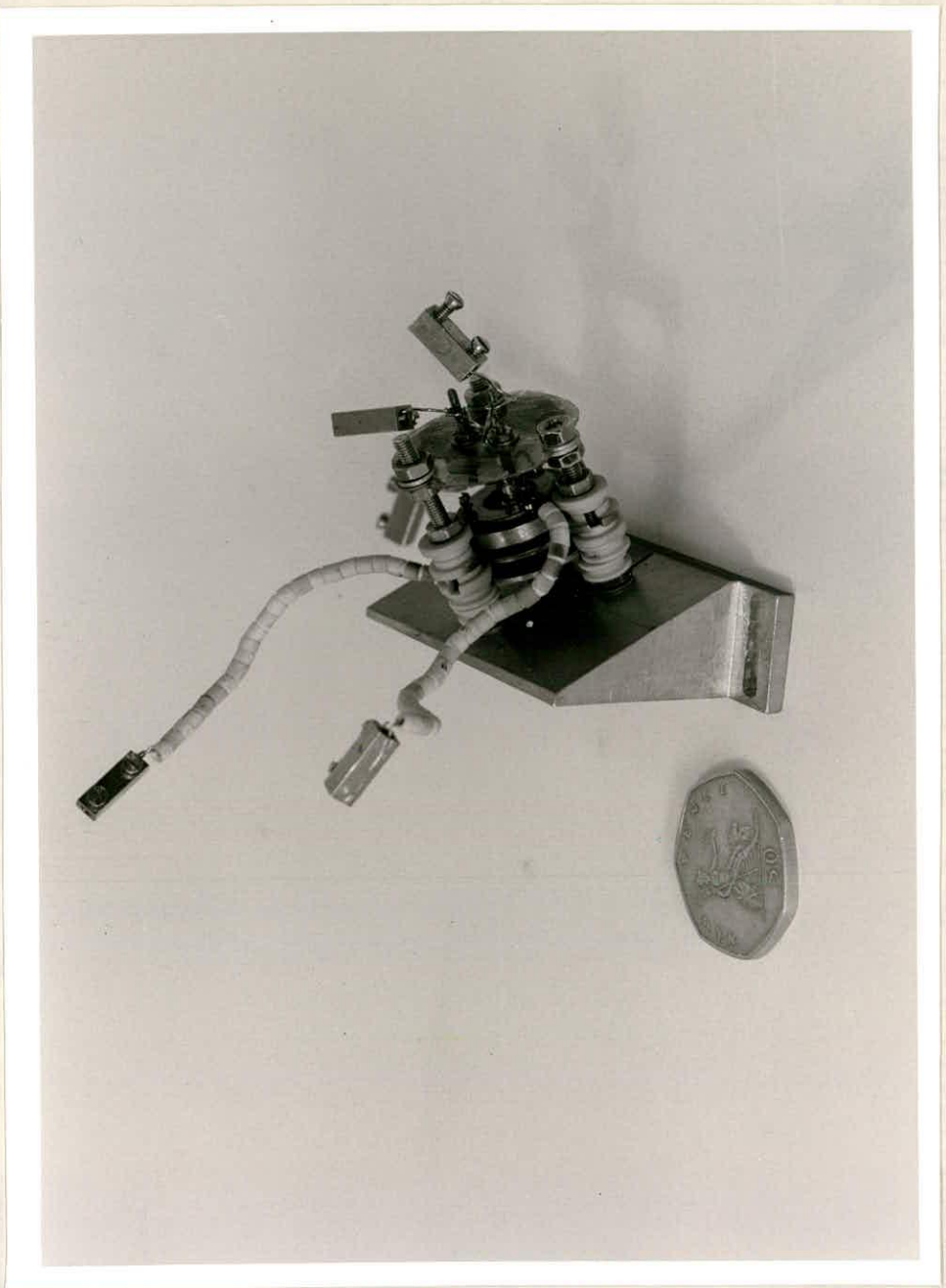

Figure 3.2 Electron Gun.

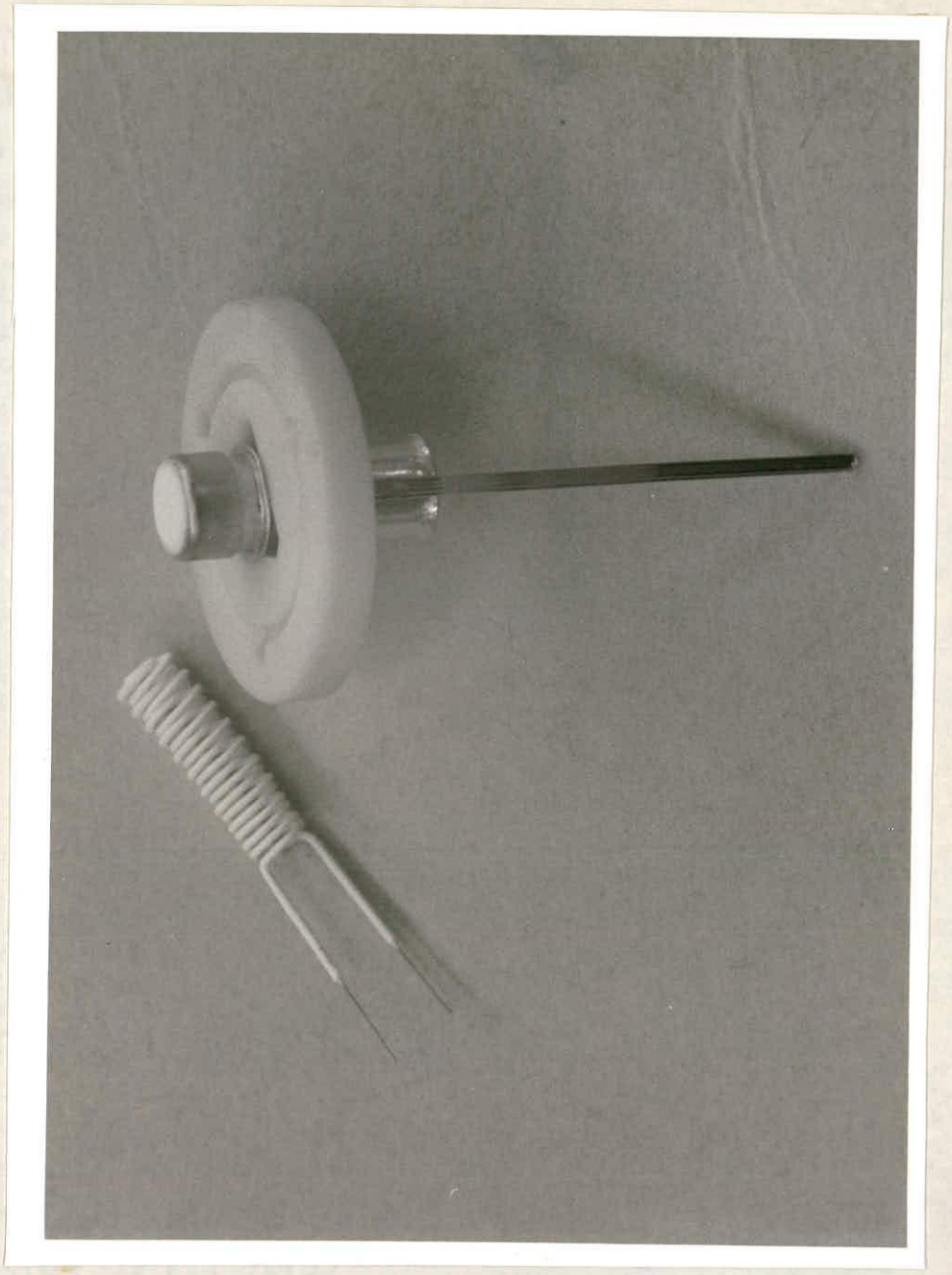

Figure 3.3 Cathode & Heater.

3.2 Electron Gun

The electron gun consisted of an indirectly heated oxide coated cathode, heater and two electrodes mounted on the same brass block that held the source slit. The electrodes were made from non-magnetic stainless steel, electrode d having a 2 mm diameter hole and electrode e a 1-5 mm diameter hole. (Figure 3.1). The cathode was mounted in a non-magnetic stainless steel holder which was designed to facilitate easy replacement of the cathode. The heater was spot welded to two stainless steel screws bolted to a sheet of mica. The electrodes, cathode and heater assemblies were mounted to the brass block using three M3 threaded rods and spacing was achieved using stepped ceramic insulators as shown in figure (3.2). The electrical contacts to the various parts were made by short lengths of nickel wire spot welded on.

The oxide coated cathode and heater were of the type used in 3WP cathode ray tubes. This meant that the cathode was supplied mounted on a ceramic disc as shown in figure (3.3). These cathodes were capable of being used more than once if care was taken to allow them to cool completely before exposed to the air, although the activation procedure had to be carried out each time before electron emission stabilised. The heater was of the insulated, bifilar type which meant that the cathode was of the equipotential type and there would be no stray magnetic field produced by the heater current.

The activation procedure carried out on the cathodes is described fully in appendix III.

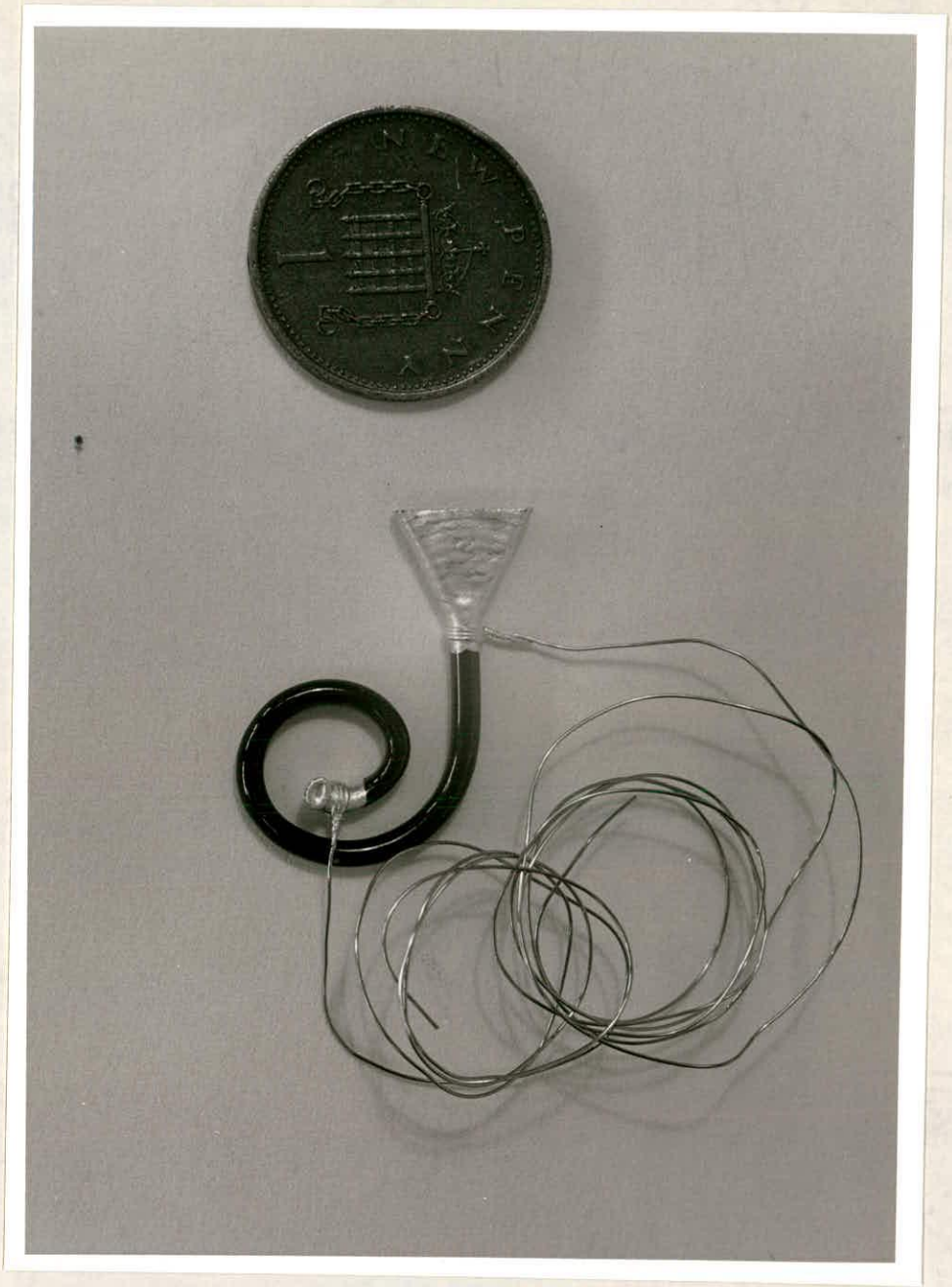

Figure 3.4 Channeltron.

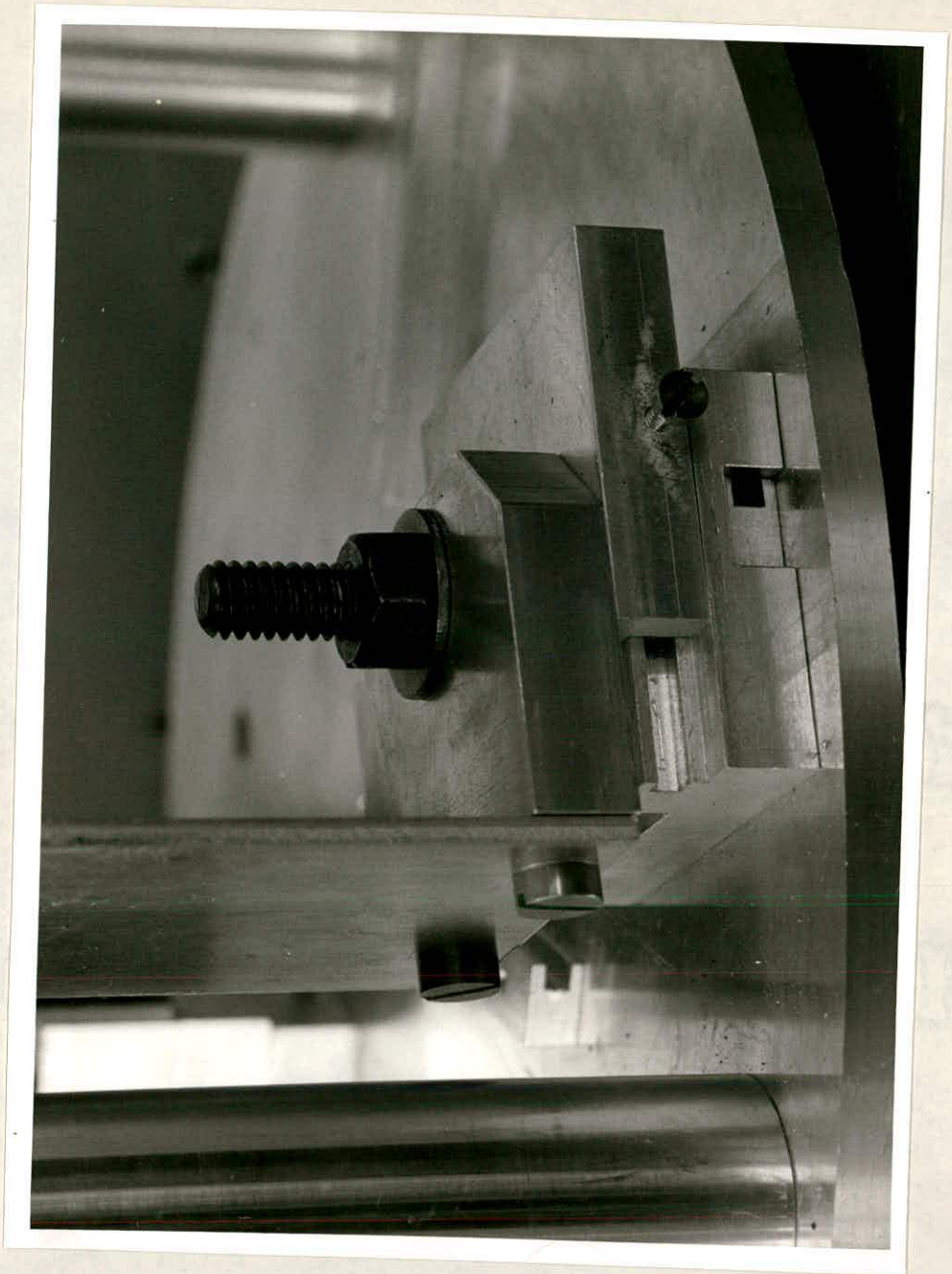

Figure 3.5 Sliding Mechanism on Baseplate.

3.3 Electron Detector

The detector was a channel electron multiplier (Channeltron) of the Mullard B312BL/01 type shown in figure (3.4). This was mounted on a sheet of mica and inserted in a copper box in such a way that the mouth of the channeltron was aligned with a small hole in the box. This box was mounted on a sliding jig which was attached to the baseplate so allowing the whole assembly to be positioned with respect to the analyser assembly (see figure 3.5). The lead to the closed end of the channeltron was screened and this screen connected to the open end of the channeltron which was at ground potential.

The channeltron was operated at about three kilovolts and this was applied through a charge sensitive preamplifier which was connected to the counting equipment. Pulses from the channeltron were fed to this preamplifier and from there to an amplifier then to the appropriate counting equipment.

Although this type of channeltron was used through most of the experiment a similar type of channel electron multiplier, developed in the Physics department of Edinburgh University by H.J. Stevens and E. Davidson, has also been used with considerable success. This channeltron had similar characteristics to the commercially available type but of course could be produced at much lower cost. Unfortunately the dimensions of the prototype were unsuitable for certain aspects of the experiment although at this present time smaller channeltrons are being developed.

3.4 Ancillary Apparatus

(a) Magnetic Shielding

Because of the low kinetic energy of the electrons passing through the analyser it is necessary to attain a condition of negligible magnetic field over the region in which the electron trajectories occupy. The presence of a magnetic field, even that caused by the earth's own magnetic properties, can cause the electrons to defocus and the plane mirror electrostatic energy analyser to behave completely "out of tune" with the theory already discussed.

The normal method of achieving a null magnetic field is to use three pairs of Helmholtz coils to cancel the field in the three dimensions involved. This approach was tried and found to be reasonably successful, however each pair of coils needed a stabilised d.c. supply adjustable independently of the others. To avoid this expense another method of shielding was adopted consisting of three layers of 0.05 mm thick Telshield wrapped around the 12" glass pipe section. To take advantage of the properties of this material to the greatest advantage overlapped joints were used and kinks in the material avoided. Each layer was interleaved with paper to take advantage of successive reflections at the shield boundaries in the case of a.c. shielding. As well as those layers of Telshield which formed a cylinder in the vertical direction, which is the direction orthogonal to the focusing plane of the analyser, a pair of Helmholtz coils was also used to help nullify the earth's magnetic field in this direction.

Measurements of magnetic flux density were made by a Hewlett-Packard milligauss meter and probe unit. With the top flange and analyser/

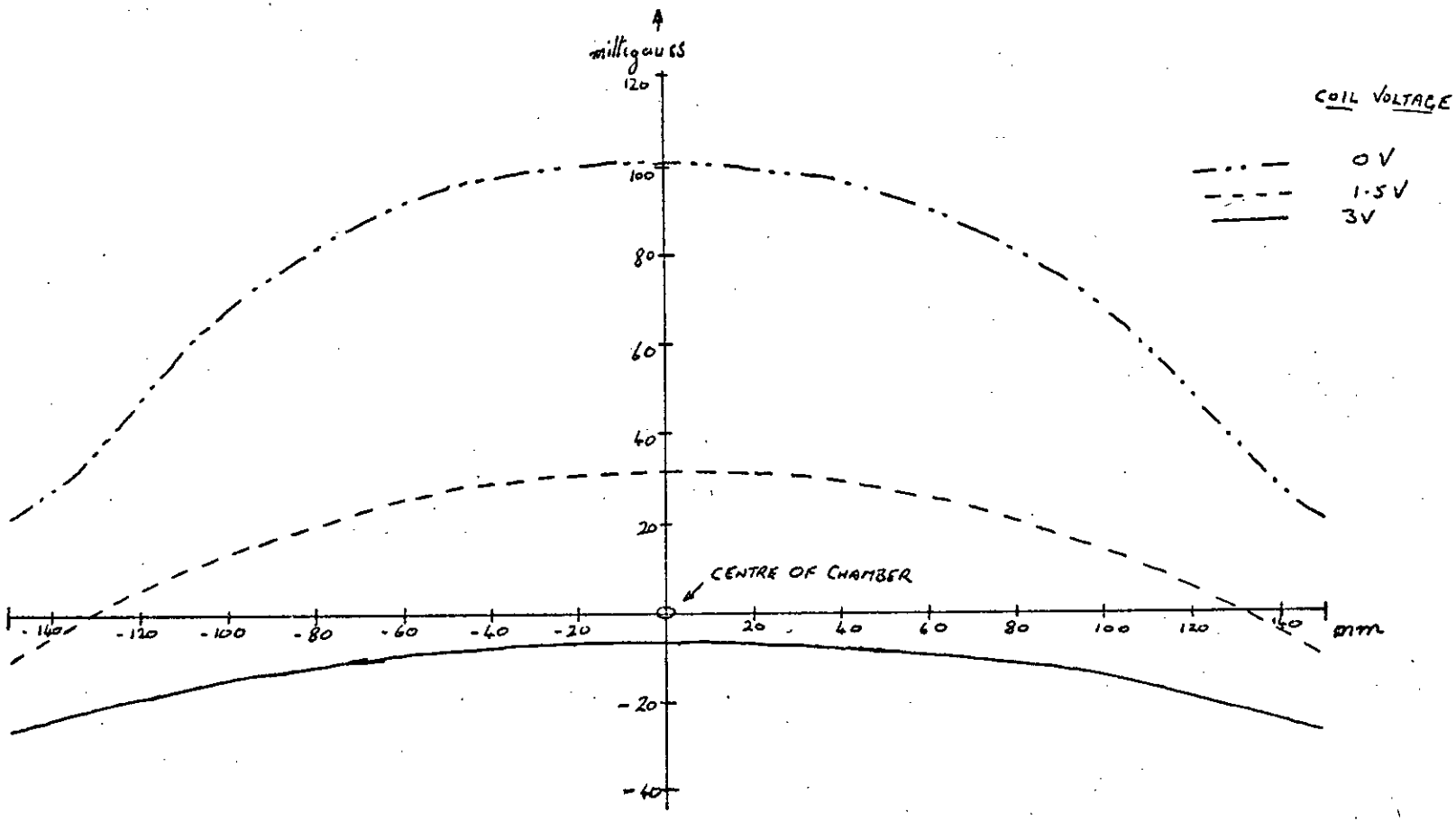

Figure 3.6 Magnetic Field Plot

analyser removed from the vacuum chamber, measurements were made of the magnetic field inside the chamber at the depth at which the electron beam passed through the analyser. These measurements were made diametrically across the chamber and the results are shown in figure (3.6). It can be seen that the Telshield alone does not reduce the residual field sufficiently, but by applying another magnetic field using the Helmholtz coils at 3 volts a reasonably uniform and for all intents and purposes negligible field can be obtained.

The power supply to control the current through the coils is shown in figure (AII.3). The circuit uses an operational amplifier to control the amount of current passed by a large power transistor which is the same current passed through the coils and a one ohm resistor which is on a heat sink. The 250 ohm potentiometer sets this value of current. Any small changes in this current will produce a change in the voltage dropped across the one ohm resistor. This is fed back to the operational amplifier which corrects this change in current and therefore the circuit is a stabilised current supply.

Coil dimensions - each coil

Radius - 400 mm

Number of turns - 52 of 22 s.w.g. enamelled copper wire

Resistance - 5.5 ohms.

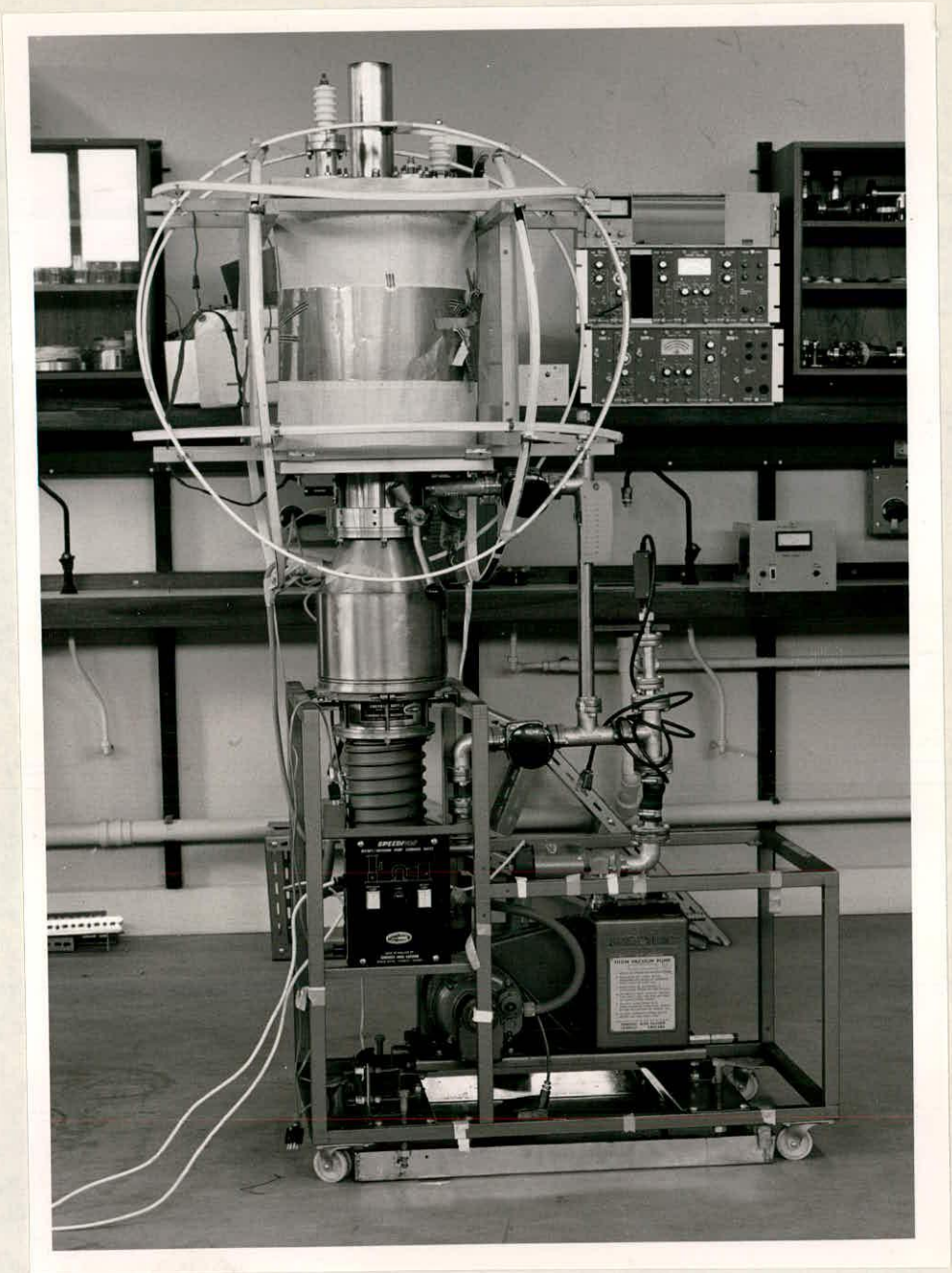

Figure 3.8 Vacuum System.

(b) The Vacuum System

The electron gun, analyser and channeltron were contained in a glass pipe section of nominal diameter 300 mm and length 450 mm sealed at the top by a dural plate to which the various feedthroughs were attached; the bottom being connected to a fairly fast pumping system consisting of an ES200 rotary pump, E04 water cooled oil diffusion pump, water cooled chevron baffle, liquid nitrogen trap and butterfly valve shown in figure (3.8). The rotary pump was connected to the system in such a way that it could "back" the diffusion pump and "rough" out the system independently. This greatly simplified any changes which were necessary inside the vacuum chamber as there was no need to allow the diffusion pump to cool down and therefore a great deal of time could be saved. The diffusion pump was filled with Santovac 5 fluid and the system was capable of attaining a pressure of 1×10^{-7} torr inside the glass chamber. Pressure was measured using an IG5G glass ionisation gauge.

There were several good reasons why a good vacuum was necessary; firstly it was essential that most of the air and gas molecules were removed as their presence could result in the scattering of the electrons; secondly the type of cathode used was susceptible to "poisoning" if the surrounding area contained any contaminants; thirdly any monolayer of hydrocarbon from the pumping oil could cause electrodes and surfaces with electrical potentials on them to behave in a peculiar fashion; fourthly the channeltron only operates satisfactorily at pressures below 1×10^{-4} torr.

The top dural flange had several electrical feedthroughs and a cold finger sealed to it using 1 mm diameter extruded indium wire. The cold finger was part of the system originally as a method of cooling/

cooling the mercury vapour cell in the inelastic scattering experiment but it also served to increase the pumping speed of the system. The baseplate containing the analyser and other parts was suspended from the top flange by three 25mm diameter dural rods and the whole assembly could be removed from the vacuum chamber in one piece.

All the components inside the vacuum system were made from non-magnetic materials and the insulators were of mica or ceramic which have a lower rate of outgassing than nylon, perspex or p.t.f.e. the use of which were avoided.

All the components, with the exception of the cathode, heater and channeltron, were cleaned first with trichloroethylene, then with acetone and dried in a stream of hot air. The channeltron could be cleaned using iso-propyl alcohol and being air dried at a temperature not exceeding 70° C.

The liquid nitrogen cold traps were filled using the automatic level controllers described later in the appendix. These units were developed and used in preference to the commercial units available. The commercial units were expensive and tended to waste a great deal of liquid nitrogen because they replenished the cold traps too often, having only one level detector. In the constructed type two level detectors, an upper and a lower, were found to be more economic in liquid nitrogen costs.

Similarly, in view of the expense and general unsuitability of commercially built units, a unit was built to protect the vacuum pumps and components in the case of failure of cooling water or system pressure. This unit is described in the appendix and proved invaluable in preventing expensive equipment being ruined.

CHAPTER 4

EXPERIMENTAL METHOD

4.1 Setting of basic experimental parameters.

The vacuum system was pumped until the system pressure was less than 2×10^{-6} torr. The cathode of the electron gun was then activated following the procedure described in the appendix. This was necessary after the cathode had been exposed to the air or if a new cathode was being used. The voltages for the electron gun were supplied by the unit described in the appendix. With the voltage on the cathode set to some predetermined value, the voltage on the first electrode (the one nearest the cathode) was set to the same value, or if the cathode was nearly exhausted, slightly positive with respect to the cathode. The voltage on the second electrode was normally fixed at +10V with respect to earth, which was found to be the setting which allowed a fairly high intensity of beam to enter the analyser. The voltage on the heater was normally about 6.8V when the cathode was new, but could be as high as 7.8V if the oxide layer on the cathode was nearly exhausted. All the voltages on the gun, as well as the voltage on the back plate of the analyser, were measured on a digital voltmeter and could be read to two decimal places.

The channel electron multiplier was normally operated at just over three kilovolts, the voltage being applied slowly to avoid breakdown in the charge sensitive preamplifier. This voltage was also decreased slowly before switching off.

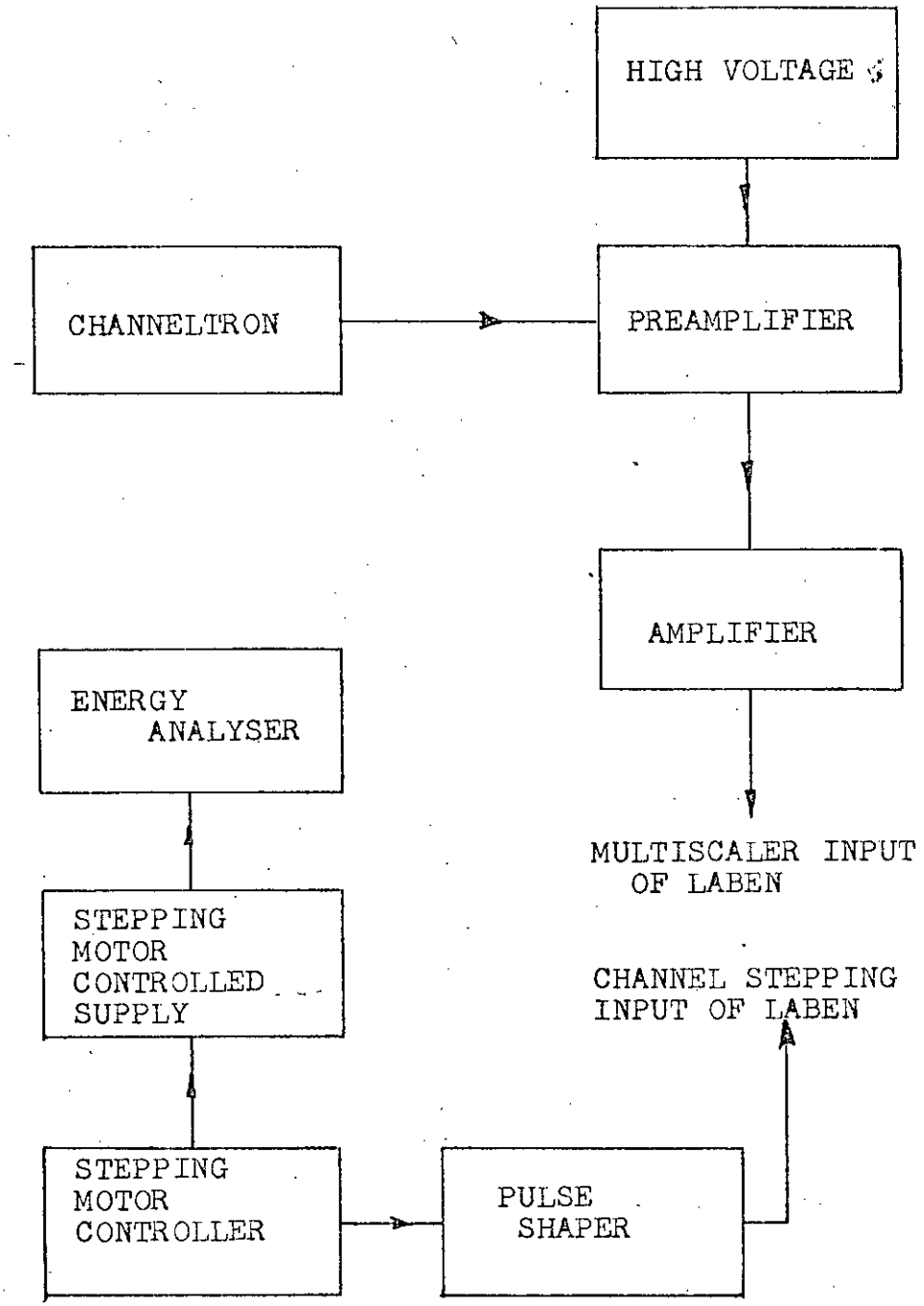

Figure 4.1 Method 1 of Data Collection

4.2 Data Measurement and Recording.

The back plate voltage (Eb), when varied, passes through the value required to deflect the beam, which has entered the analyser, out of the exit aperture and focuses it on to the collector slit. This procedure could be carried out manually by noting the back plate voltage (Eb) and recording the counting rate of the channeltron for all values of Eb.

To overcome this rather tedious task, two methods were developed which automated the collection of the data. The first method enabled Eb to be changed in steps from a low value upwards and the counting rate for each voltage to be recorded. The second method involved sweeping Eb at a constant rate upwards, then repeating sweeps and recording the counting rates for different values of Eb during these sweeps.

a) Method (1).

The cathode and electrode voltages are set to suitable values for the emission of a beam of electrons with energy U. The method of experimentally displaying the relationship between Eb and the counting rate obtained from the channeltron is illustrated in block diagram form in figure (4.1). The voltage supplied to the back plate of the analyser, the front plate being at earth potential, is controlled by a ten-turn potentiometer connected to a stabilised d.c. supply in such a way that the voltage developed across the potentiometer can be varied using two other potentiometers and the datum point of this voltage drop can also be varied. This means that with a d.c. supply of about 20 volts, a voltage variation using the main potentiometer of zero to 20 volts can be obtained; or a small variation of as low as under one volt with a starting

point anywhere between zero and 19 volts can also be obtained. This main potentiometer is driven by a small stepping motor, the controller of which is described in the appendix. The back plate voltage of the analyser can be varied by very small increments as the stepping motor does 48 steps for every revolution and so there are a total of 480 steps for the full range of the potentiometer, 400 of which are used in the recorded scan. The rate of stepping is also variable so that the rate of scan of the back plate voltage of the analyser can be slow to obtain long counting rates, or fast to do performance checks.

The stepping motor controller is also connected through a pulse correcting circuit to a multichannel analyser (Laben) in such a way that every time the motor advances a step, the Laben advances a channel up to its maximum of 400 channels then switches to the stop mode. The Laben is set up in the multiscaler mode so that signals collected from the channeltron are amplified and counted in channel 0 for a certain length of time, determined by the stepping motor controller, then when the stepping motor steps, the signals are counted in channel 1 and so on up to channel 399. The analyser back plate voltage at channel 0 and channel 399 is noted so that a linear scale of Eb can be set up along the X axis of the Laben. As the counts in the various channels of the Laben are directly related to the number of electrons focused on the image slit of the analyser, then a graphical display of electron intensity against deflecting voltage for an electron beam emitted from the gun is obtained. This display can be transferred to an X-Y recorder, typed in numerical fashion, or recorded on punch

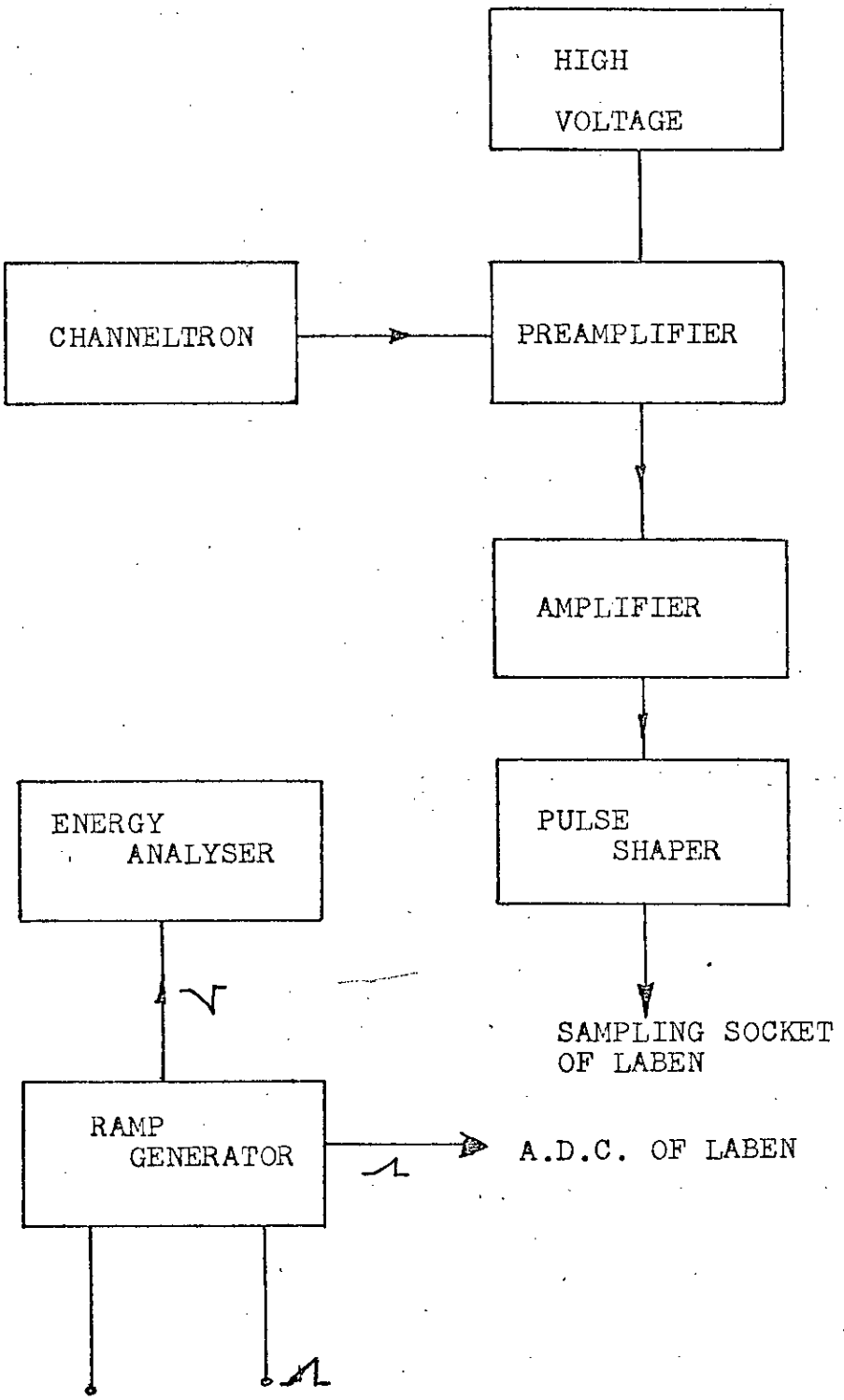

Figure 4.2 Method 2 of Data Collection

tape for computer analysis.

There is also the facility of switching out the stepping motor driven potentiometer and switching in an ordinary potentiometer so that the deflecting voltage can be varied manually and its effect on the count rate observed on an oscilloscope or ratemeter.

Advantages:- 1) The value of Eb at any time during the scan can be monitored by the digital multimeter.

2) The range of Eb swept can be very small or up to the maximum available.

Disadvantages:- 1) If any change in experimental parameters occurs during the scan, which is normally set for 15 minutes, then the run had to be repeated.

2) The data collected could not be monitored during the run.

3) At the end of the scan the stepping motor controlled potentiometer had to be switched off manually after 400 steps exactly.

b) Method (2).

The method of data collection shown in block diagram form in figure (4.2) involves the use of a linearly variable voltage (ramp voltage) on the back plate of the analyser and a directly proportional voltage to address the analogue to digital converter (A.D.C.) of the Laben. The counts from the channeltron are amplified and fed through a pulse shaping network before being connected to the sampling input of the Laben. This in effect means that at any instant in time, pulses counted by the channeltron for

a specific value of Eb will be recorded in a channel of the Laben corresponding to the voltage level of the ramp function in the A.D.C. at that time. The values of Eb corresponding to channel 0 and channel 399 are noted and the same type of display as in method (1) is obtained and can be extracted from the Laben in both analogue and digital forms. The ramp function can be obtained externally from the X output of a cathode ray oscilloscope, or internally from the unit described in the appendix.

Advantages:-

1) The scanning of the back plate voltage can be continued for very long counting times and any change in experimental parameters might be statistically averaged.

2) A constant monitoring of the results being recorded could be carried out using the "live display" mode.

Disadvantages:-

1) The range of Eb swept could not be varied to such narrow values as in method (1), so that most scans were taken between 1.0 and 10.5 volts for Eb.

CHAPTER 5

EVALUATION OF RESULTS.

All the measurements were produced in the form of graphs of number of counts from the channeltron against analyser back plate voltage for given values of voltage on the cathode.

5.1 Electron Ballistics.

The peak of each curve obtained was taken to correspond to the value of back plate voltage, Eb, which allows the most electrons to be transmitted through the analyser and then focused on the image slit. Typical graphs obtained using both methods (1) and (2) of data collection are shown in figures (5.1 & 5.2), but with method (1) being used to obtain graphs of the important part of the scan; i.e. in the region of the peak. By plotting the value of back plate voltage (Eb) at which the maximum counting rate occurs against the voltage on the cathode (U_k) for the same heater voltage and the same cathode but various values of cathode voltage, a graph is plotted as in figure (5.3). In all cases, with the results obtained, a straight line can be drawn through the plotted points. The slope of this line gives the ratio of Eb to the energy of the electrons entering the analyser and being focused on the image slit. It is apparent that this line does not pass through the origin and therefore the voltage applied to the cathode is not the actual energy (U) of the electrons leaving the electron gun. The difference between U_k and U is the voltage required to move the electrons from just inside the cathode surface to just outside the cathode surface. This is the 'contact potential' (Beck:1953) and is denoted by ϕ. In the case of an oxide coated cathode ϕ can vary from less than 1 volt upwards, depending on

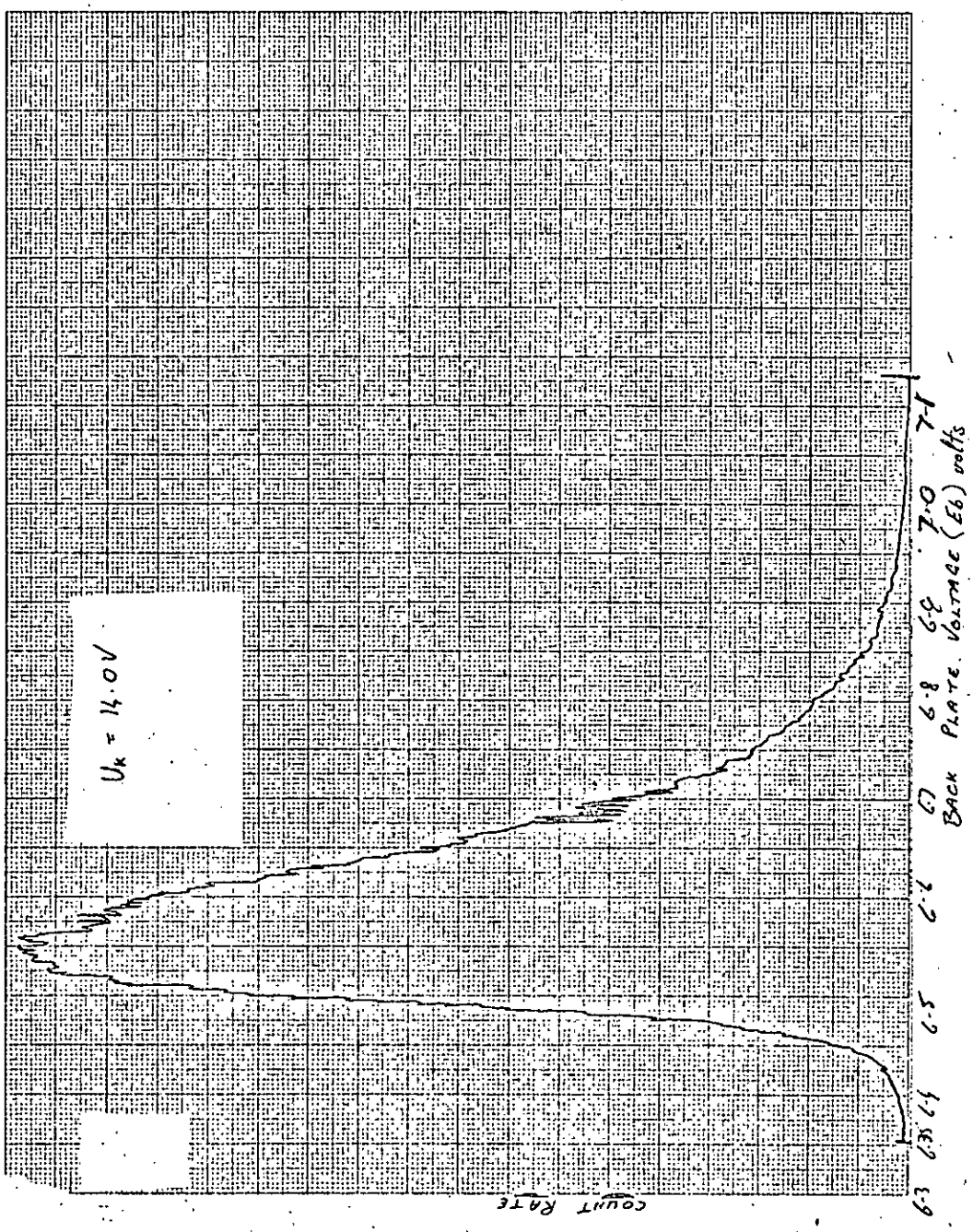

Figure 5.1 Result Obtained Using Method (1)

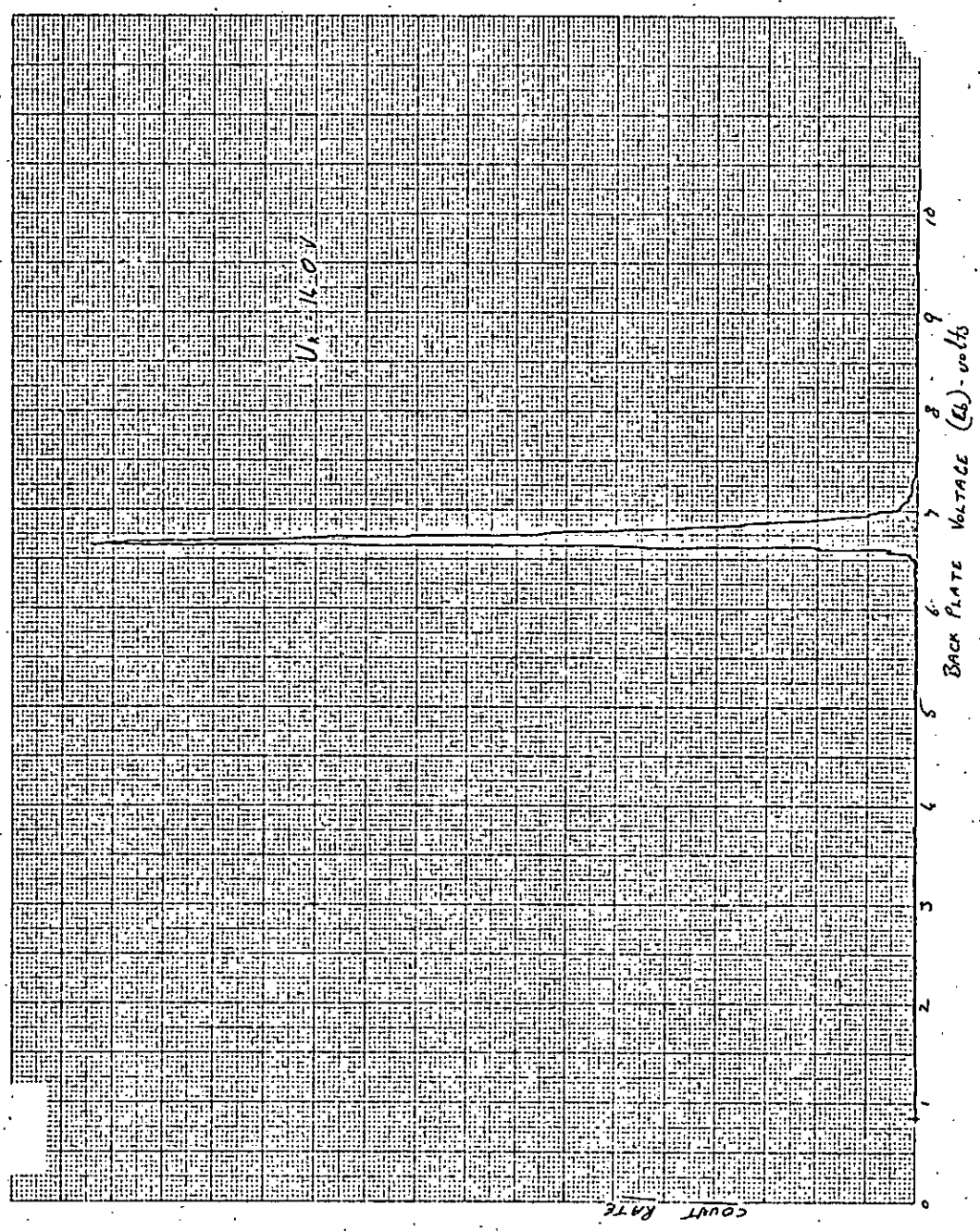

Figure 5.2 Result Obtained Using Method (2)

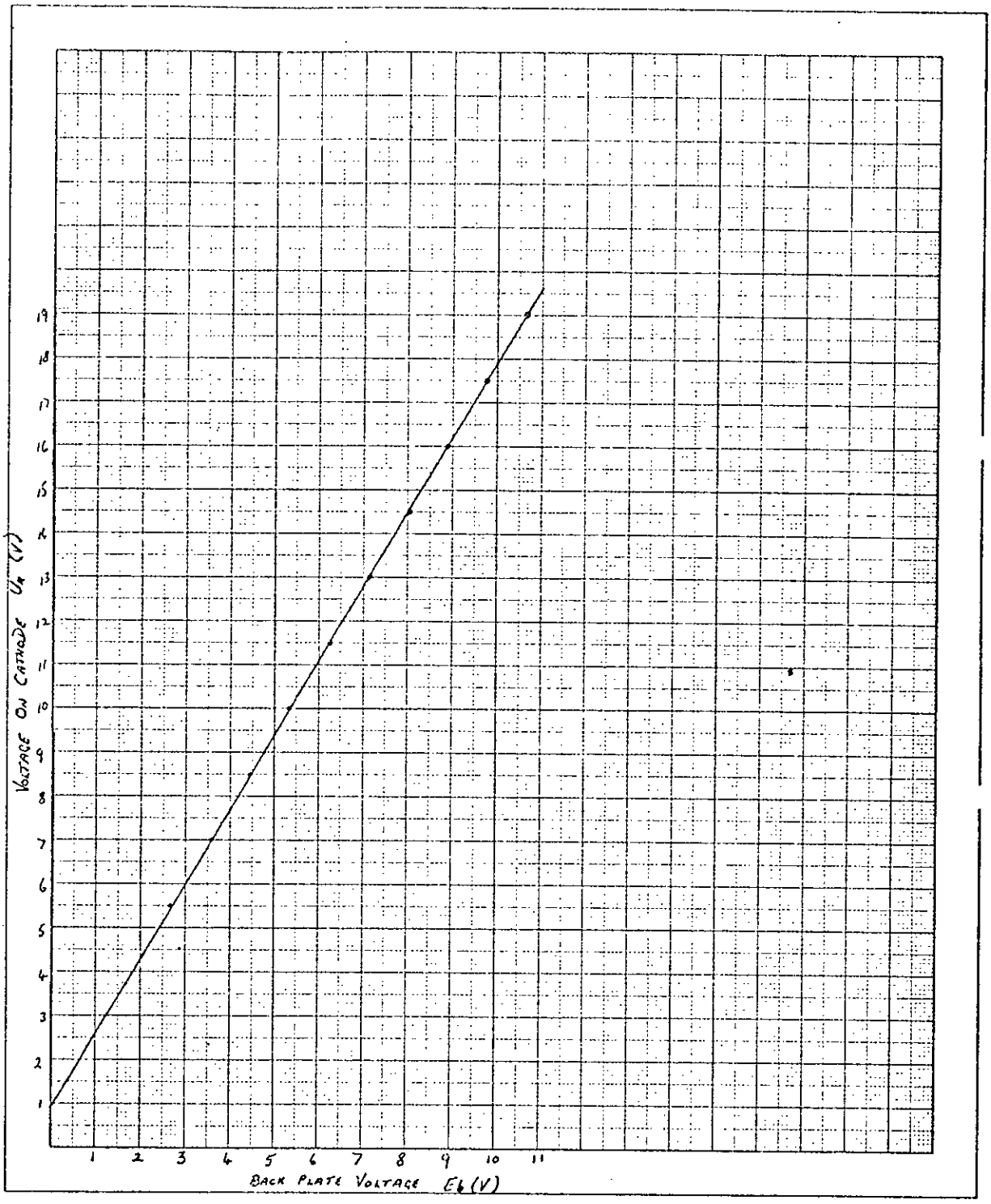
VOLTAGE ON CATHODE U_k (V)
BACK PLATE VOLTAGE E_b (V)
1
2
3
4
5
6
7
8
9
10
11
12
13
14
15
16
17
18
19

Figure 5.3

the condition of the cathode surface. In fact, values of ϕ as high as 2.5 volts were measured although these occured when the oxide layer was very thin. Of the various experimental runs taken, the relationship between Eb and U agreed with the theoretical value to within a few percent. For this particular part of the experiment, method (2) of data collection could be used because only the position of the peaks were taken into account, although by using method (1) the same results were obtained. However, when method (1) was used, the curves obtained were conspicuously assymetric and so the following procedure was carried out to investigate these shapes.

5.2 Interpretation of shapes of measured spectra.

The various mathematical steps for the following discussion can be found in the appendix.

Electrons emitted from a hot cathode have a distribution of speeds which is well approximated by the Maxwell distribution law.

$$n(u)du = \left(\frac{4N}{\sqrt{\pi}}\right)\left(\frac{m}{2kT}\right)^{\frac{3}{2}} u^2 e^{\frac{-mu^2}{2kT}} du$$

$$= \text{constant} \times u^2 e^{-\frac{1}{2}m\lambda u^2} du$$

Then the probability that an electron in a beam subtending unit solid angle has a velocity between u and u + du is given by

$$p(u)du = C' u^2 e^{-\frac{1}{2}m\lambda u^2} u\, du$$

C' is a normalisation constant chosen such that

$$\int_0^\infty p(u)du = 1$$

As the plane mirror electrostatic energy analyser measures energy, an expression for energy distribution is required such that $p(u)du = p(U)dU$. Such a distribution can be written as

$$p(U)dU = C\, U\, e^{-\lambda U} dU \qquad \text{where } U \geq 0$$

C is a normalisation constant numerically different from C'. λ is dependent on the cathode temperature, work function and space charge conditions and, although its precise value is not required for the present, it is noted that λ has the dimension of $(\text{energy})^{-1}$. This equation for energy distribution describes an asymmetric distribution of which the mean energy $\langle U \rangle$ and the standard deviation $\langle \Delta U^2 \rangle$ (mean square deviation) can be calculated.

$$\langle U \rangle = \frac{2}{\lambda} \quad ; \quad \langle \Delta U^2 \rangle = \frac{2}{\lambda^2}$$

If the analyser had infinitely good resolution then these two quantities could be measured, because the mean and the mean square deviation could be obtained from the measured data. The problem, however, is to disentangle the spread of the energy spectrum due to the nature of the thermionic emission dealt with so far, from that arising from the finite resolution of the analyser.

A "generating function" for the probability distribution of the electron energies is now introduced and this is the Laplace transform of this equation.

$$\mathcal{L}(v) = \int_0^\infty e^{vU}\, p(U)dU = C\int_0^\infty U\, e^{-(\lambda - v)U}\, dU$$

When the integral is evaluated, then

$$\mathcal{L}(v) = \frac{\lambda^2}{(\lambda - v)^2}$$

The natural logarithm of this function is called the logarithmic generating function.

$$H(v) = \ln \mathcal{L}(v) = 2\ln\lambda - 2\ln(\lambda - v)$$

The important property of this function is that its consecutive derivatives with respect to v, taken at v = 0, can be used to calculate the "central moments" of the distribution. In particular

$$\left(\frac{dH}{dv}\right)_{v=0} = \langle U \rangle$$

and

$$\left(\frac{d^2H}{dv^2}\right)_{v=0} = \langle \Delta U^2 \rangle$$

When considering the effect of the finite resolution of the energy analyser on the observed results it is assumed that the analyser has a Gaussian "instrument function". This means that if the analyser is set or tuned to transmit electrons of energy U_0 then the probability of observing an incident electron of energy U is given by

$$g(U - U_o) = K\, e^{-\frac{(U - U_o)^2}{2\sigma^2}}$$

The factor K is a normalisation constant such that

$$\int_{-\infty}^{\infty} g(U - U_o)dU = 1$$

This Gaussian distribution has its mean at U_o

$$\langle U \rangle = U_o$$

and the mean square deviation is $\langle \Delta U^2 \rangle = \sigma^2$

Introducing a generating function as before

$$\mathcal{L}(v) = K \int_{-\infty}^{\infty} e^{vU}\, g(U - U_o)dU$$

which gives $\mathcal{L}(v)' = e^{(U_o v + \frac{1}{2}\sigma^2 v^2)}$

The logarithmic generating function becomes

$$H(v) = U_o v + \tfrac{1}{2}\sigma^2 v^2$$

The first two central moments of the distribution become

$$\left(\frac{dH}{dv}\right)_{v=0} = U_o \; ; \qquad \left(\frac{d^2H}{dv^2}\right)_{v=0} = \sigma^2$$

Having now manipulated the Maxwellian distribution of the emitted electrons and the Gaussian distribution inherent in the energy analyser the problem now is to see how the observed spectrum from the results arose and how it can be described.

Suppose the electrons emitted from the cathode are accelerated to an energy U_a. Then the probability that an electron of energy $U_a + U$ enters the analyser is

$$p(U_a + U) = p(U) = C\, U\, e^{-\lambda U}$$

i.e. electrons entering the analyser have the same probability of occurence as electrons being emitted from the cathode.

The property of the analyser leads to an energy spectrum different from $p(U_a + U)$ in that it is a convolution of $p(U_a + U) = p(U)$ with $g(U - U_o)$. This spectrum is observed by scanning the nominal energy of the analyser and observing the convoluted spectrum on the U_o scale.

Then the probability of an electron of energy U, emitted from the cathode and accelerated to an energy (U_a+U), getting through the analyser set to accept electrons of energy U_o is

$$P(U_o) = \int_{-\infty}^{\infty} p(U)\, g(U_o - U)\, dU$$

The generating function for $P(U_o)$ is

$$\mathcal{L}(v) = \int_{-\infty}^{\infty} e^{vU_o} P(U_o) dU_o$$

$$\mathcal{L}(v) = \int_{-\infty}^{\infty} e^{vU_o} \int_{-\infty}^{\infty} p(U)\, g(U - U_o) dU dU_o$$

$$= \int_{-\infty}^{\infty} e^{vU} p(U) dU \int_{-\infty}^{\infty} e^{vA} g(A)\, dA$$

where $A = U_o - U$

If this generating function is called $\mathcal{L}_{P(v)}$ and noting that the first integral on the right hand side is a generating function as is the second integral, then

$$\mathcal{L}_{P(v)} = \mathcal{L}_{p(v)}\, \mathcal{L}_{g(v)}$$

or forming the logarithms

$$H_{P(v)} = H_{p(v)} + H_{g(v)}$$

Hence the mean and mean square deviation can be obtained by differentiating this with respect to v. Denoting the observed mean energy by $\langle W \rangle$ and the mean square deviation by $\langle \Delta W^2 \rangle$

$$H_{P(v)} = 2 \ln \lambda - 2 \ln(\lambda - v) + \tfrac{1}{2}\sigma^2 v^2$$

Taking account of the acceleration to U_a

$$\langle W \rangle = \frac{2}{\lambda} + U_a$$

$$\langle \Delta W^2 \rangle = \frac{2}{\lambda^2} + \sigma^2$$

The nature of the analyser is such that it gives a constant fractional resolution, i,e. the ratio of the mean spread of the transmitted spectrum to the mean of the transmitted energy is constant.

$$\frac{\sigma}{\langle W \rangle} = R = \text{constant}$$

and therefore $$\langle \Delta W^2 \rangle = \frac{2}{\lambda^2} + R^2 \langle W \rangle^2$$

The factor $2\lambda^{-2}$ is an energy spread characteristic of the electron gun; it may change slightly with different settings of the electrode potentials because they affect the space charge conditions; it may be affected by uncontrollable changes in the work function of the cathode and by small changes in cathode temperature. If, however, these conditions vary within a range which keeps λ virtually constant, then from the previous equation the mean square width $\langle \Delta W^2 \rangle$ as a function of the mean energy squared $\langle W \rangle^2$ gives a straight line, the slope of which is the square of the percentage resolution of the analyser. The extrapolated intercept gives the mean square of the thermal spread of the incident beam.

Linear relationships between the width of the observed spectrum and the mean energy can only be expected if in the range of measurement

$$\frac{2}{\lambda^2} \ll R^2 \langle W \rangle^2$$

This would be the case if the electrons had an incident energy greater than about 100 eV with a cathode temperature of approximately 1200 ^{o}K. Then the resolution of the analyser would be the slope of the line obtained when the half widths of the spectra were plotted against the energy of the electron beam (Harrower:1955). In this case the intercept is vanishingly small, the spectrum is of Gaussian shape, so that the mean and peak of the spectrum coincide and the thermal spread is negligible. In the low energy range in which the present analyser is working this is not the case.

5.3 Calculation of Resolution.

The measured energy spectra obtained from the Laben using method (1) of data collection were reproduced graphically and also on punch tape. Each set of data was run through a computer program to help to evaluate the mean observed energy $\langle W \rangle$ and the standard deviation $\langle \Delta W^2 \rangle$. The results obtained from the computer established the mean value of the curve by denoting the value of Eb at which it occured by a channel number X. The extent of each scan was known (M), and the number of channels used in that scan was N. This gave a channel step size for a scan of M/N. The start of the scan (E_1) was known and therefore the position of back plate voltage $\langle E \rangle$ for the mean observed energy was

$$\langle E \rangle = E_1 + \frac{X\,M}{N}$$

The ratio between Eb and the electron energy U was known by using the results from 5.1 and therefore the observed mean energy was

$$\langle W \rangle = \frac{U}{Eb} \langle E \rangle$$

Similarly the value of mean square deviation of the measured spectrum was in channel numbers (Y^2) and so the mean square deviation of the back plate voltage was

$$\langle \Delta E^2 \rangle = \left(\frac{M}{N}\right)^2 Y^2$$

The mean square deviation of energy can be found

$$\langle \Delta W^2 \rangle = \left(\frac{U}{Eb}\right)^2 \langle \Delta E^2 \rangle$$

The values of $\langle W \rangle^2$ against $\langle \Delta W^2 \rangle$, for the same cathode and same heater voltage, were plotted and the best straight line fitted to these points using the method of least squares. From this the resolution R and the thermal spread of the beam were found as described in section 5.2.

RUN (1) Figures (5.4 to 5.11)

Heater voltage = 7.50 volts

Cathode Voltage U_k	19	16.5	14	11.5	9	6.5	Volts
Peak value of Eb	10.63	9.175	7.71	6.24	4.73	3.27	Volts

Graph plotted shown in figure(5.4)

By method of least squares:-

Slope of line = $\frac{U}{Eb}$ = 1.6955

Intercept on axis = contact potential = 0.951 volts

From computer print out & graphs (see text).

X	Y	M	N	E_1	$\langle W^2 \rangle$	$\langle \Delta W^2 \rangle$
153.5	71.8	0.77	400	10.41	329.5	0.0549
148.3	63.4	0.78	400	8,95	245.4	0.0439
161.7	60.3	0.77	400	7.44	172.7	0.0387
174.3	57.4	0.77	400	5.94	113.2	0.0351
152.5	51.6	0.80	400	4.48	65.8	0.0306
207.3	48.0	0.79	400	2.90	31.5	0.0258

Graph plotted shown in figure (5.11)

By method of least squares:-

Slope of line = R^2 ; Intercept = mean square of thermal spread

Resolution = R = 0.00952 = 0.952%

Thermal Spread of electron source = $\frac{\sqrt{2}}{\lambda}$ = 154 mV

Error in resolution = $\frac{\Delta R}{R}$ = 3.1 %

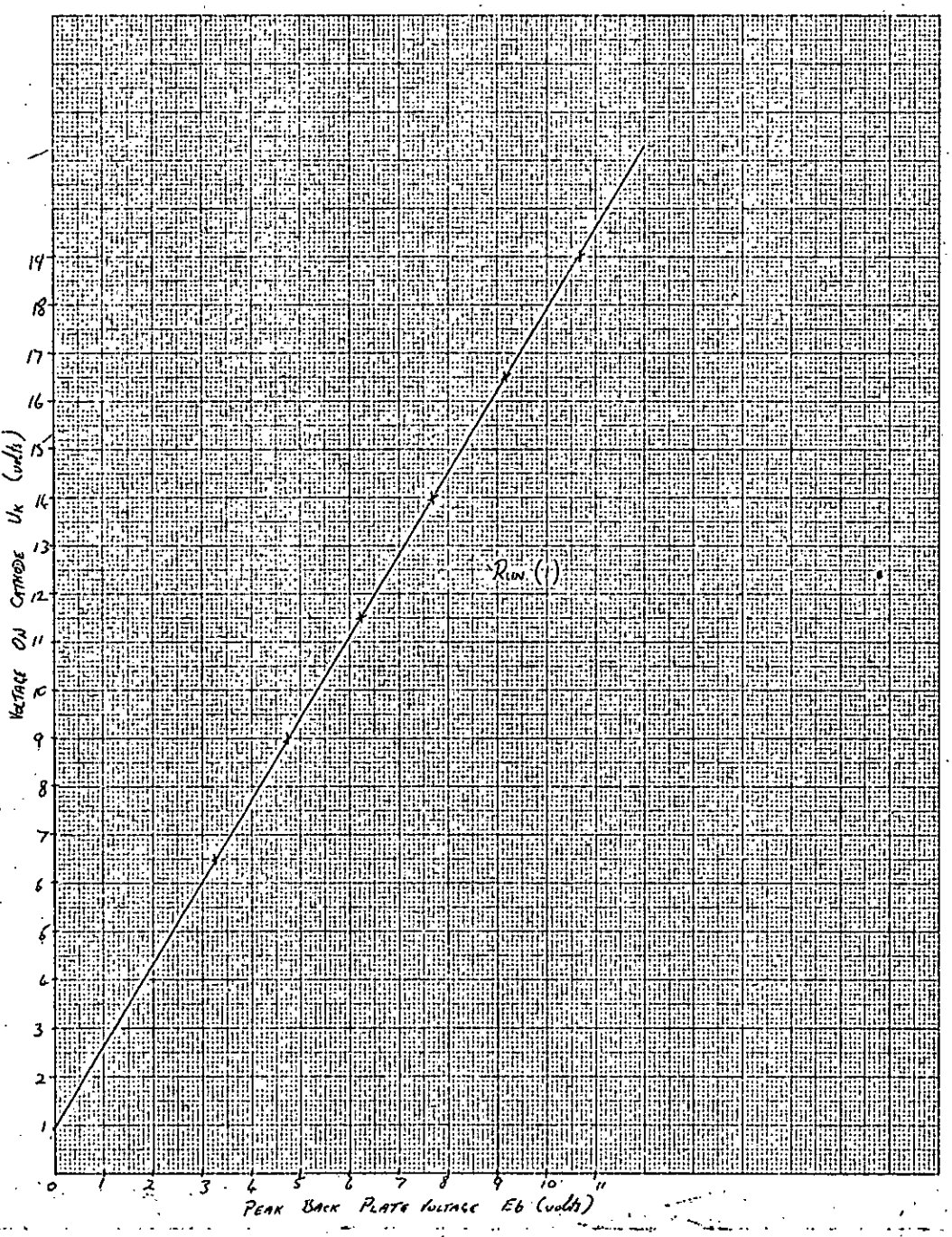
VOLTAGE ON CATHODE U_K (volts)
PEAK BACK PLATE VOLTAGE E_b (volts)
R_{GEN} (1)
0
1
2
3
4
5
6
7
8
9
10
11
12
13
14
15
16
17
18

Figure 5.4

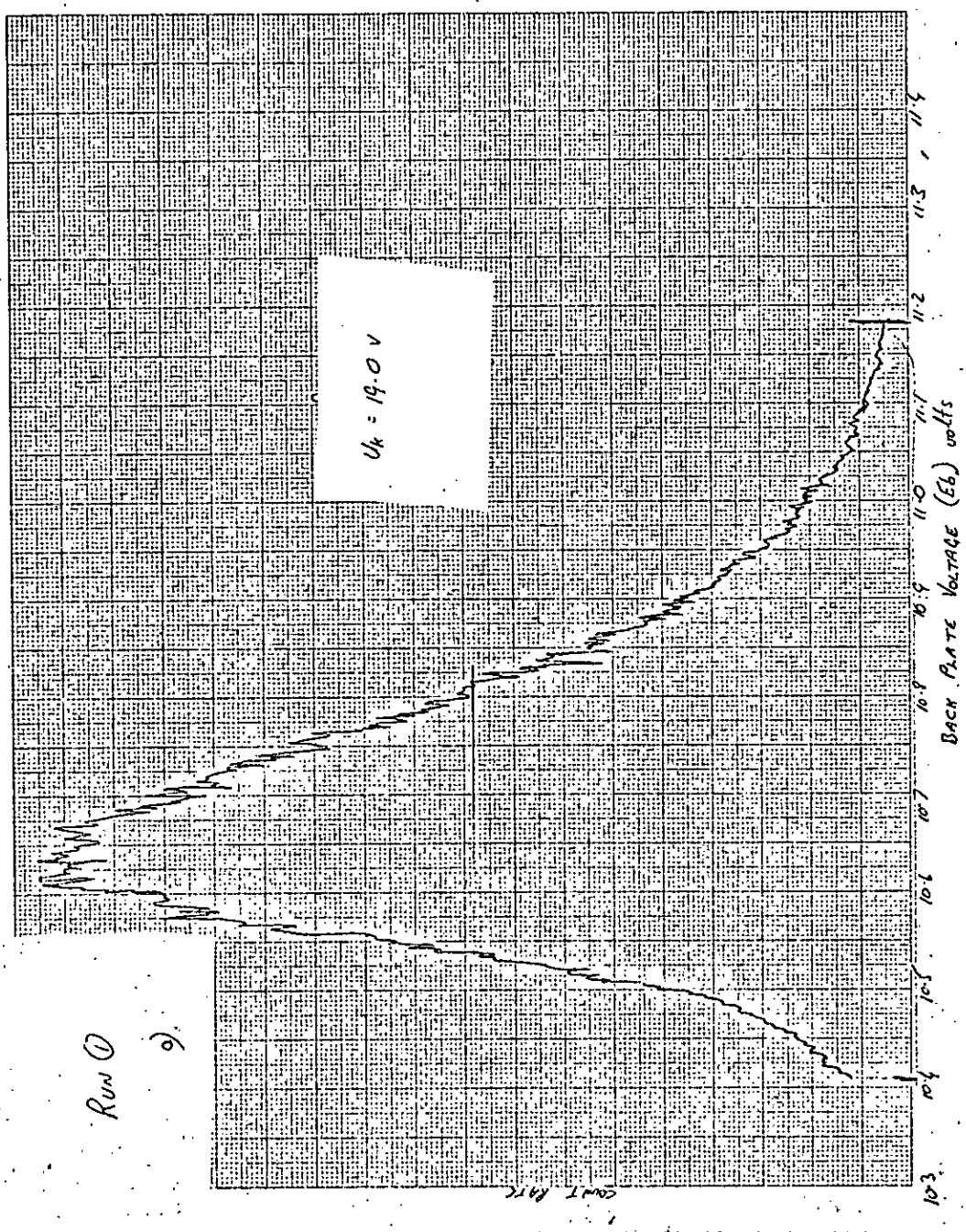
U_k = 19.0 v
Run 0
9
Count Rate
Back Plate Voltage (E_b) volts
11.4
11.3
11.2
11.1
11.0
10.9
10.8
10.7
10.6
10.5
10.4
10.3

Figure 5.5

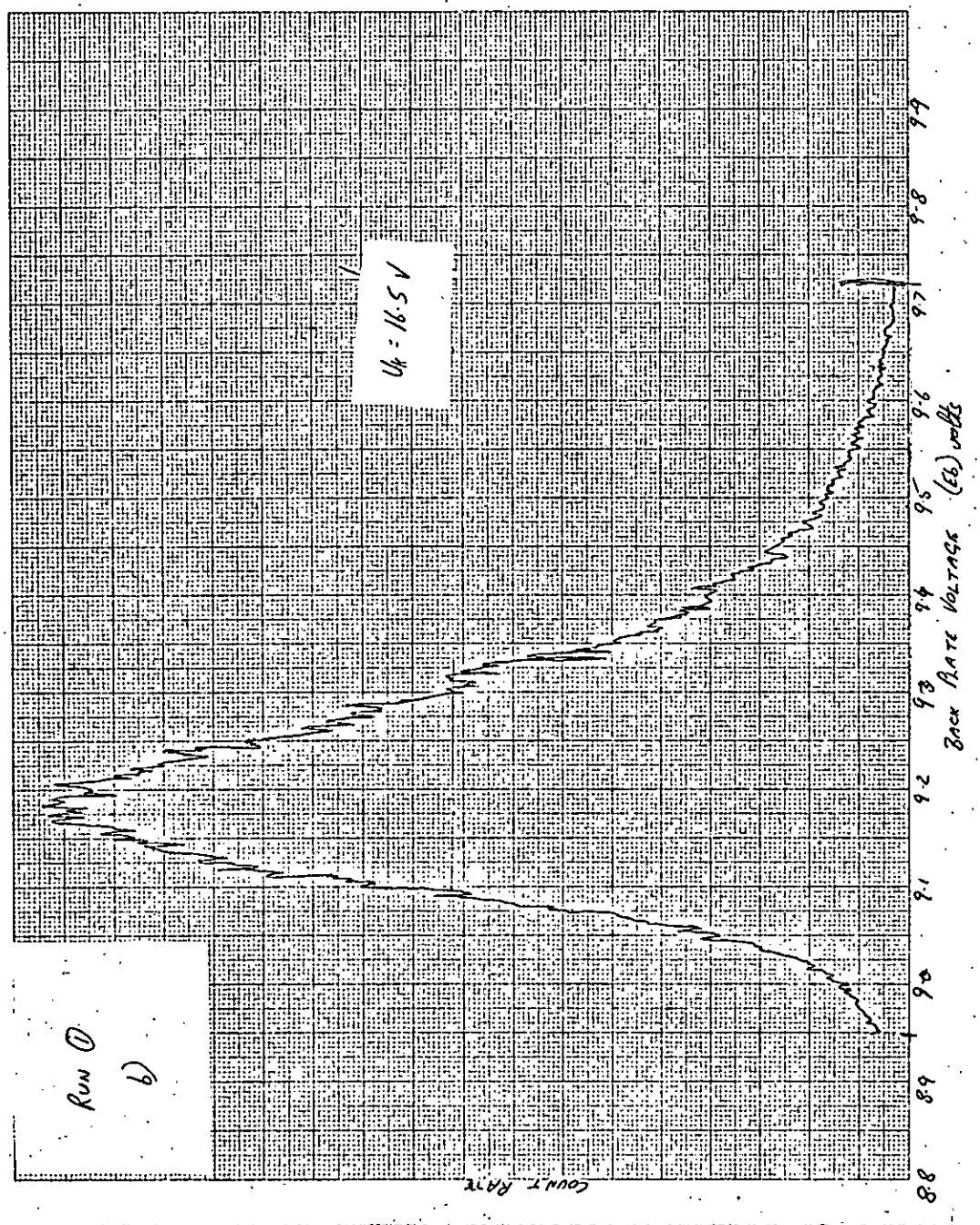
Run 0
b)
$V_k = 16.5$ V
Count Rate
Back Plate Voltage (Eb) Volts
8.8
8.9
9.0
9.1
9.2
9.3
9.4
9.5
9.6
9.7
9.8
9.9

Figure 5.6

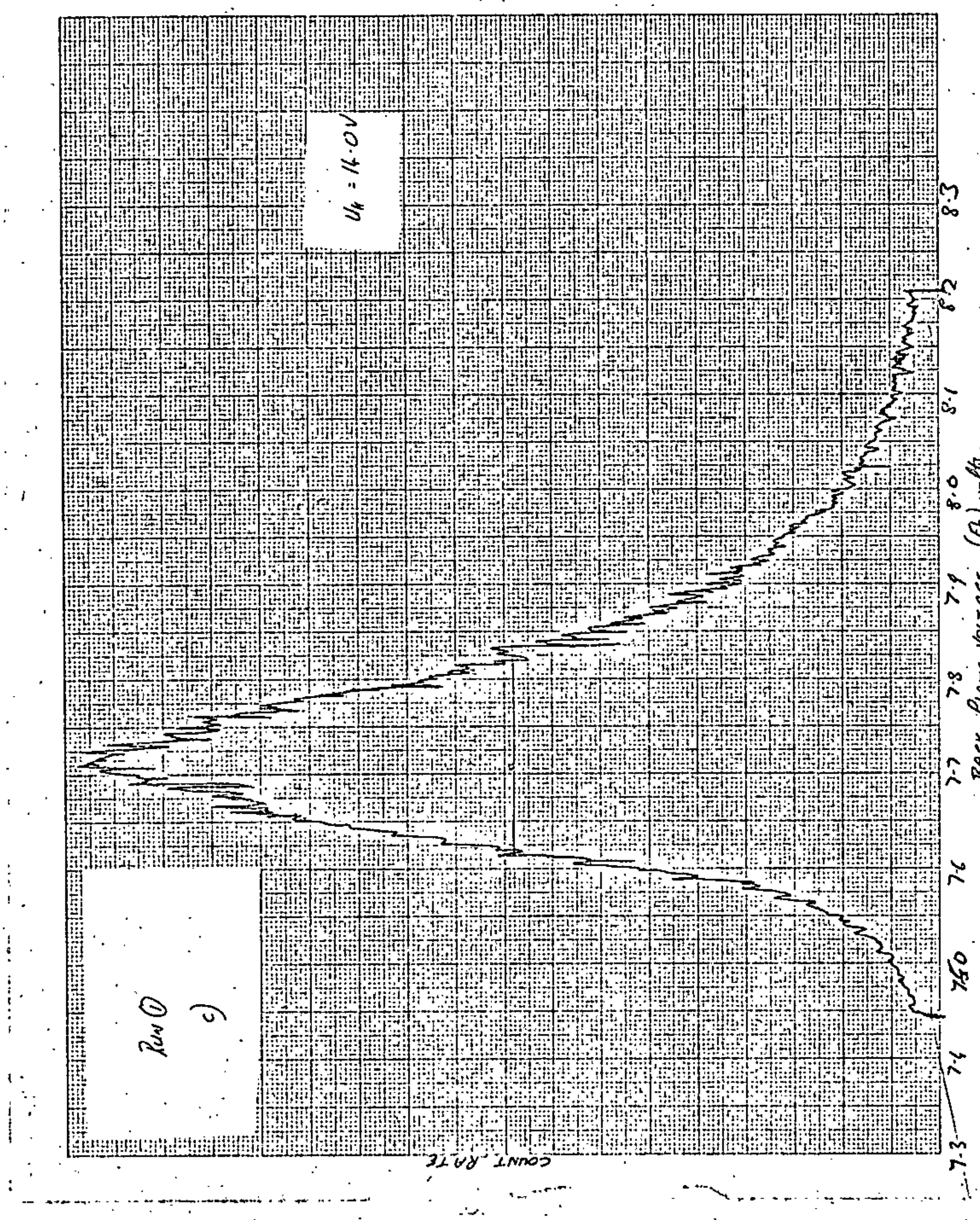

Figure 5.7

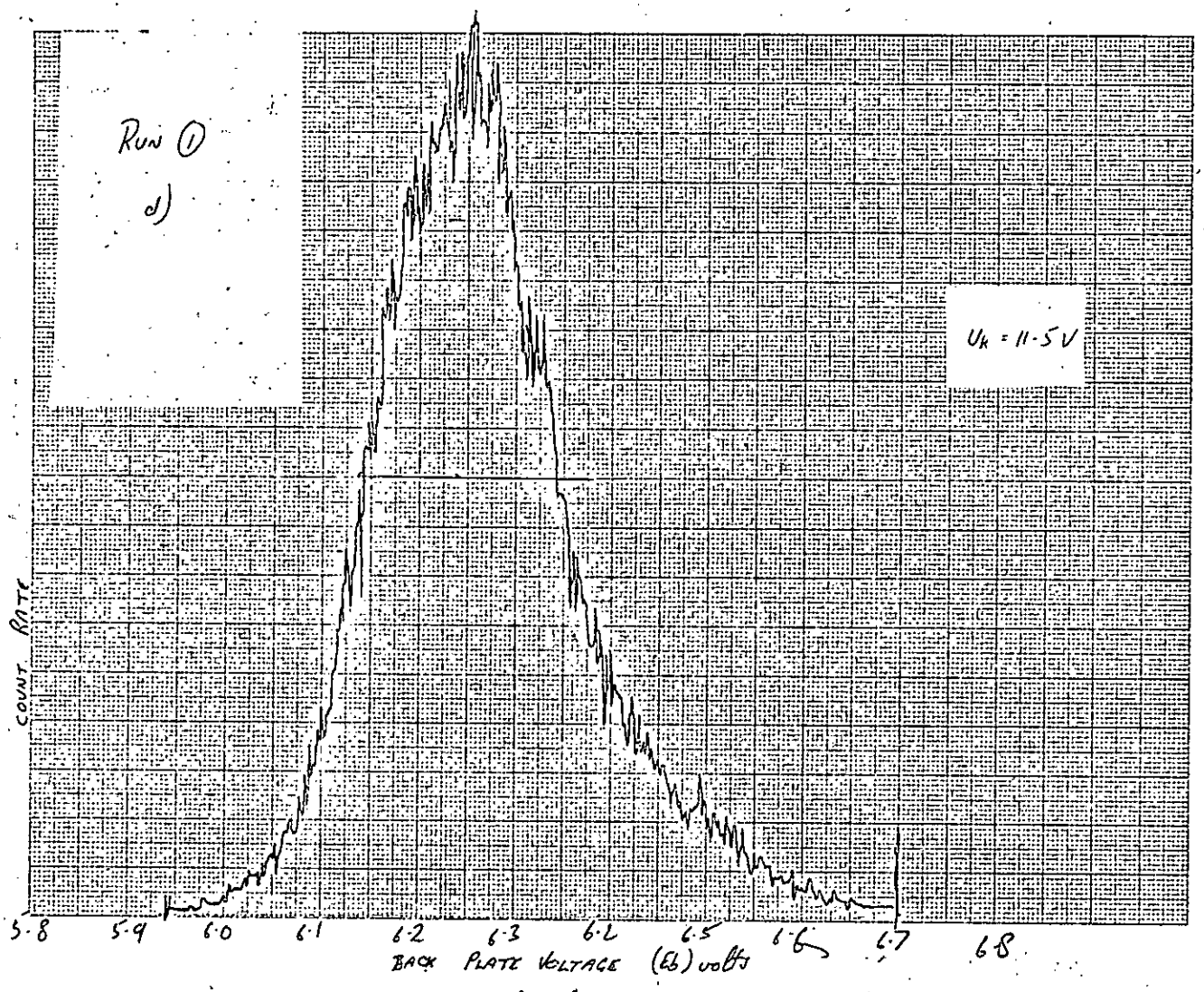
Run ①
d)
$U_k = 11.5\,V$
COUNT RATE
5·8
5·9
6·0
6·1
6·2
6·3
6·4
6·5
6·6
6·7
6·8
BACK PLATE VOLTAGE (Eb) volts

Figure 5.8

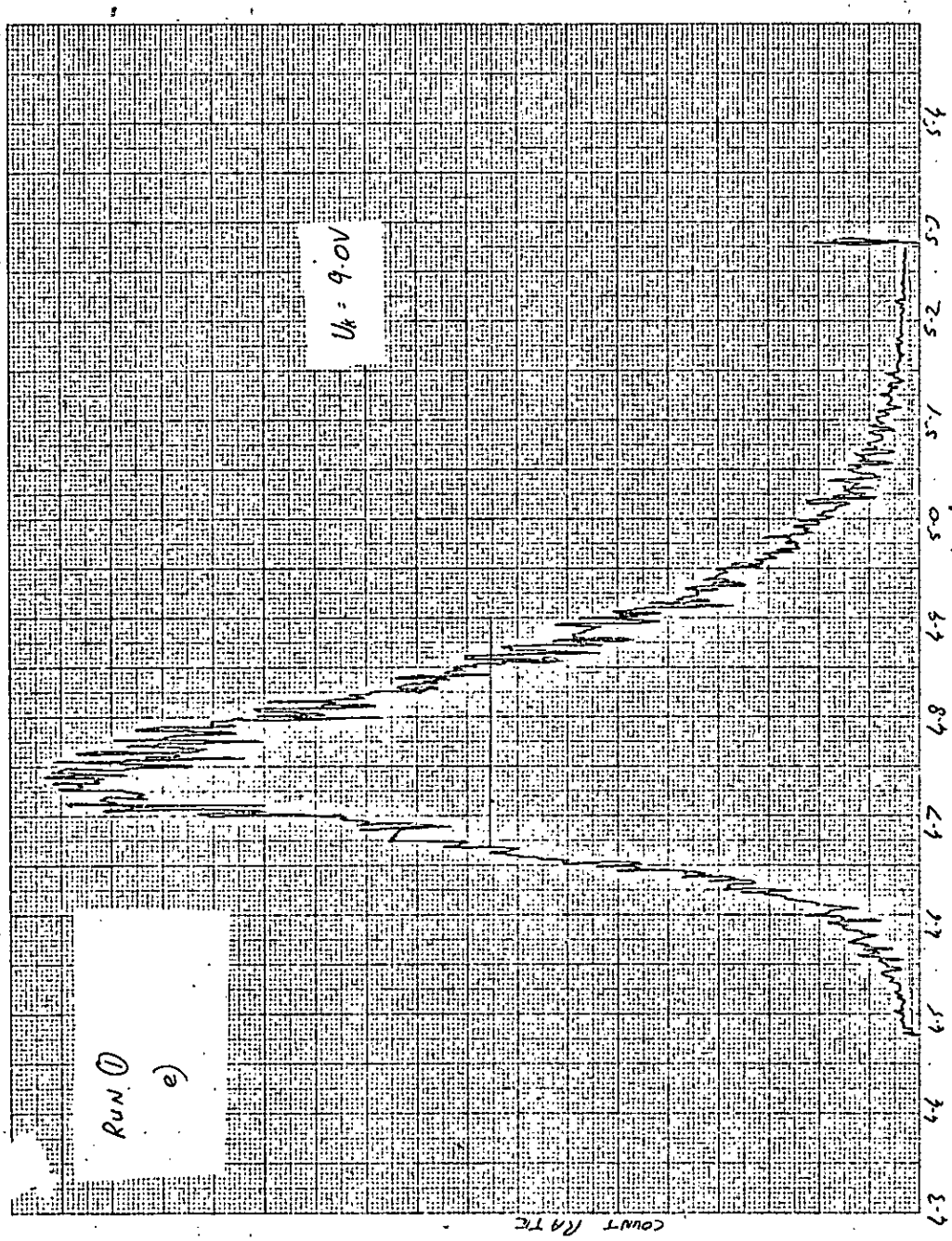
RUN ①
e)
U_K = 9.0V
COUNT RATE
4.3
4.4
4.5
4.6
4.7
4.8
4.9
5.0
5.1
5.2
5.3
5.4
BACK PLATE VOLTAGE (EB) volts

Figure 5.9

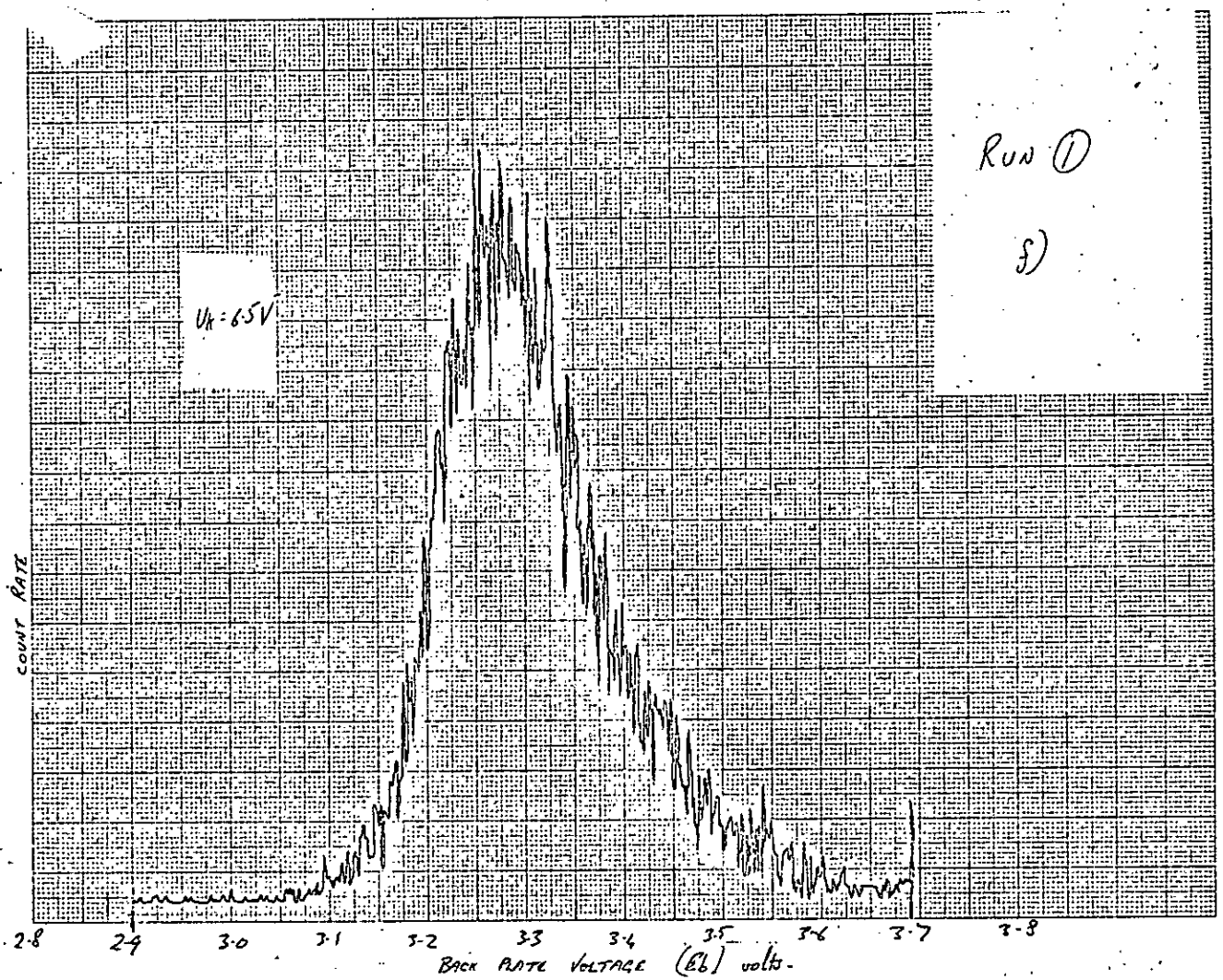
Run ①
$U_k = 6.5V$
count rate
2·8
2·9
3·0
3·1
3·2
3·3
3·4
3·5
3·6
3·7
3·8
Back plate voltage (Eb) volts.

Figure 5.10

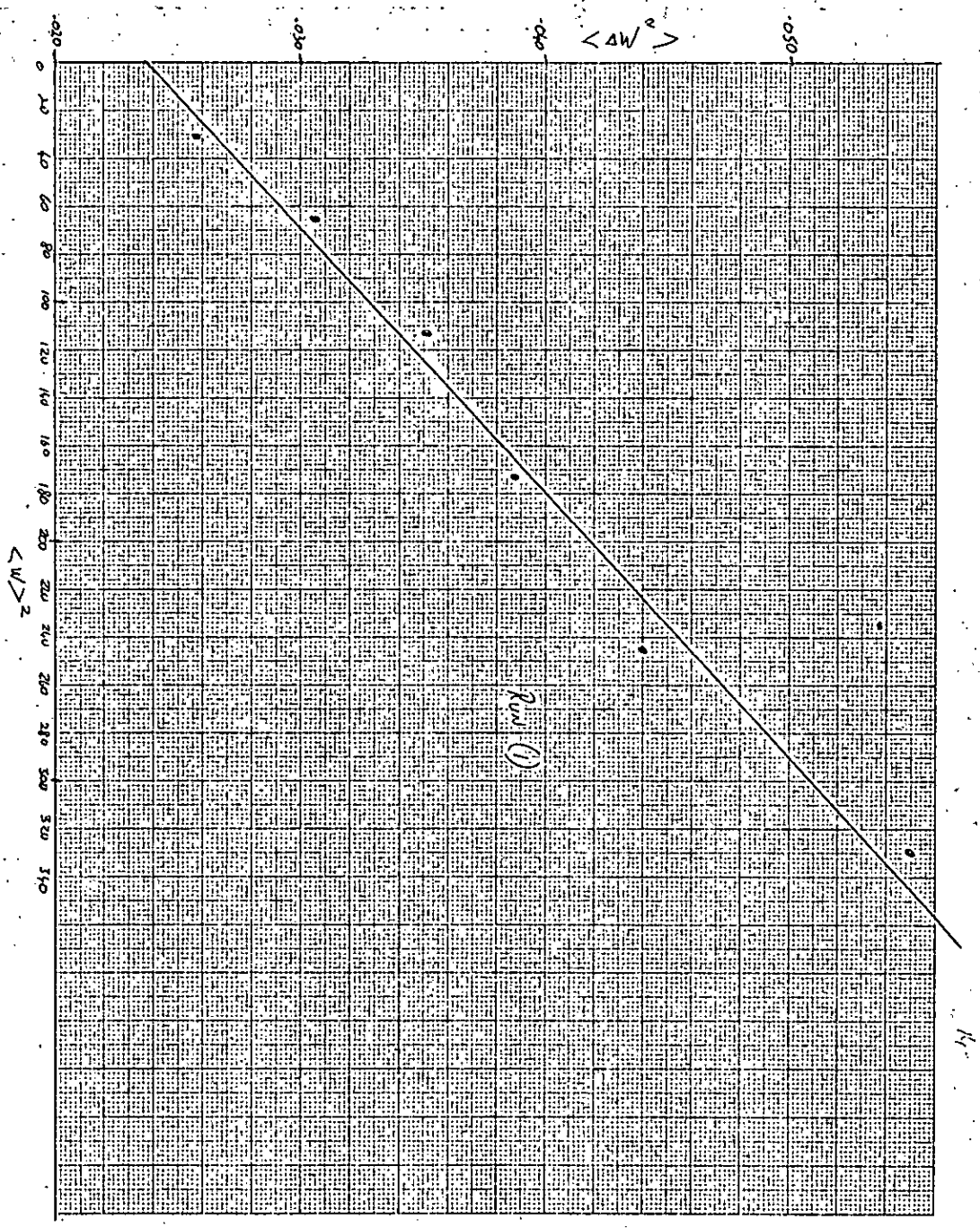

Figure 5.11

RUN (2)

Heater voltage = 7.89 volts

U_k	19	17	15	13	11	9	7	5	volts
Eb peak	10.575	9.40	8.22	7.03	5.85	4.75	3.49	2.30	volts

Graph plotted shown in figure (5.12)

By method of least squares:-

Slope of line = $\frac{U}{Eb}$ = 1.7029

Intercept on axis = contact potential = 1.034 volts

From computer print out & graphs.

X	Y	M	N	E_1	$\langle W \rangle^2$	$\langle \Delta W^2 \rangle$
195.3	82.1	0.69	400	10.28	326.9	0.0582
207.0	78.6	0.69	400	9.09	258.8	0.0533
197.9	77.0	0.675	400	7.93	198.0	0.0490
154.8	76.1	0.66	400	6.83	145.6	0.0457
192.3	68.8	0.65	400	5.58	100.7	0.0362
220.9	55.3	0.77	400	4.29	64.5	0.0329
162.1	47.9	0.68	340	3.21	36.2	0.0266
159.8	45.3	0.655	320	2.02	16.0	0.0249

Graph plotted shown in figure (5.13)

By method of least squares:-

Slope of line = R^2 ; Intercept = mean square of thermal spread

Resolution = R = 0.0105 = 1.05%

Thermal spread of electron source = $\frac{\sqrt{2}}{\lambda}$ = 158 mV

Error in resolution = $\frac{\Delta R}{R}$ = 4.2%

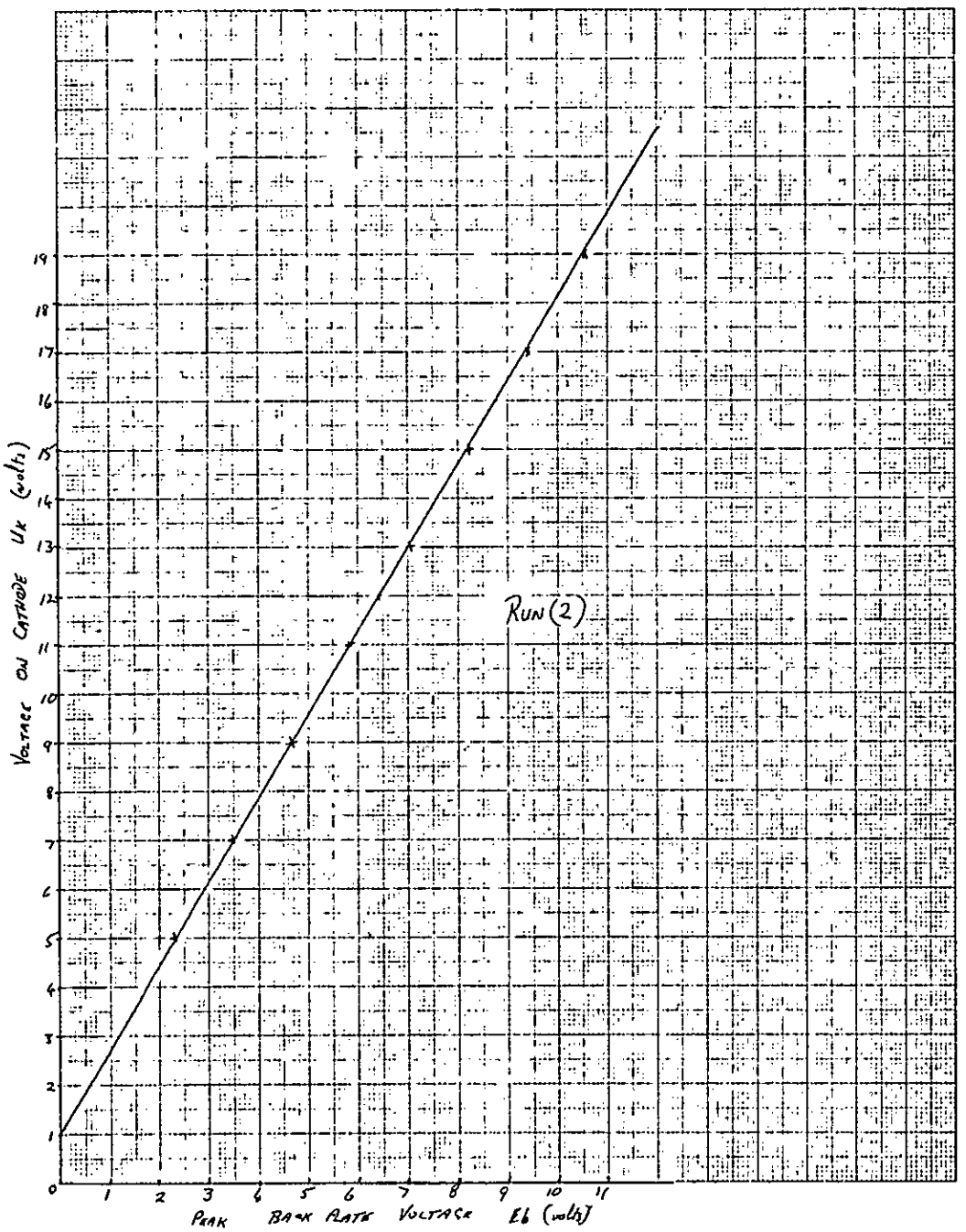
Voltage on Cathode Uk (volts)
Peak Back Plate Voltage Eb (volts)
Run (2)
0
1
2
3
4
5
6
7
8
9
10
11
12
13
14
15
16
17
18
19

Figure 5.12

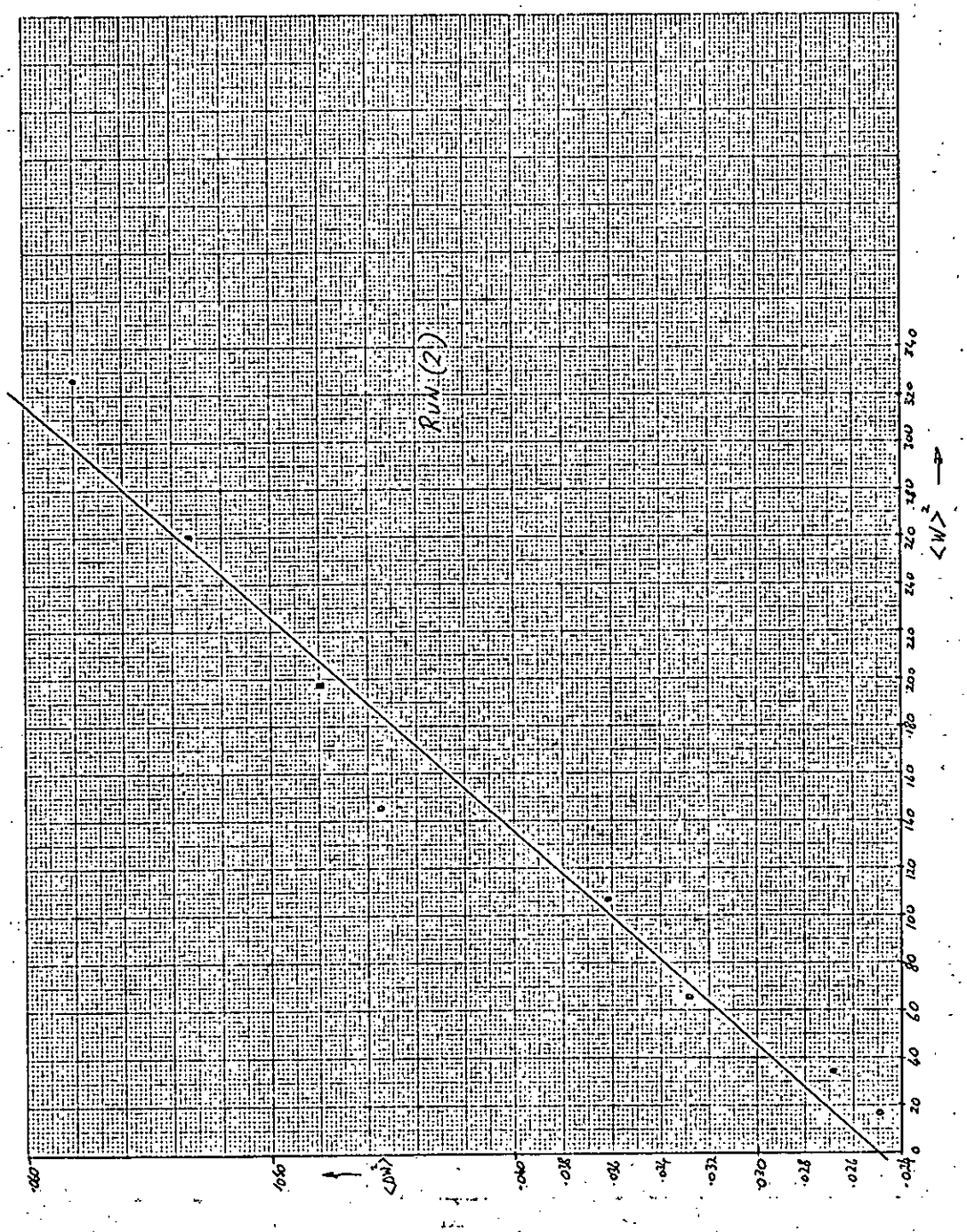
RUN (2)
$\langle \Delta W^2 \rangle$
$\langle W \rangle^2$
.060
.058
.056
.054
.052
.050
.048
.046
.044
.042
.040
0
20
40
60
80
100
120
140
160
180
200
220
240
260
280
300
320
340

Figure 5.13

Run (3)

Heater voltage = 7.32 volts.

U_k	19	17	15	13	11	9	volts
Eb peak	10.63	9.48	8.18	6.97	5.72	4.49	volts

By the method of least squares;-

Slope of line = $\frac{U}{Eb}$ = 1.6152

Intercept on axis = contact potential = 1.7564

From computer print out & graphs.

X	Y	M	N	E_1	$\langle W \rangle^2$	$\langle \Delta W^2 \rangle$
165.7	44.2	0.79	400	10.35	297.4	0.0199
235.7	56.3	0.78	400	9.05	235.9	0.0314
140.8	45.6	0.83	400	7.95	177.2	0.0234
139.0	50.7	0.85	400	6.75	129.5	0.0303
148.2	42.9	0.89	400	5.43	86.5	0.0238
156.4	41.1	0.95	400	4.16	53.6	0.0249

By the method of least squares:-

Slope of line = R^2 ; Intercept = mean square of thermal spread

Resolution = R = 0.0054 = 0.54%

Thermal spread of electron source = $\frac{\sqrt{2}}{\lambda}$ = 151 mV

Error in resolution = $\frac{\Delta R}{R}$ = 95%

CONCLUSION

The experiments carried out confirmed the analyser electron optics theory to within a small percentage of experimental error. The relationship between the electron energy of the beam selected by the analyser and the deflecting voltage necessary to achieve this selection was borne out by the results obtained.

The measurements of energy resolution of the analyser are comparable with predictions. Although in some runs the experimental error is quite large, there were enough results with small percentage errors to justify the claim that the energy resolution of the analyser is not worse than one percent.

The assymetries of the energy spectra obtained are similar to those explained by Dietrich (1958). The actual temperature of the cathode was not determined as there was no way of directly observing the face of the cathode with an optical pyrometer and therefore results deduced from the energy spectra could not be directly confirmed. The value of $2\lambda^{-2}$, although taken as a constant for any particular set of runs, may have varied slightly due to variations in beam density. (Boersch:1954).

The experiment to observe the inelastically scattered electrons from mercury vapour at an angle of scattering of 180 degrees appeared to be feasible, although, from the few qualitative results obtained, no firm conclusion is drawn.

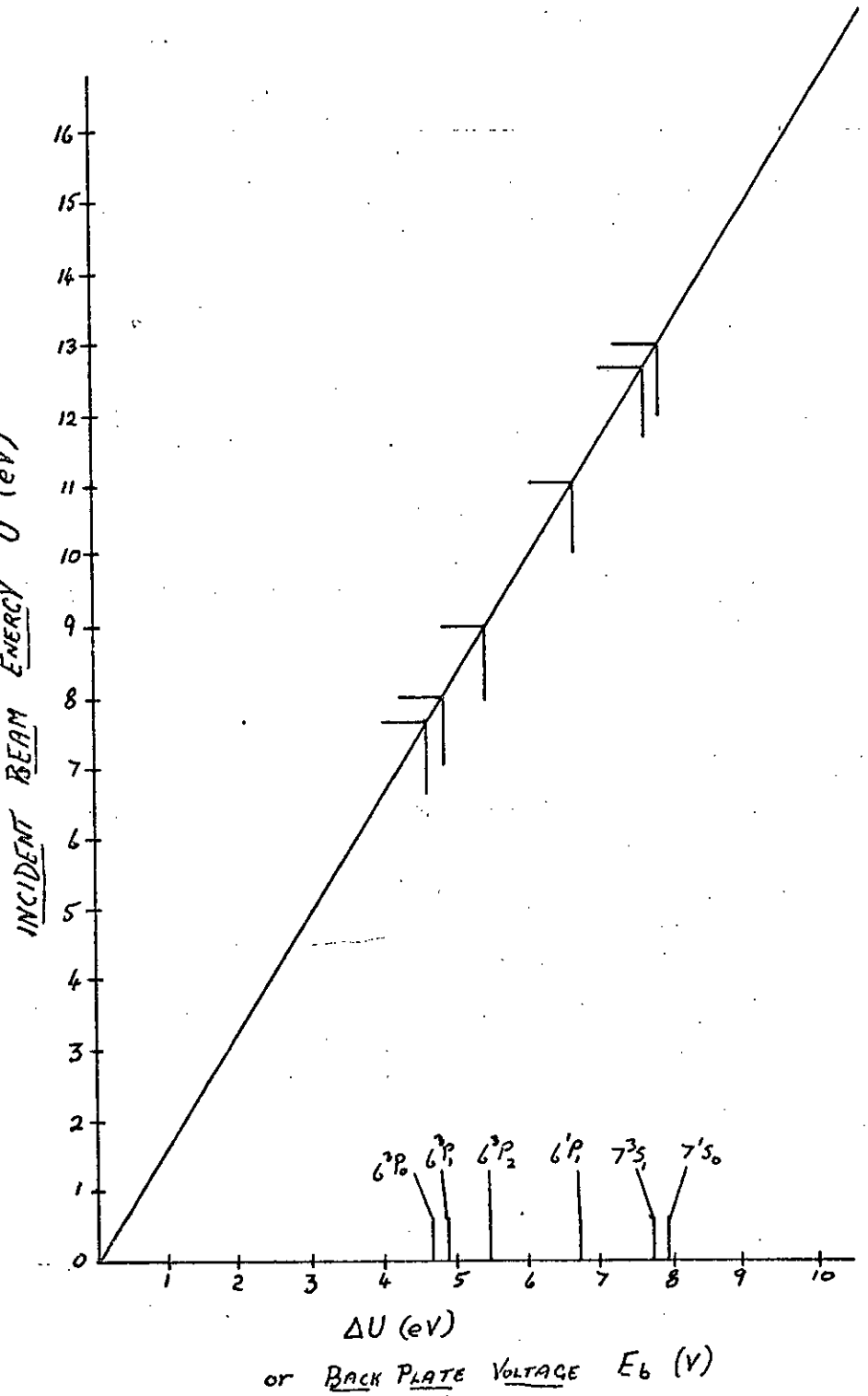
INCIDENT BEAM ENERGY U (eV)
16
15
14
13
12
11
10
9
8
7
6
5
4
3
2
1
0
1
2
3
4
5
6
7
8
9
10
6^1P_0
6^3P_1
6^3P_2
6^1P_1
7^3S_1
7^1S_0
ΔU (eV)
or BACK PLATE VOLTAGE E_b (V)

Figure AI.1

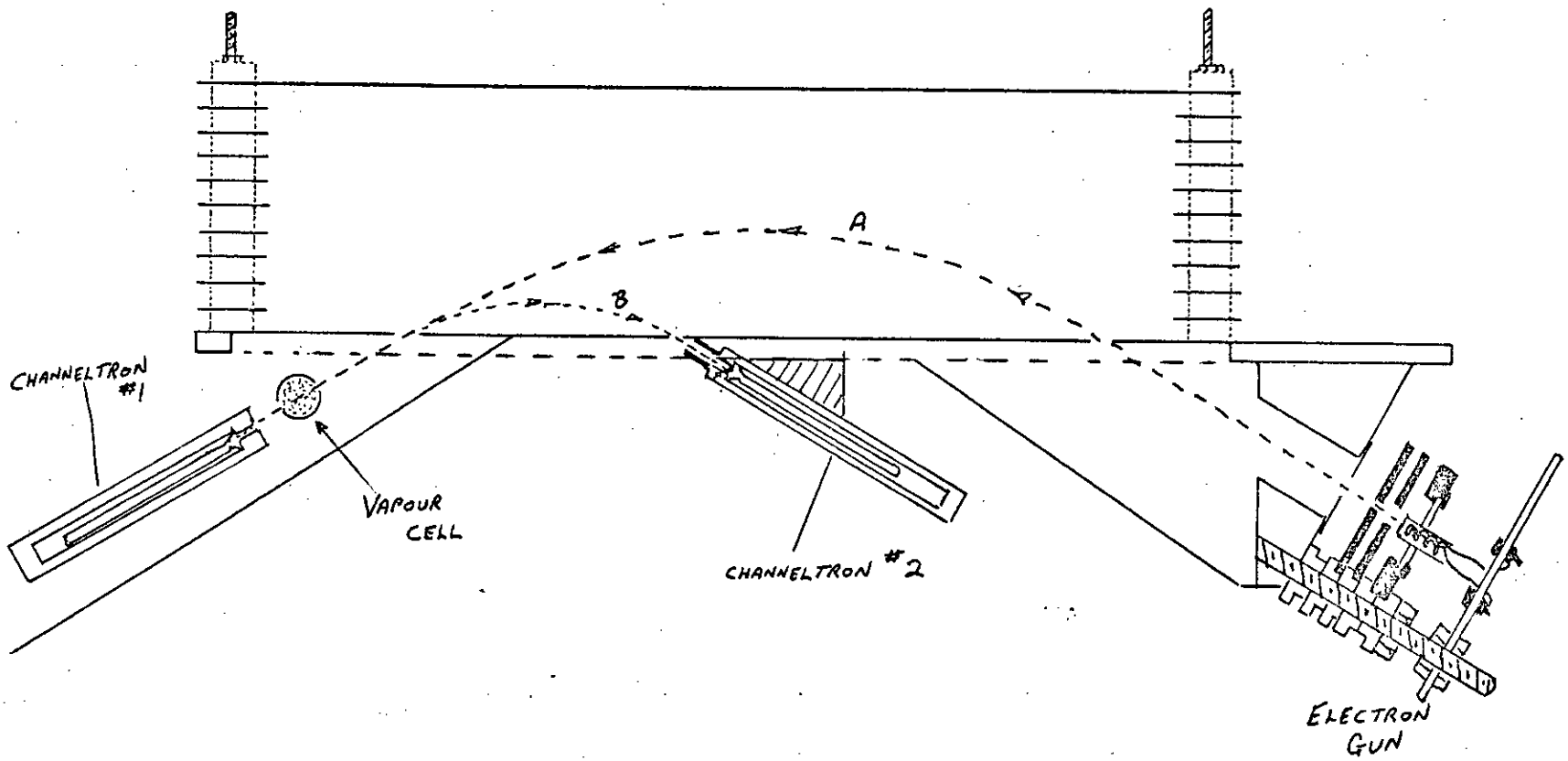

Figure AI.2 Experimental Arrangement to Measure Back-Scattering.

APPENDIX I.

MEASUREMENTS OF INELASTIC SCATTERING FROM THE MERCURY ATOM.

The plane mirror electrostatic energy analyser seemed to be ideally suited as an instrument with which to observe inelastically scattered electrons at an angle of scattering of 180 degrees from a gaseous source. Since the energy spread of the electrons being focused on leaving the analyser seemed to be in the extreme no greater than ± 250 millivolts about the mean energy, it was thought that the examination of inelastically scattered electrons from the neutral mercury atom was possible. From figure (AI.1) it can be seen that scattering from the 6^1P_1 state should be fairly easy to separate from scattering due to the other states. Electrons of a certain energy, which interact with the mercury atoms and excite any of the states of the atom, when scattered at 180 degrees to the incoming electrons, will have lost an amount of energy dictated by the particular level excited. These electrons, on re-entering the analyser, will be deflected in a different path to the incoming electrons and refocused on their exit from the analyser.

The apparatus, shown in figure (AI.2), consists of the plane mirror electrostatic analyser which has already been discussed in depth, the electron gun, and, instead of an image slit, there is a mercury vapour cell. This has two slits in the direction of motion of the electron beam; one to allow the entry of the incoming electron beam and the exit of the resulting inelastically scattered electrons; the other for the purpose of monitoring the incident beam intensity by means of a channeltron. At the focus point for the backscattered electrons there is another channeltron which

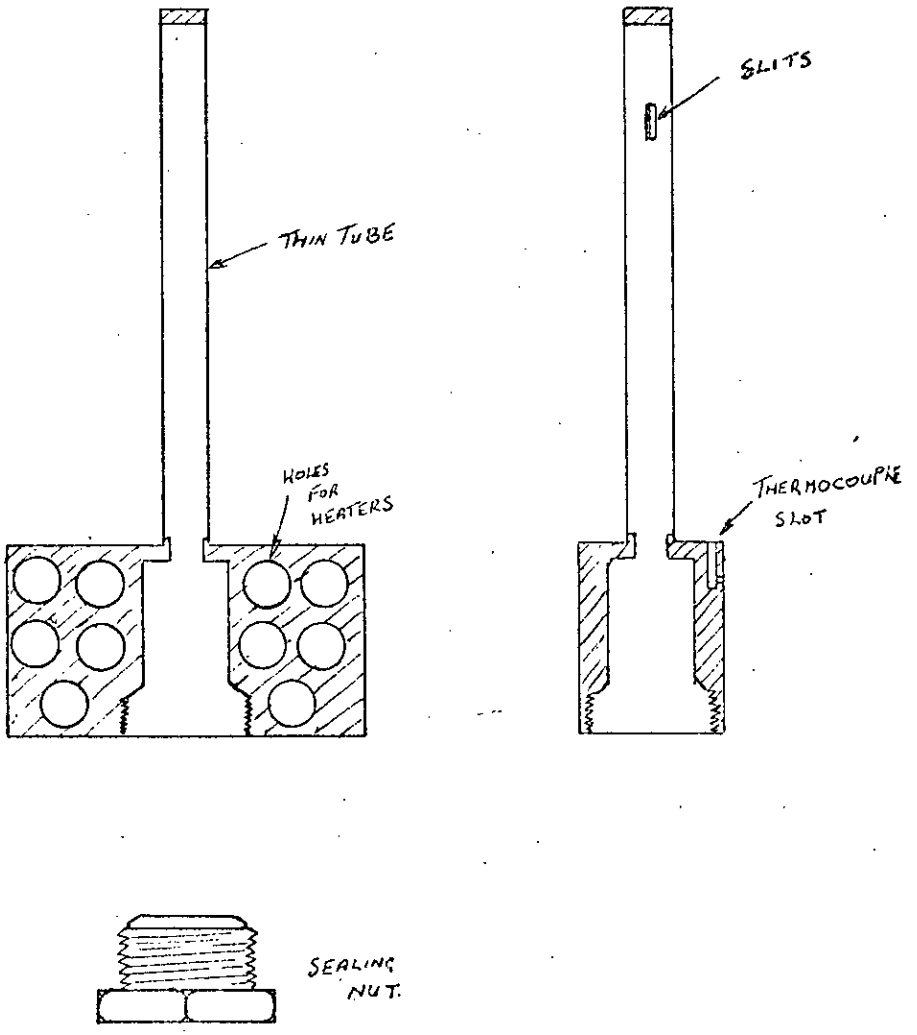

Figure AI.3 Vapour Cell

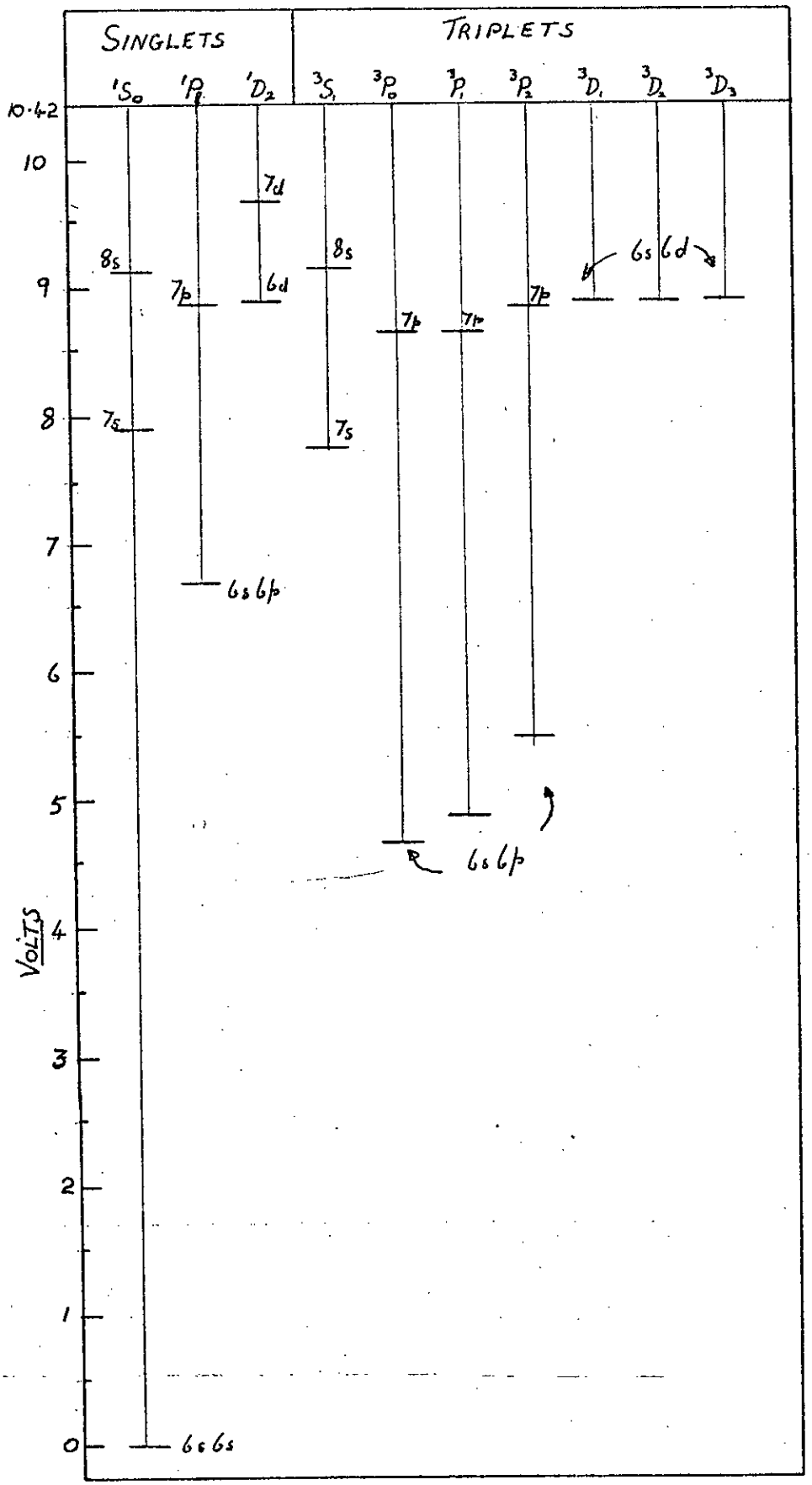

FIG. AI.4 Important energy levels for Hg

measures the intensity of the inelastically scattered electrons.

The vapour cell shown in figure (AI.3) consists of an oven block inside which a small amount of mercury is placed and a thin tube which has two slits spark machined in it. The oven block has a heater inserted in the various holes and the tube has a separate heater wound round it in a bifilar fashion. This means that the oven block and the tube can be heated independently thus enabling a greater control to be kept over the temperature of the mercury vapour in the tube. As the tube is much lighter in its construction the temperature can be varied at a much faster rate than that of the oven block. The vapour cell was constructed of non-magnetic stainless steel of the EN58J type and was mounted using ceramic bushes and insulators on a dural sliding mechanism mounted on the baseplate of the apparatus. As previously, the incident beam monitoring channeltron was also mounted on a sliding mechanism on the baseplate. The other channeltron was mounted directly on the front plate of the analyser with its angle set at 30 degrees to the front plate using a brass mounting block. The mercuryvapour cell could be cooled to a temperature of $-40^{o}C$ by filling the top cold trap with liquid nitrogen. This cold trap is connected to the vapour cell by a flexible copper braid.

The configuration of the apparatus was such that electrons with an initial energy U are deflected through the analyser and focused on a point at the centre of the vapour cell by the voltage between the front plate and the back plate of the analyser (Eb). Nearly all of these electrons then enter the channeltron and an indication of incident beam intensity is obtained. Any electrons which interact with the mercury vapour and scatter inelastically

at 180 degrees to the direction of the incident electrons, then re-enter the analyser, are deflected by the same electric field, and are focused on the other channeltron only if they have lost the appropriate energy to which the analyser is "tuned". Electrons of any other energy loss will, on being deflected by the electric field, be collected on the front plate of the analyser and do not interfere with the count rate.

As the analyser used was basically the same as used in the measurements of resolution, then the value of deflecting voltage Eb to focus an electron beam at the centre of the vapour cell was in the same ratio to the incident beam energy as before.

$$U = 1.6735\ Eb$$

$Z_{max} = 50$ mm. $\qquad Z'_{max} = 20$ mm.

$d_o = 20$ mm. $\qquad d_1 = 8.9$ mm.

input slit = 2×4 mm.

output slit = 1×4 mm. $\qquad$ backscattering slit = 1×4 mm.

$$d_1 + d'_1 = \frac{Z'_{max}}{\sqrt{3}}$$

$$d'_1 = 3.65 \text{ mm.}$$

From the relationship

$$\frac{Z'_{max}}{Z_{max}} = 1 - \frac{\Delta U}{U}$$

$$\frac{\Delta U}{U} = 1 - 0.4 = 0.6$$

$$\Delta U = 0.6U = 0.6 \times 1.6735\ Eb = Eb$$

This ratio of Z max to Z'max simplifies the use of the analyser as a direct measurement of energy loss will be obtained from the deflecting voltage.

The level of the mercury atom to be excited is chosen and the value of back plate voltage Eb is known to be the same as

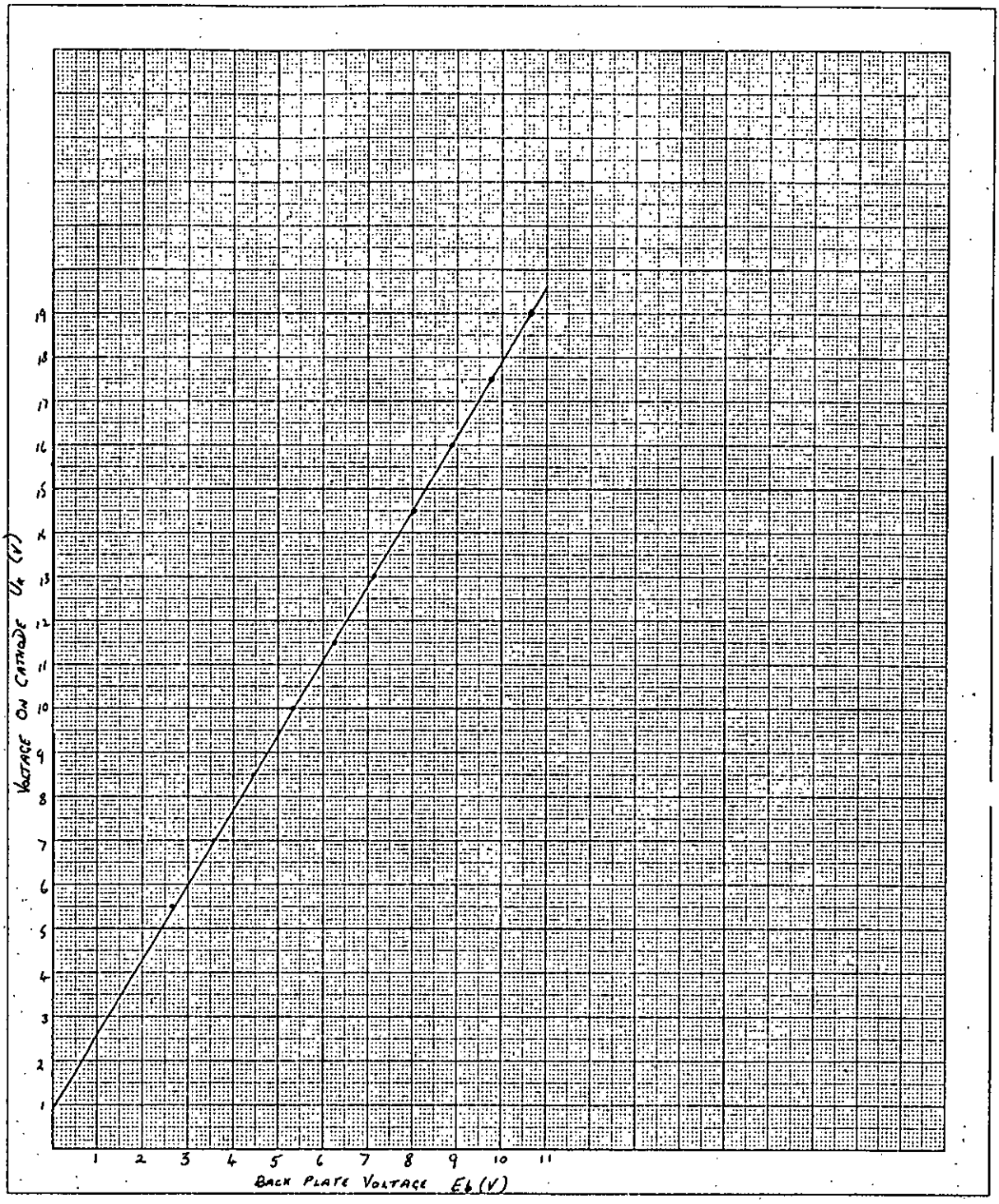
VOLTAGE ON CATHODE U_k (V)
BACK PLATE VOLTAGE E_b (V)
1 2 3 4 5 6 7 8 9 10 11
1 2 3 4 5 6 7 8 9 10 11 12 13 14 15 16 17 18 19

Figure AI.5

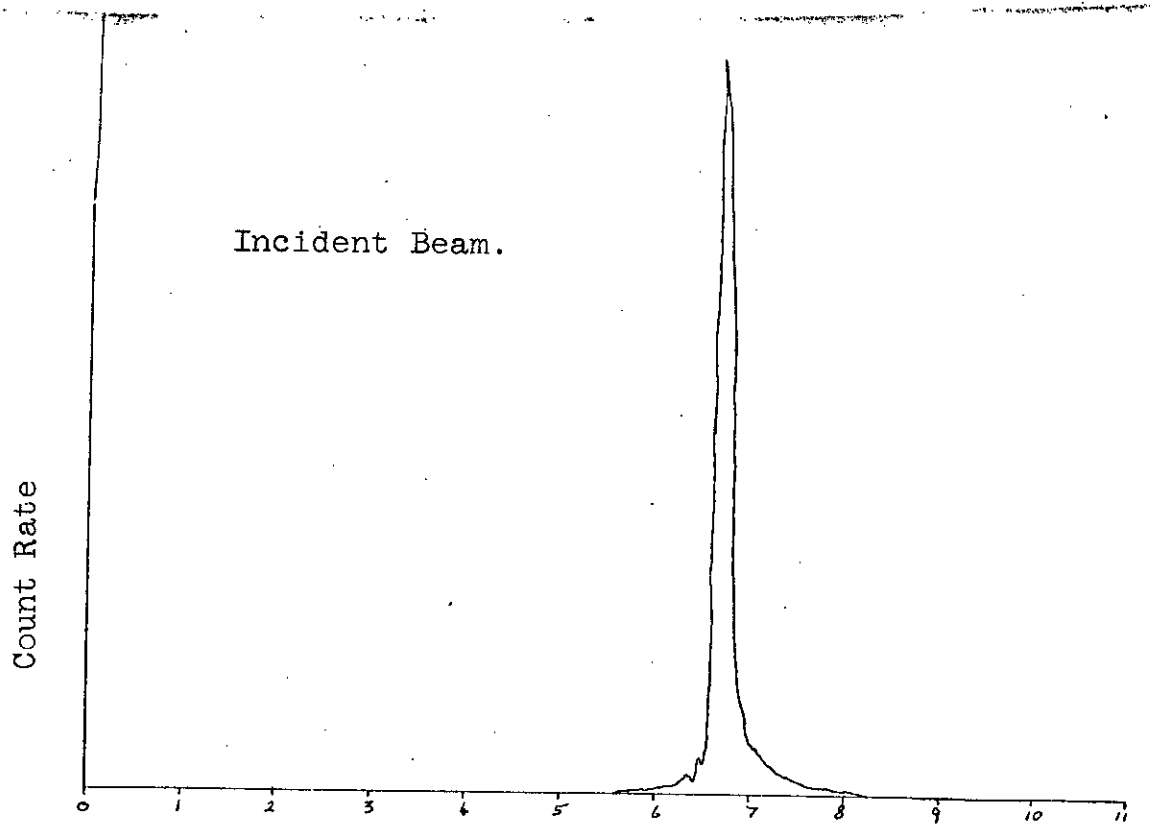

a) Back Plate Voltage (volts)

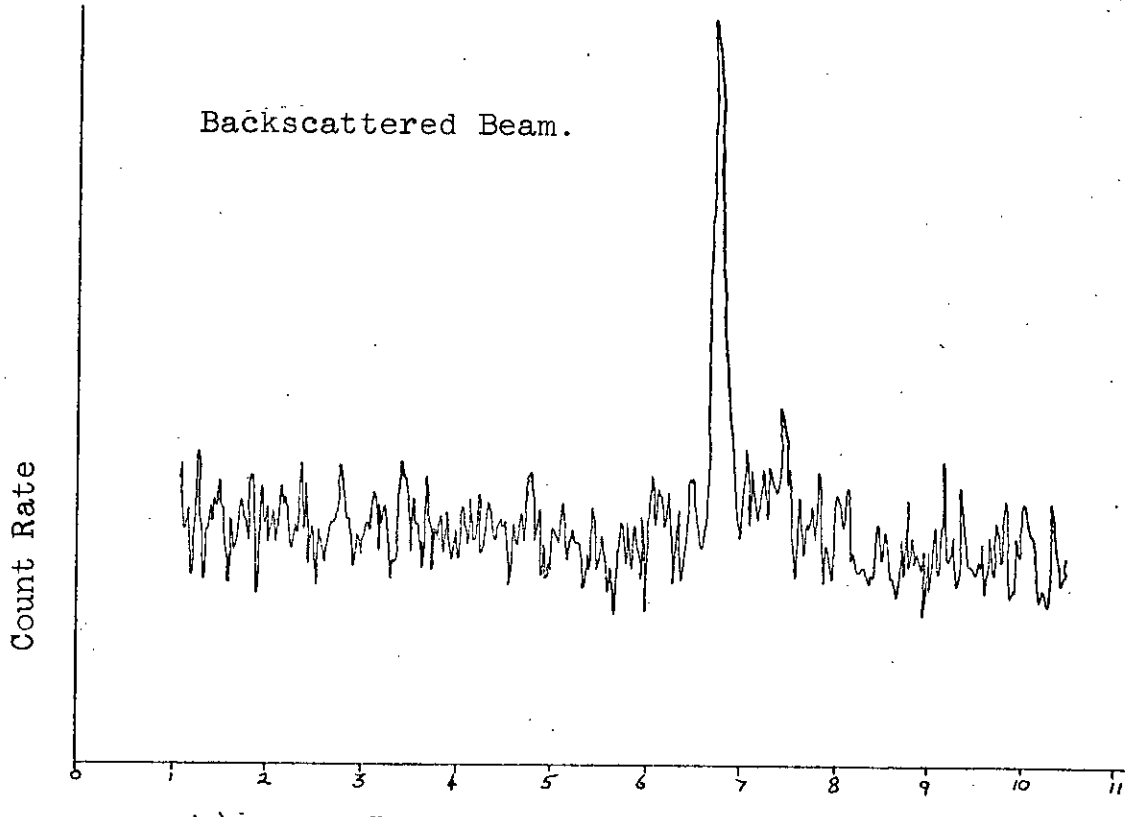

b) Back Plate Voltage (volts)

Figure AI.6

this energy loss. If the contact potential of the cathode is known, then by using the value of U found from figure (AI.5) and adding the contact potential, a value of cathode voltage is found. If however, as was sometimes the case, the contact potential was not known to any great accuracy, then with Eb set, the values of cathode voltage U_k and the electrode potentials are set such that a maximum count rate can be observed from the incident beam channeltron using the ramp generator in the d.c. position. Having made sure that the peak of the count rate occurs at the correct value of Eb, the ramp generator is then switched to either internal or external ramp function. The limits of this sweep are measured and using method (2) of data collection and the counts from the incident beam channeltron, a display of count rate against Eb is observed on the Laben as shown in figure (AI.6a). Similarly, by using the other channeltron as the detector, a display of count rate of inelastically scattered electrons through 180 degrees against Eb can be obtained (figure AI.6b). This is also an energy loss spectrum for the appropriate interaction between the incident electrons and the mercury vapour.

The results obtained are given along with the experimental parameters.

Run (1). Figure (AI.6)

Oven temp. = 20°C Cathode voltage U_k = 12.20 V

Contact Potential = 1.0 V Electron energy = U = 11.20V

Heater voltage = 7.45 V

Incident beam: Eb for maximum counts = 6.69 V

count time = 30 seconds

max. no. of counts = 28,000

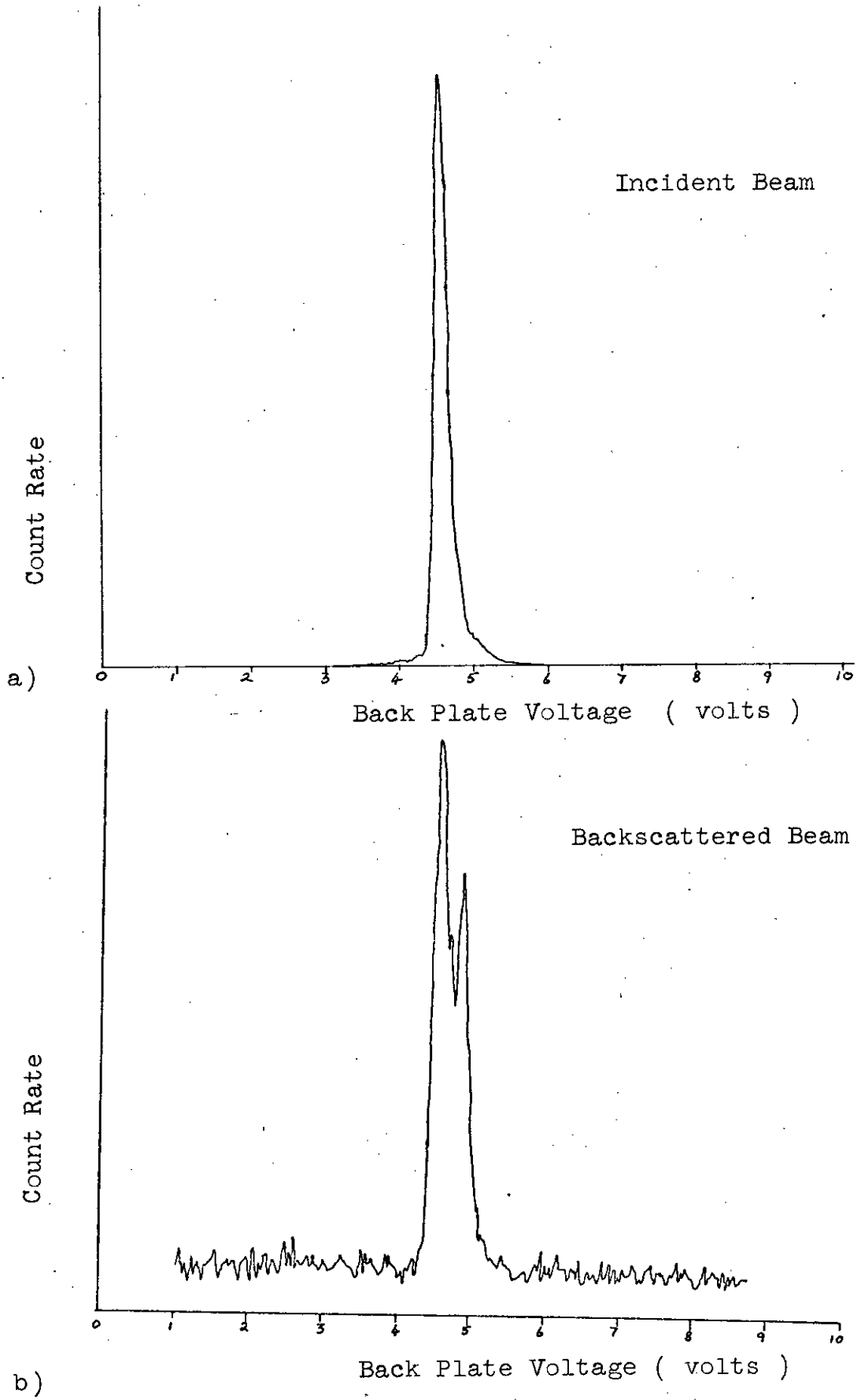
Incident Beam
Count Rate
a)
0 1 2 3 4 5 6 7 8 9 10
Back Plate Voltage (volts)
Backscattered Beam
Count Rate
b)
0 1 2 3 4 5 6 7 8 9 10
Back Plate Voltage (volts)

Figure AI.7

Backscattered beam: Eb for peak = 6.69V = energy loss

count time = 2 hours

maximum number of counts = 210

Run (2) Figure (AI.7)

Oven temp. = 40°C U_k = 8.50 V

Contact potential = 1.00 V U = 7.50 V

Heater voltage = 7.48 V

Incident beam: Eb for peak = 4.70 V

count time = 30 seconds

maximum number of counts = 30,000

Backscattered beam: Eb for peak = 4.65 & 4.90 V = energy loss

count time = 2 hours

maximum number of counts = 250

From the results obtained, and there were at least ten experimental runs which produced similar results, the observation of energy loss, or inelastically scattered electrons, from the mercury atom using the analyser seems possible. In the first run the incident beam interaction with the 6^1P_1 state is observed and in run (2) the interaction with both the 6^3P_0 and 6^3P_1 states is observed. In fact when the experiment was carried out for this second run, the intention was to excite the 6^3P_0 state only, but the fact that the two states are very close accounts for both energy losses being recorded. The voltage on the cathode was also adjusted so that the back plate voltage caused a peak for the incident electrons at values not corresponding to any energy loss peaks. In these cases, when long runs of measurement of backscattering were made, there were no peaks apparent on the spectra obtained. This is consistent with the theory of the

analyser as inelastically scattered electrons should only be observed when the back plate voltage and the incident energy are set to values which correspond to the focusing of the incident beam on the vapour cell, and the focusing of electrons which have lost a certain energy on the second channeltron.

Due to the long counting times involved and the instability of the oxide coated cathode when exposed to mercury vapour, it took a considerable period of time to achieve any success and this was rather short-lived as the vacuum system became very contaminated as did the channeltrons. No real conclusions for this particular experiment are drawn except to say that the results obtained seemed comparable with the theory of the analyser although no quantitative measurements were possible in the time available. It may well be useful to pursue this technique with different vapour sources, especially those which do not have such a detrimental effect on the vacuum and components.

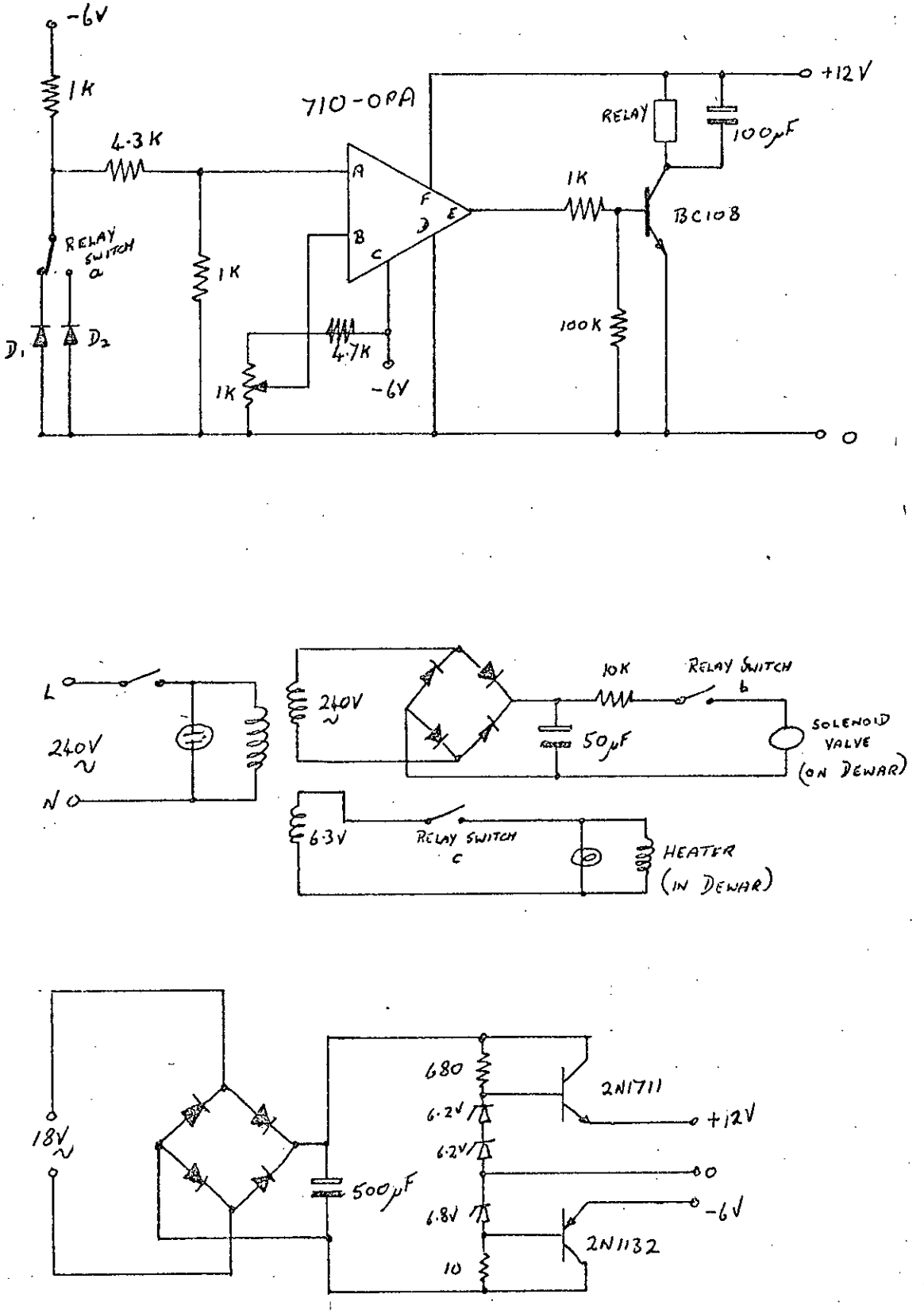

Figure AII.1 Liquid Nitrogen Replenisher

APPENDIX II

ELECTRONIC CIRCUITS

(a) Automatic Level Controller for Liquid Nitrogen

This circuit was designed to maintain the level of liquid nitrogen in the cold traps. Two circuits were required as one cold trap is on the top flange of the vacuum system and the other is an Edwards NTM4 trap situated above the chevron baffle.

The basic idea was that liquid nitrogen was to be delivered until the level reached a certain point in the trap and then delivery would stop until the level fell below another predetermined point when it would start up again. The devices used to sense the presence of the liquid nitrogen were two general purpose germanium diodes. These were found to have a forward resistance of 500 ohms at room temperature which rose to fifty kilohms at liquid nitrogen temperatures. This characteristic was used in the circuit in figure (AII.1).

This is basically a voltage comparator circuit so that when the voltage on the input of the operational amplifier crosses a value equal to that of the reference voltage, the state of the output changes. When the unit is first switched on with no coolant in the cold trap then the voltage at point A is smaller than the reference voltage maintained at B and set by the potentiometer. This means that the output of the operational amplifier is positive and the transistor and the relay are switched on. The relay switch then has the following functions:-

(1) Upper sensor D_2 in circuit.

(2) Solenoid valve on top of supply dewar in closed position.

(3) Heater under the liquid nitrogen in the supply dewar is switched on.

This/

This causes liquid nitrogen to be delivered to the cold trap. When the coolant reaches the upper sensor, the voltage at A increases above the reference voltage value so causing the output of the operational amplifier to drop to near zero and switching the relay off. The following then happen:-.

(1) The lower sensor D_1 is then in circuit and under liquid nitrogen.

(2) The solenoid valve switches off and vents the supply dewar.

(3) The heater in the supply dewar is switched off.

The power supplies to drive the unit are very basic and stable enough for the purpose. The heater in the supply dewar is simply a low value resistor of approximately 6 ohms. The distance between the sensors was adjusted so that in the large Edwards cold trap the liquid nitrogen was replenished about every 12 hours.

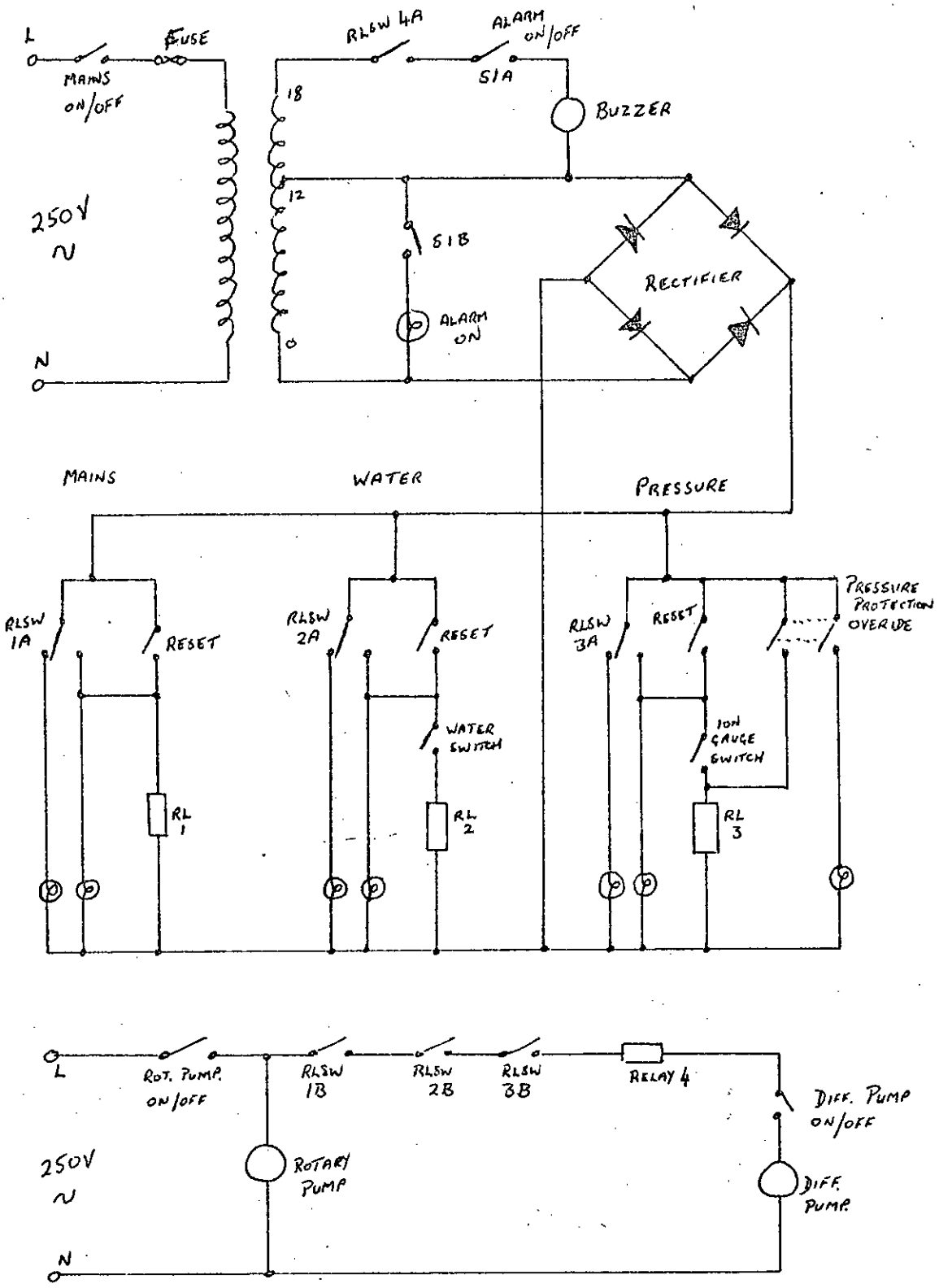

Figure AII.2 Vacuum Protection Circuit.

(b) Vacuum System Protection

The circuit shown in figure (AII2) was designed to provide protection for the oil diffusion pump in the event of pressure, water or mains failure. It is basically a network of switches and relays which latch into the circuit in certain positions such that if failure of any of the three parameters involved occurs then the diffusion pump will be switched off and can not be restarted until the fault has been attended to and that part of the circuit associated with the fault reset manually. The wiring is such that the diffusion pump cannot be switched on without the rotary pump being switched on. The flow of water is monitored by a cup connected to a lever type of switch so that when the recirculated cooling water flow decreases sufficiently or stops then the switch changes to the open position and switches the diffusion pump off. The pressure inside the vacuum chamber is monitored by an ionisation gauge and the controller for this has a suitable relay switch built in such that when the pressure rises above a predetermined value the ionisation gauge switches off and the relay switch opens so switching off the diffusion pump. A bypass switch for the pressure part of the circuit has been included because on starting the system up, the ionisation gauge cannot be switched on until the diffusion pump has been on for some time. By wiring a mains outlet in parallel with the diffusion pump certain other pieces of equipment such as high voltage power supplies and electron gun heater can also be switched off in the event of vacuum failure.

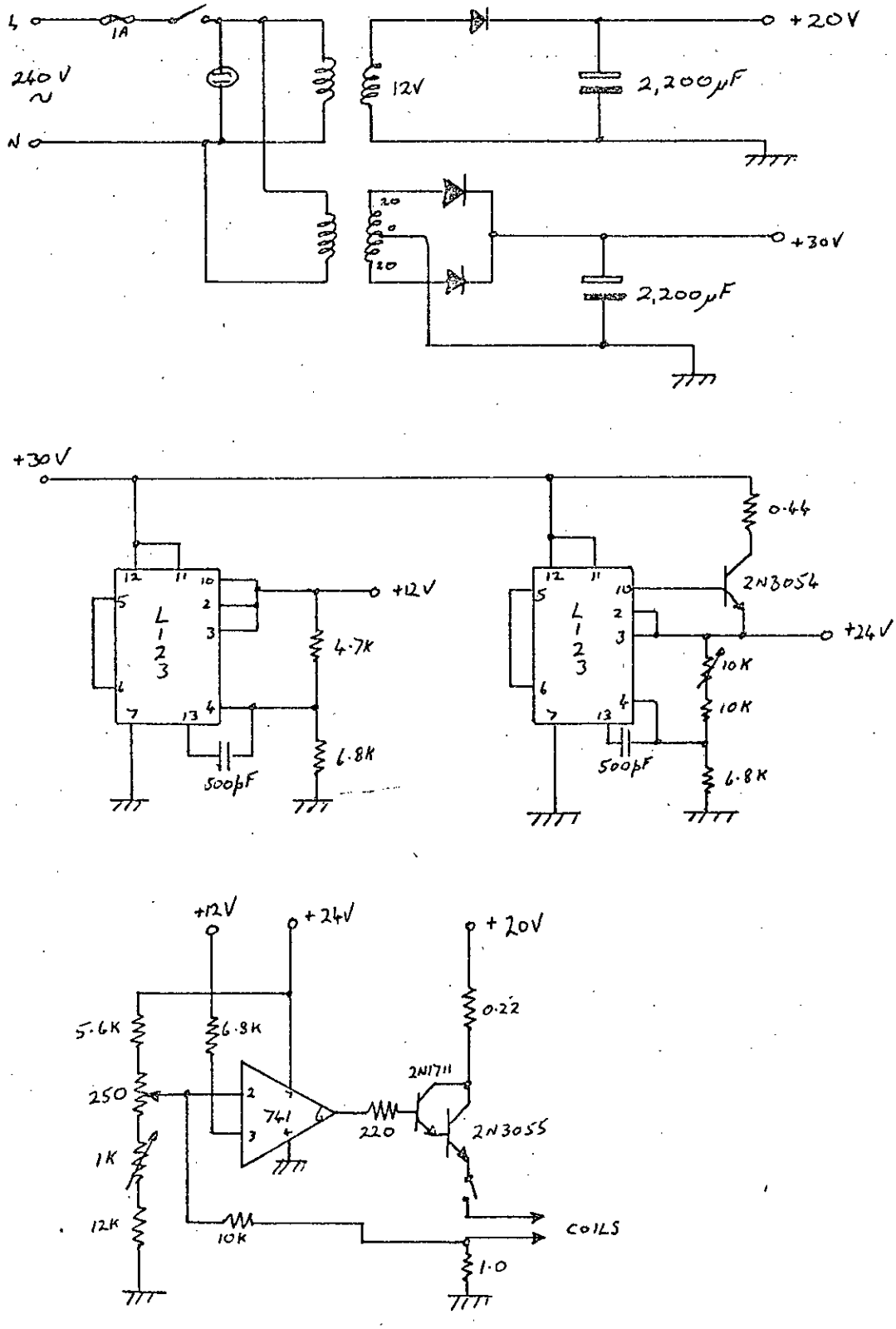

Figure AII.3 Helmholtz Coils Power Supply.

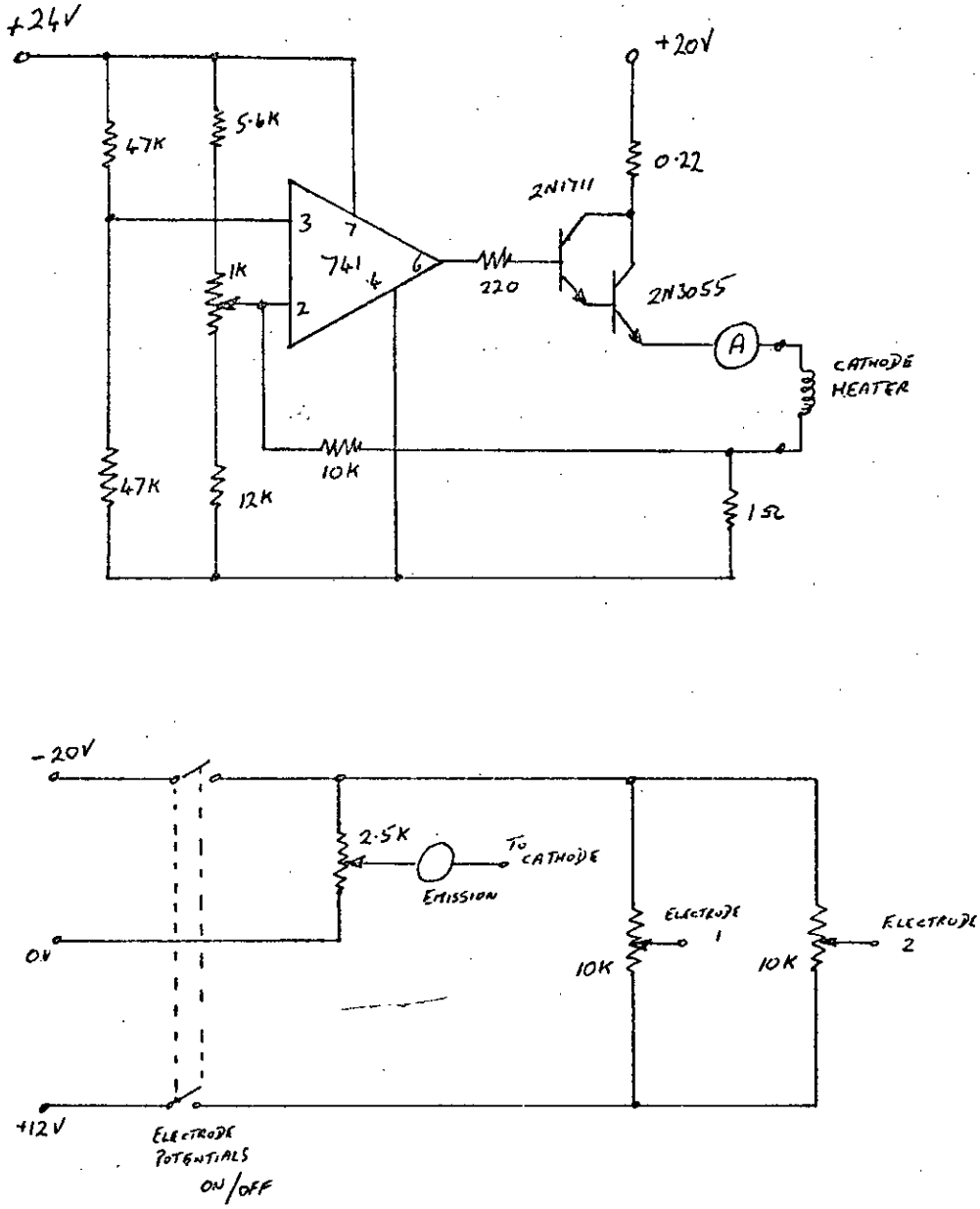

Figure AII.4 Electron Gun Power Supply.

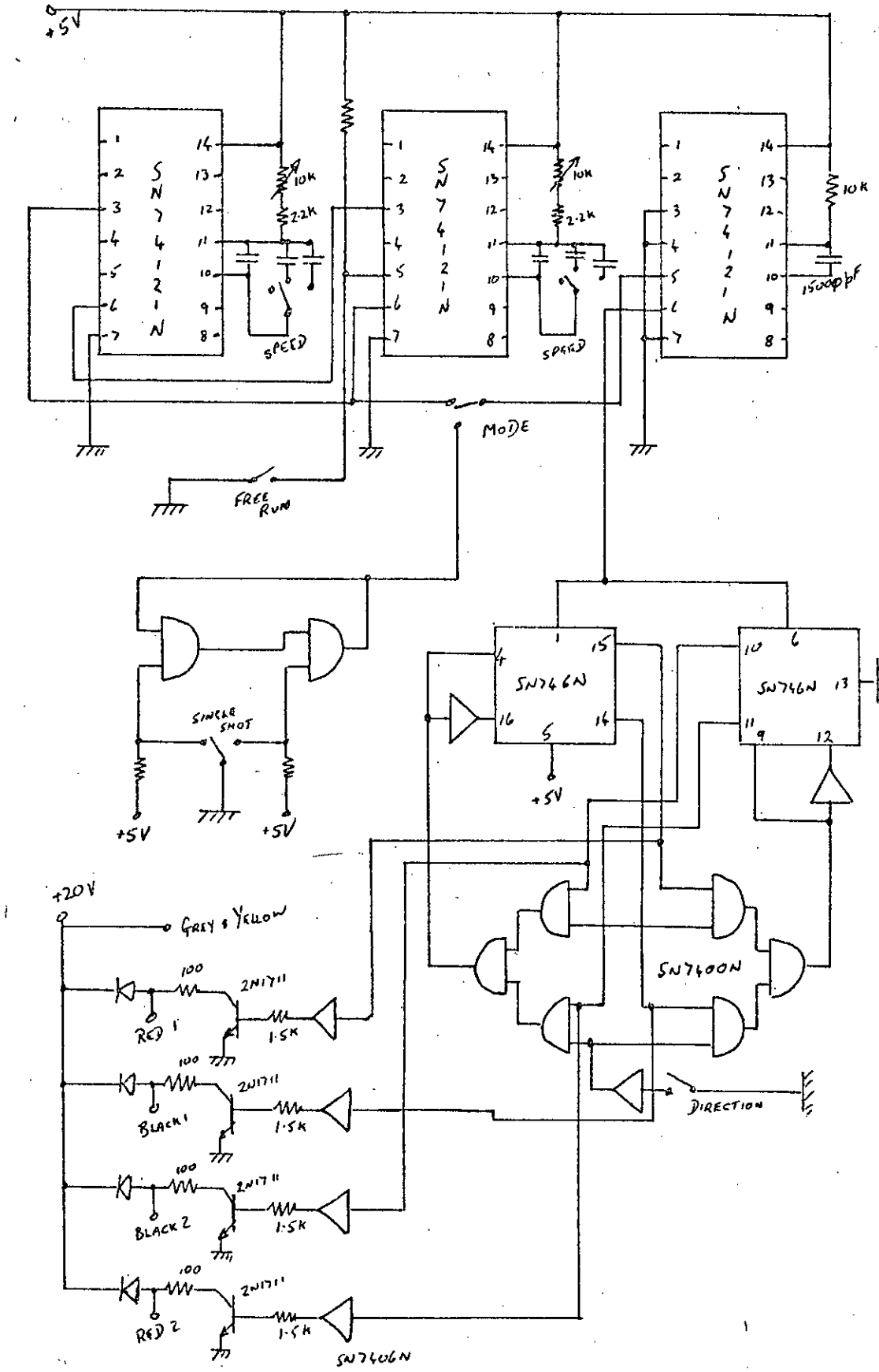

Figure AII.5 Stepping Motor Controller.

(c) Helmholtz coil power supply

The circuit is shown in figure (AII.3) and is powered by two stabilised supplies of 12V and 24V and an unstabilised supply of 20V. The stabilised supplies are provided by two L123 regulators with appropriate "programming" resistors. The supplies are connected to the 741 operational amplifier the 12V supply being the reference voltage. By adjusting the 250 ohm multi-turn potentiometer the output of the amplifier is varied which in turn determines the amount of collector current passed by the 2N3055 transistor which is connected to the 20V supply. This current also passes through the Helmholtz coils and a lohm heat sunk resistor. If when the current has been set a small change in this current occurs then the voltage across the lohm resistor changes and is fed back to pin 2 of the 741 and the change in current is remedial so producing a constant current condition.

(d) Electron gun power supply

This is shown in figure (AII4) and consists of a cathode heater supply and electrode voltage supply. The cathode heater supply is similar in operation to the Helmoltz coil power supply. The elec-:trode voltage supply is simply three multi-turn potentiometers connected across stabilised d.c. power supplies. In this case these power supplies are of a commercial type. The heater supply is isolated from the electrode supply and the voltage on the cathode can never be made positive with respect to earth.

(e) Stepping motor controller: figure (AII5)

Two SN74121N monostables are wired to be a multivibrator circuit and it is this part of the controller which regulates the speed of the stepping motor by changing the capacitors or varying the 10 kilohm/

kilohm ganged potentiometer. The output of the multivibrator is fed to a SN74121N monostable so that a clock pulse is fed from the output and into a dual flip-flop. The outputs of these flip-flops are connected to a system of NAND gates which produce logic outputs via the invertors to the bases of the four 2N1711 transistors. These transistors power the four coils of the stepping motor and the circuit has to be wired correctly so that the sequence of the transistors switching on and off is such that the stepping motor shaft rotates and does not just step backwards and forwards. The clock pulse can also be provided manually using two NAND gates.

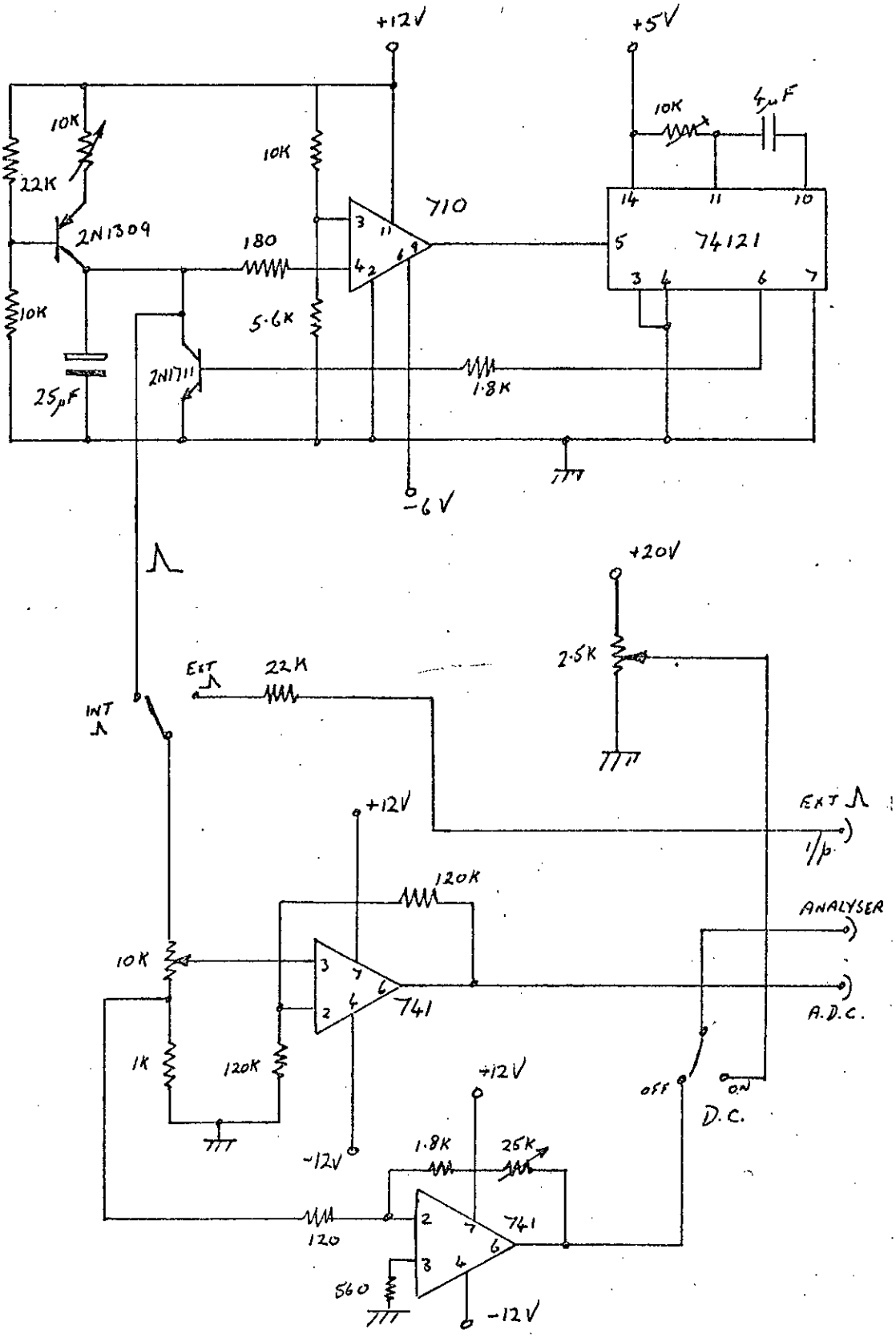

Figure AII.6 Ramp Generator

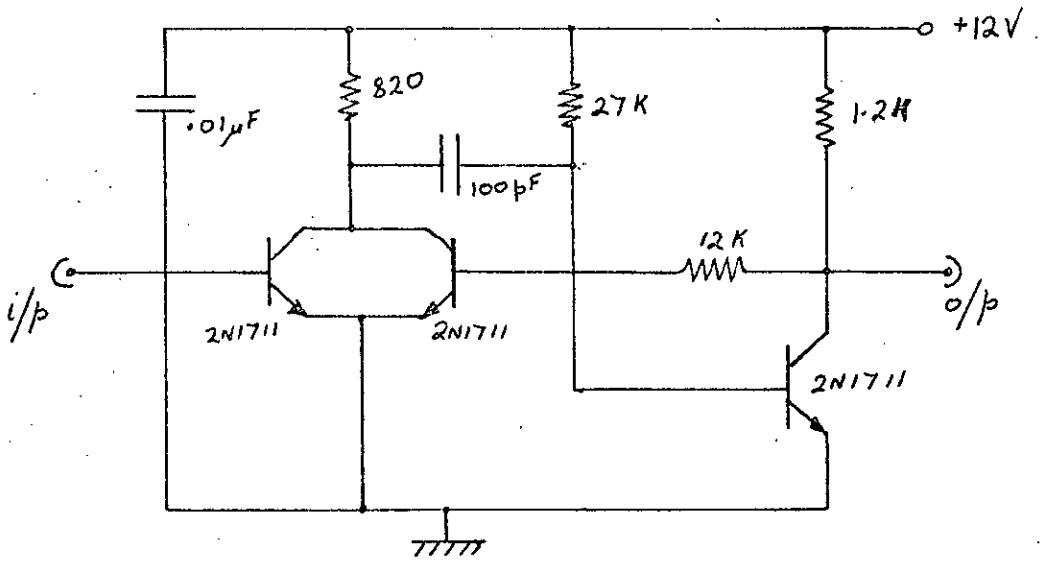

Figure AII.7 Pulse Shaper to Suit Sampling Input of Laben

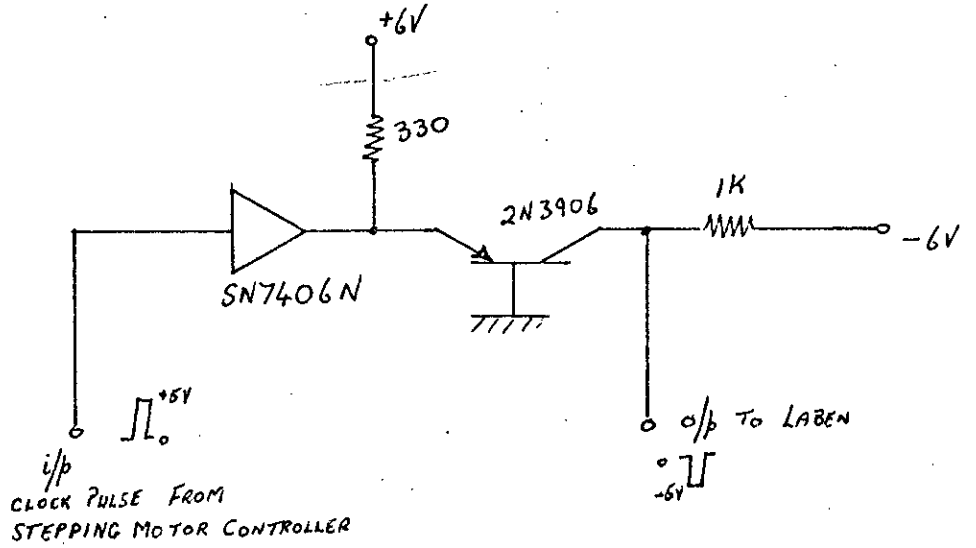

Figure AII.8 Pulse Shaper for Channel Stepping

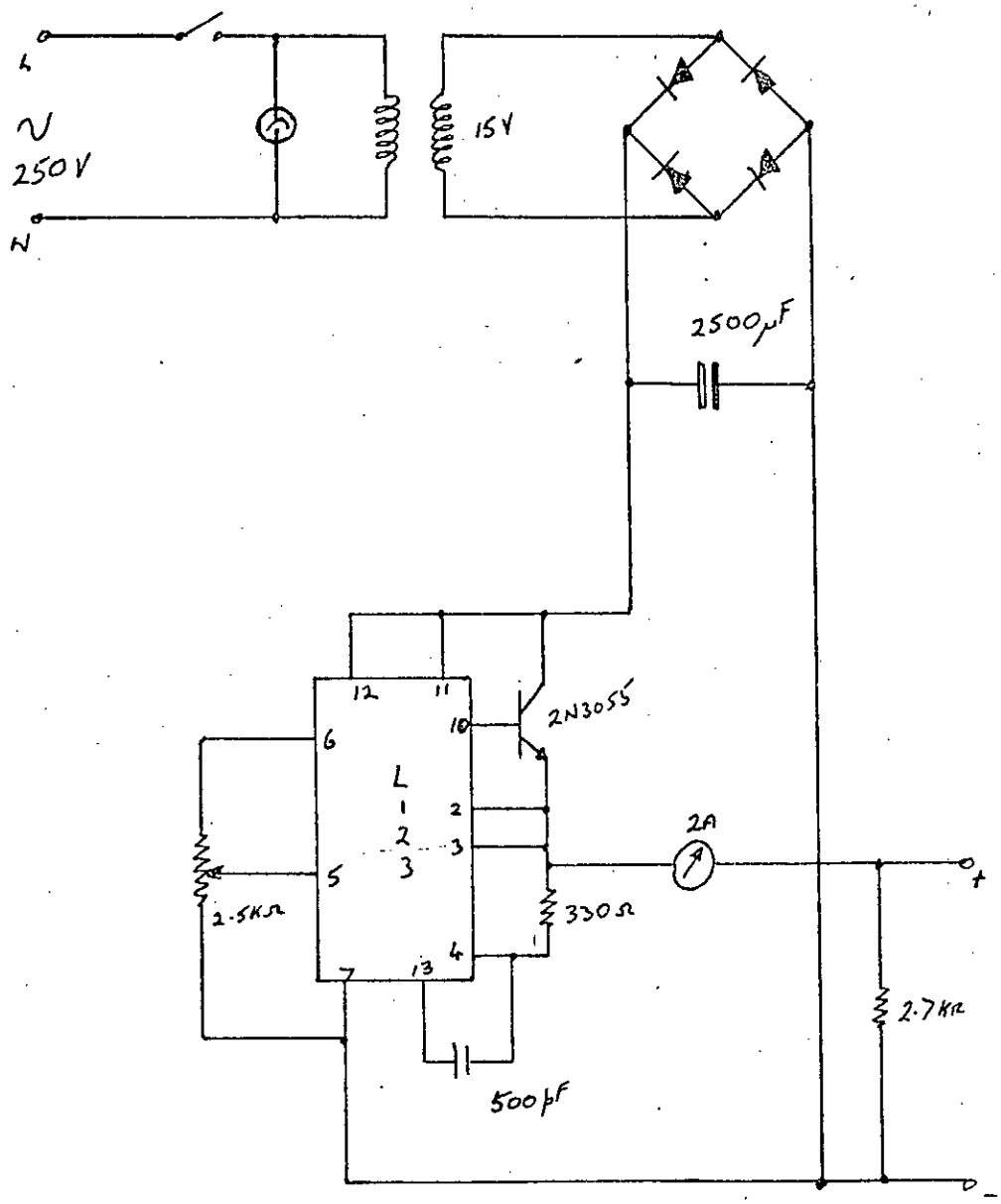

Figure AII.9 Power Supply for Oven Heaters

(f) Ramp Generator. (figure (AII.6)

The upper part of the circuit diagram shows the internal ramp source. This is produced by the charging and discharging action of the 25 microfarad capacitor. The capacitor charges until it reaches a voltage which is of the same value as the reference voltage of the 710 operational amplifier. At this point the output of the 710 changes and causes the monostable SN74121 to pulse and discharge the capacitor very quickly through the 2N1711 transistor. This produces a voltage which increases linearly from zero to about 4 volts, then drops quickly to zero again and repeats the cycle.

Either this waveform or that from the X output of an oscilloscope is fed to the two 741 operational amplifiers. One of these amplifiers acts as a voltage controller for the A.D.C. of the Laben while the other inverts the waveform to supply the back plate voltage for the analyser. The switching to provide a d.c. back plate voltage is also incorporated in the unit.

(g) Pulse Shaping Network for sampling input of Laben (figure (AII.7)

This circuit sharpens the edges of the channeltron pulses which have already been amplified, before the sampling input of the Laben will accept them.

(h) Pulse Shaper for channel stepping figure (AII.8)

This unit is required to change the clock pulse from the stepping motor controller from a + 5V pulse from zero to a -5V pulse from zero which the Laben needs before it will step channels.

(j) Power supply for oven heaters. figure (AII.9)

Two of this type of supply were built to operate the two heaters on the mercury vapour cell. The unstabilised d.c. voltage from the rectifier/

rectifier was regulated by the L123 voltage regulator to a value determined by the 2.5 kilohm potentiometer. This voltage was fed to the base of a 2N3055 transistor to regulate the collector current through the transistor which is proportional to the current drawn by the heater. The supply was capable of giving from 2 to 7 volts at up to 2 amps.

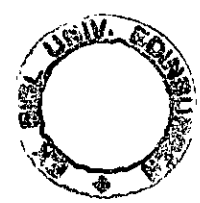

APPENDIX III

Procedure for Activating Cathode

The activation must not commence until the vacuum chamber pressure is better than 1.5×10^{-6} torr. A voltage of 3 volts is then applied to the heater so preheating the cathode for about 15 minutes and then the heater voltage is raised to 5.5V. At this stage any rise in pressure due to increase in temperature is due largely to the evolution of carbon dioxide with, perhaps, some water vapour and other gasses. It is also advisable to make sure that the pressure is not allowed to rise above 4×10^{-6} torr. After about 15 minutes at this voltage another 15 minutes at 7.5 volts is allowed, followed by 5 minutes at 9.0 volts. At this stage, the heater voltage is raised to 11.0 volts and 12.5 volts for 1 minute each and then reduced to 8.0 volts at which it must be kept for at least 15 minutes. At no time during this process must any other voltages be applied to the gun.

The heater can now be lowered in voltage to about 7.0 volts and the voltages to the other electrodes switched on. The gun is now ready for use. Although the usual heater voltage is quoted at 6.3 volts by the manufacturer, in practice, because of the fairly large electrodes and other structures, it may be found that 7.0 to 7.5 volts is necessary on the heater to attain a reasonable performance.

APPENDIX IV.

MATHEMATICAL STEPS FOR THE INTERPRETATION OF SHAPES OF MEASURED SPECTRA.

Maxwellian distribution:

$$n(u)du = \left(\frac{4N}{\sqrt{\pi}}\right)\left(\frac{m}{2kT}\right)^{\frac{3}{2}} u^2 \, e^{\frac{-mu^2}{2kT}} \, du$$

$$= \text{constant} \times u^2 \, e^{-\frac{1}{2}m\lambda u^2} \, du$$

$$p(u)du = n(u)du \times \text{constant} \times u$$

$$= C'\left(u^2 \, e^{-\frac{1}{2}m\lambda u^2} \, du\right) u$$

$$= C' \, u^2 \, e^{-\frac{1}{2}m\lambda u^2} \, u \, du$$

$$\int_0^\infty p(u)du = 1$$

$$U = \tfrac{1}{2}mu^2 \qquad \therefore \quad dU = mu \, du$$

$$p(u)du = C' \frac{\frac{1}{2}mu^2}{\frac{1}{2}m} \, e^{-\frac{1}{2}m\lambda \frac{\frac{1}{2}mu^2}{\frac{1}{2}m}} \frac{mu}{m} \, du$$

$$= C' \frac{1}{\frac{1}{2}m} U \, e^{-\lambda U} \frac{1}{m} \, dU$$

$$= C \, U \, e^{-\lambda U} \, dU = p(U)dU$$

$$\langle U \rangle = \frac{\int_0^\infty U p(U)dU}{\int_0^\infty p(U)dU}$$

$$\langle \Delta U^2 \rangle = \langle (U - \bar{U})^2 \rangle = \langle U^2 \rangle - \langle U \rangle^2$$

$$\langle U^2 \rangle = \frac{\int_0^\infty U^2 \, p(U)dU}{\int_0^\infty p(U)dU}$$

$$\int_0^\infty U^2 \, p(U)dU = \int_0^\infty U^2 \, C \, U \, e^{-\lambda U} \, dU = C\int_0^\infty U^3 \, e^{-\lambda U} \, dU$$

$$= \frac{C}{\lambda^4}\int_0^\infty (\lambda U)^3 \, e^{-(\lambda U)} \, d(\lambda U)$$

Integration by parts gives:-

$$\int_0^\infty U^2 \, p(U) \, dU = \frac{C \times 3 \times 2 \times 1}{\lambda^4} = \frac{(C \times 3 \times 2)}{\lambda^{(3+1)}}$$

$$\therefore \quad I(n) = \frac{C(n+1)}{\lambda^{(n+2)}}$$

$$\langle U \rangle = \frac{I_{(1)}}{I_{(0)}} = \frac{C \times 2}{\lambda^3} \times \frac{\lambda^2}{C \times 1} = \frac{2}{\lambda}$$

$$\langle U^2 \rangle = \frac{I_{(2)}}{I_{(0)}} = \frac{C \times 6}{\lambda^4} \times \frac{\lambda^2}{C \times 1} = \frac{6}{\lambda^2}$$

$$\langle \Delta U^2 \rangle = \langle U^2 \rangle - \langle U \rangle^2 = \frac{6}{\lambda^2} - \left(\frac{2}{\lambda}\right)^2 = \frac{2}{\lambda^2}$$

Laplace transform

$$\mathcal{L}(v) = \int_0^\infty e^{vU} p(U)dU = C \int_0^\infty e^{-(\lambda - v)U} dU$$

$$= \frac{C \int_0^\infty U e^{-(\lambda - v)U} dU}{C, \int_0^\infty U e^{-\lambda U} dU} \qquad \text{where denominator} = 1.$$

$$= \frac{I_{(0, \lambda - v)}}{I_{(0, \lambda)}} = \frac{C \times 1}{(\lambda - v)^2} \quad \frac{\lambda^2}{C \times 1}$$

$$= \frac{\lambda^2}{(\lambda - v)^2}$$

$$H(v) = \ln \mathcal{L}(v) = 2 \ln \lambda - 2 \ln(\lambda - v)$$

$$\frac{dH}{dv} = \frac{dH}{d(\lambda - v)} \times \frac{d(\lambda - v)}{dv} = - \frac{dH}{d(\lambda - v)}$$

$$= \frac{2}{\lambda - v} = \frac{2}{\lambda} \qquad \text{at } v=0$$

$$\left(\frac{dH}{dv}\right)_{v=0} = \langle U \rangle$$

$$\frac{d^2H}{dv^2} = \frac{d\left(\frac{2}{\lambda - v}\right)}{d(\lambda - v)} \times \frac{d(\lambda - v)}{dv} = \frac{2}{(\lambda - v)^2} = \frac{2}{\lambda^2} \quad \text{at } v=0$$

$$= \langle \Delta U^2 \rangle$$

Gaussian distribution:-

$$G(U - U_0) = K e^{- \frac{(U - U_0)^2}{2\sigma^2}}$$

K is constant to make $\int_{-\infty}^{\infty} G(U - U_0) dU = 1$

Mean of gaussian $= \langle U \rangle = \dfrac{\int_{-\infty}^{\infty} U\, G(U - U_0)\, dU}{\int_{-\infty}^{\infty} G(U - U_0)\, dU} = U_0$

Generating function:-

$$\mathcal{L}(v) = K \int_{-\infty}^{\infty} e^{vU}\, g(U - U_o)\, dU = K \int_{-\infty}^{\infty} e^{vU}\, e^{-\frac{(U-U_o)}{2\sigma^2}}\, dU$$

$$= e^{\left(U_o v + \frac{1}{2}\sigma^2 v^2\right)}$$

Logarithmic generating function:-

$$H(v) = \ln \mathcal{L}(v) = U_o v + \tfrac{1}{2}\sigma^2 v^2$$

$$\frac{dH}{dv} = U_o + \sigma^2 v = U_o \quad \text{at } v=0$$

$$\frac{d^2H}{dv^2} = \sigma^2 \quad \text{at } v=0$$

$$\frac{d^3H}{dv^3} = 0 \quad \text{at } v=0$$

$$p(U_a + U) = C\, U\, e^{-\lambda U}$$

$$P(U_o) = p(U)\, g(U - U_o)\, dU = \int_{-\infty}^{\infty} C\, U\, e^{-\lambda U}\, K\, e^{-\frac{(U-U_o)^2}{2\sigma^2}}\, dU$$

Introducing the generating function,

$$\mathcal{L}(v) = \int_{-\infty}^{\infty} e^{vU_o}\, P(U_o)\, dU_o$$

$$= \int_{-\infty}^{\infty} e^{vU_o} \int_{-\infty}^{\infty} p(U)\, g(U - U_o)\, dU\, dU_o$$

Now if $A = U_o - U$ then $dU_o = dA$

$$e^{vU_o}\, P(U_o) = e^{v(U_o - U + U)} \int_{-\infty}^{\infty} p(U)\, g(U - U_o)\, dU$$

$$= e^{vU}\, e^{vA} \int_{-\infty}^{\infty} p(U)\, g(U - U_o)\, dU$$

$$\mathcal{L}(v) = \int_{-\infty}^{\infty} e^{vU}\, e^{vA} \int_{-\infty}^{\infty} p(U)\, g(-A)\, dU\, dU_o$$

$$= \int_{-\infty}^{\infty} e^{vA}\, g(A) \int_{-\infty}^{\infty} e^{vU}\, p(U)\, dU\, dA$$

$$= \int_{-\infty}^{\infty} e^{vA}\, g(A)\, dA \int_{-\infty}^{\infty} e^{vU}\, p(U)\, dU$$

$$\mathcal{L}_{P(v)} = \mathcal{L}_{p(v)}\, \mathcal{L}_{g(v)}$$

$$H_{P(v)} = H_{p(v)} + H_{g(v)}$$

$$H_{P(v)} = 2 \ln \lambda - 2 \ln (\lambda - v) + \tfrac{1}{2}\sigma^2 v^2$$

As function **gA** describes a Gaussian centred at 0 then $U_o = 0$

$$\frac{dHp}{dv} = \langle W \rangle \qquad \text{as in previous arguments}$$

$$= \left\{ -2 \left(\frac{1}{\lambda - v} \right)(-1) + \sigma^2 v \right\}$$

$$= \frac{2}{\lambda} \qquad \text{at } v=0$$

Taking account of acceleration $\langle W \rangle = \frac{2}{\lambda} + U_a$

$$\frac{d^2 H_p}{dv^2} = \left\{ \frac{-2}{(\lambda - v)^2} (-1) + \sigma^2 \right\}$$

$$= \frac{2}{(\lambda - v)^2} + \sigma^2$$

$$= \frac{2}{\lambda^2} + \sigma^2 \qquad \text{at } v=0$$

$$= \langle \Delta W^2 \rangle$$

REFERENCES.

Aksela, S., Karras, M., Passa, M. & Suoninen, E. (1970) Rev. Sci. Inst. 41 , 351 - 355.

Beck, A.H.W. (1953) Thermionic Valves, Cambridge Univ. Press.

Blauth, E. (1957) Z. Phys. 147 , 228 - 240.

Boersch, H. (1954) Z. Phys. 139 , 115.

Dietrich, W. (1958) Z. Phys. 152 , 306 - 313.

Eland, J.D.H. & Danby, C.J. (1958) J. Sci. Inst. 1 , 406 - 408.

Gagge, A.P. (1933) Phys. Rev. 44 , 808 - 814.

Green, T.S. & Proca, G.A. (1970) Rev. Sci. Inst. 41 , 1409- 1414; 41 , 1778 - 1782.

Hafner, H., Simpson, J.A. & Kuyatt, C.E. (1968) Rev. Sci. Inst. 39 , 33 - 35.

Harrower, G.A. (1955) Rev. Sci. Inst. 26 , 850 - 854.

Lassetre, E.N., Berman, A.S., Silverman, S.M. & Krasnow, M.E. (1964) J. Chem. Phys. 40 , 1232.

Malcolm, I.C. (1976) Ph.D. Thesis, Univ. of Edinburgh.

Pierce, J.R. (1949) Theory and Design of Electron Beams, D. Van Nostrand Co.

Sar-el, H.Z. (1967) Rev. Sci. Inst. 38 , 1210 - 1216.

Schulz, G.J. (1962) Phys. Rev. 125 , 229 - 232.

Yarnold, G.D. & Bolton, H.C. (1949) J. Sci. Inst. 26 , 38 - 40.

Zashkvara, V.V., Korsunskii, M.I. & Kosmachev, O.S. (1966) Sov. Phys. 11 , 96 - 99.